Distribution of $^{3}He/^{4}He$ ratios and geotectonic structure of the Japanese Islands

By

Yuji SANO

Submitted in partial satisfaction of the requirements for degree of

DOCTOR OF SCIENCE

in

Geophysics

in the

GRADUATE SCHOOL

OF THE

UNIVERSITY OF TOKYO

Acknowledgments

I would like to express my grateful thanks to Professor H. Wakita of University of Tokyo for his invaluable advice and collaboration in all stage of this study. I am indebted to Professor M. Ozima of University of Tokyo for his valuable suggestions and careful reviews of this manuscript. My grateful thanks are expressed to Professor T. Tominaga of University of Tokyo. He gave me the freedom to choose my own project and encouragement in the cource of this work. I acknowledge Dr. I. Kaneoka of University of Tokyo for fruitful discussions and the improvement in English of this thesis. Thanks are also expressed to Dr. Y. Nakamura of University of Tokyo for his valuable suggestions and help in field work. I am grateful to Professor H. Sakai of University of Okayama and Dr. K. Notsu of University of Tsukuba for kindly providing samples. I thank Mr. H. Hiyagon and Mr. S. Zashu of University of Tokyo for invaluable technical assistance and Mrs. A. Urabe for her data of chemical analyses of gaseous samples. Grateful thanks are expressed to many people for their generous assistences in collction of gas samples.

Abstract

Isotopic ratios of $^3He/^4He$ in various natural gases and thermal fluids were examined to reveal the spatial distribution of the ratio and its relation to geotectonic conditions. They include 144 gas and water samples such as bubble gases from hot springs, mineral springs and water wells, CH_4-rich fuel gases, petroleum gases and volcanic fumaroles, which were collected at 100 sites in Japan. Concentrations of CO_2, N_2 and CH_4 in these samples vary significantly, ranging from 0 to nearly 100 %.

The $^3He/^4He$ ratios were measured by a 6-inch magnetic deflection type mass spectrometer with a double collector system and a resolving power of about 600 to separate ^3He beams completely from those of H_3 and HD. A standard sample for $^3He/^4He$ measurement was prepared by mixing known amounts of pure ^3He and ^4He gases. The mass discrimination factor of the system was calculated using the standard sample. The mean value of the $^3He/^4He$ ratio in the air obtained by 31 repeat runs was $(1.42\pm0.04) \times 10^{-6}$.

The elemental abundances and isotopic ratios of rare gases in gaseous samples were measured by a conventional QMS system with experimental errors of about 2% except for $^3He/^4He$, $^{78}Kr/^{84}Kr$, $^{124}Xe/^{132}Xe$ and $^{126}Xe/^{132}Xe$.

Several samples collected at a single location at different times show almost the same $^3He/^4He$ ratios. Hence, even a single measurement performed at a location may be

assigned as an approximate value for the site.

Observed $^{3}He/^{4}He$ and $^{20}Ne/^{4}He$ ratios in Japan vary significantly, from 7.47×10^{-8} to 9.65×10^{-6} and from 8.8×10^{-4} to 4.49, respectively. There is no correlation between the $^{3}He/^{4}He$ and $^{20}Ne/^{4}He$ ratios. The data for these samples in the $^{3}He/^{4}He$-$^{20}Ne/^{4}He$ diagram distribute in a triangle-like region, which suggests the existence of three end members for He: atmospheric He, mantle He (subduction-type He) and continental crustal He. the calculated mantle contribution of subduction-type He for samples from volcanic geothermal areas is about 90% at maximum. The $^{3}He/^{4}He$ ratio of this type is slightly lower than that of MOR-type He. Island Arc type magma in Japan may be characterized as having 80 % of the MOR-type He and 20 % of the crustal He. This crustal He may be attributed to the remelted subducted oceanic crust or to sedimentary materials.

(1) The $^{3}He/^{4}He$ ratios generally correlate with the subduction-related tectonic structure of the Japanese Islands. The $^{3}He/^{4}He$ ratios are as low as on the order of 10^{-7} for samples in areas along the Pacific coast side and in most of the alluvial plains. In the zone along the volcanic front and the areas immeadiately west of the front, the ratios are as high as $(5 - 9) \times 10^{-6}$. The tendency is most significant in the Tohoku district. Perpendicular to the trench axis the $^{3}He/^{4}He$ ratios gradually increase toward the

back arc region. This tendency suggests that there is a passage of primordial He from the mantle in the west side of the volcanic front region but not in the east side.

(2) The spatial distribution of sites with high $^3He/^4He$ ratios reflect well the regional volcanic activities. A more extensive investigation was made for samples around Mt. Ontake. The emission of primitive He becomes higher closer to the central cone than the circumference. This tendency implies that a carrier of primitive He is material flow of uprising magma containing volatiles.

(3) The $^3He/^4He$ ratio is applicable to estimation of the sources of hot springs and the origin of natural gases. There is a close relation between the $^3He/^4He$ ratios and the heat-discharging rates of hot spring. For the high heat-discharging spring the $^3He/^4He$ ratio is generally high, which implies direct transport of both heat and mass from magma to fluids. The source of springs with medium high heat-discharging and radiogenic $^3He/^4He$ ratio is thought to be the normal conductive heat flow of the earth. Several CH_4-rich petroleum gases on the coast of the Japan Sea have significantly high $^3He/^4He$ ratios, approximately equal to that of volcanic fumarole. A mantle-derived CH_4 is thought to be included partly in those petroleum gases.

(4) Icelandic gases and thermal fluids are measured in

order to compare the He isotope signature of the subduction zone with that of the Mid-Oceanic Ridge. Results indicate that He isotopic compositions of the Icelandic samples are attributed to the mixing of three components: MOR-type He, Plume-type He and atmospheric He. Gaseous samples collected at the northeastern part of the central belt (median zone) have typical MOR-type ratios, whereas those from the southern part of the island have apparently higher $^{3}He/^{4}He$ ratios than that of MOR-type. The extremely low contribution of crustal He in these samples compared to Japanese samples is explained by the absence of crustal materials in a divergent type of plate boundary.

Résumé

Le rapport isotopique de l'hélium ($^3He/^4He$) a été examiné dans divers gaz naturels et fluides géothermaux dans le but de révérler la distribution spatiale des valeurs de ce rapport et sa relation avec l'environnement tectonique. Pour cela, 144 échantillons de gaz et d'eau furent analysés, tels que des bulles de gaz dans less sources chaudes, les sources minérales et les forages, des gaz riches en CH_4 (gaz dit "naturel"), des gaz de champs pétrolifères et des gaz volcaniques. Ces échantillons furent prélevés dans 100 sites du Japon. Les concentrations de CO_2, N_2, CH_4, varient significativement de 0 ā près de 100%. Les abondances élémentaires et les rapports isotopiques des gaz rares dans les échantillons gazeux furent déterminés a l'aide d'un spectrométre de masse quadrupole avec une erreur expérimentale d'environ 2% sauf pour les rapports $^3He/^4He$, $^{78}Kr/^{84}Kr$, $^{124}Xe/^{132}Xe$ et $^{126}Xe/^{132}Xe$.

Le rapport $^3He/^4He$ fut determiné à l'aide d'un spectromètre de masse a déflection magnétique d'un rayon de 6 pouces equipè d'un système a double collection. Le pouvoir de résolution de l'appareil est de 600 (a 2% de vallée), ce qui permet la complète séparation des faisceaux d'ions ^3He d'une part et $HD+H_3$ de l'autre. Un échantillon standard fut réalisé en mélangeant des quantités connues d'isotopes ^3He et ^4He. Le facteur de discrimination de masse du système fut determiné a l'aide de ce standard. La valeur moyenne du

rapport $^{3}He/^{4}He$ dans l'air, obtenue d'après 31 analyses d'hélium atmosphérique, est de $(1.42 \pm 0.04) \times 10^{-6}$. Le rapport isotopique de l'hélium dans plusieurs échantillons colléctés à un site unique est pratiquement constant. Ainsi, un seul échantillon semble être représentatif d'un site donné.

Les rapports $^{3}He/^{4}He$ et $^{20}Ne/^{4}He$ observés au Japon varient significativement de 7.47×10^{-8} a 9.65×10^{-6} et de 8.8×10^{-4} a 4.49, respectivement, et il n'y a pas de corrélation entre ces deux rapports. La distribution des résultats dans un diagramme $^{3}He/^{4}He$- $^{20}Ne/^{4}He$ s'inscrit dans une aire trianglulaire, ce qui suggére l'existence de trois valeurs limites pour l'hélium: l'helium atmosphérique, l'hélium de type subduction et l'hélium crustal. La contribution calculée d'hélium de type subduction pour les échantillons de zones géothermales et volcaniques est de presque 90% dans les meilleurs cas. Le rapport de ce type est légèrement inférieur à celui du type basalte de ride medio-océanique (MORB). Ainsi le magma de type arc insulaire au Japon semble être caractérisé par un mélange du 80% d'hélium du type MORB et de 20% d'hélium crustal. Cet hélium crustal peut provenir soit de la re-fusion de la crouteocéanique subductée, soit de matériaux sédimentaires.

(1) Le rapport $^{3}He/^{4}He$ est généralement en corrélation avec la structure des îles japonaises. On observe une faible

valeur de ce rapport, de l'ordre de 10^{-7} , pour des échantillons prélevés le long de la côte pacifique et dans la plupart des plaines alluviales. Les valeurs observées le long du front volcanique et immediatement à l'ouest de celui-ci sont beaucoup plus élevées, de l'ordre de (5-9) x 10^{-6}. Cette tendence est clairement illustrée dans le district de Tohoku. Perpendiculairement à l'axe de la fosse du Japon, le rapport $^{3}He/^{4}He$ augmente graduellement lorsque'on se déplace vers l'ouest par rapport su front volcanique. Il apparait donc qu'il existe un passage pour l'hélium mantellique à l'ouest du front volcanique, ce qui n'est pas le cas à l'est de celui-ci.

(2) La distribution spatiale des sites à rapport $^{3}He/^{4}He$ élevé reflète bien l'activité volcanique régionale. Une étude extensive fut effectuée dans la région du Mont Ontake. La contribution d'hélium primitif est plus importante prés du cône central qu'à la périphérie de l'édifice. Ainsi la présence d'hélium mantellique est correlée spatialement avec celle de matériaux volcaniques. Il est probable que le magma, lors de son ascension, joue le rôle de portuer d'hélium primitif.

(3) Le rapport $^{3}He/^{4}He$ peut être utilise pour estimer l'origine des sources chaudes et celle des gaz naturels. Il existe une étroite relation entre ce rapport et le taux de décharge de chaleur des sources chaudes. A une source à taux

de décharge élevé correspond généralement un rapport $^3He/^4He$ également élevé, ce qui implique un transport direct de masse et de chaleur du magma vers les fluides. L'origine de la chaleur pour les sources à taux de decharge moyen et rapport $^3He/^4He$ radiogenique estattribuée au flux géothermique conductif normal de la Terre. Plusiurs gaz riches en CH_4 collectés dans les champs pétroliferes sur la côte de la Mer du Japon présentent des valeurs elevées du rapport $^3He/^4He$, approximativement égales à celles des fumerolles volcaniques. Il est possible qu'une partie du méthane contenu dans ces gaz soit d'origine mantellique.

(4) Des gaz et fluides géothermaux islandais ont été analysés afin de comparer la signature isotopique de l'hélium de type subduction à celle de l'hélium de type ride médio-océanique. Les resultats montrent que la composition isotopique de l'hélium dans les échantillons islandais resulte du mélange de trois composants: l'hélium de type MORB, l'hélium de type panache et l'hélium atmosphérique. Les échantillons collectés dans la partie nord-est de la ceinture centrale (zone mediane) présentent un rapport $^3He/^4He$ typique des rides médio-océaniques, alors que ce rapport est generalement plus élevé pour des échantillons prélevé dans la partie sud de l'île. La contribution extremèment faible d'hélium crustal dans ces échantillons par rapport aux échantillons japonais s'explique par l'absence de matériaux crustaux dans cette zone de divergence de plaques.

List of Figures

List of Tables

Contents

I. Introduction

The principal purpose of geochemistry is to investigate (1) the abundance and distribution of elements and isotopes in each part of the earth, for example atmosphere, crust, mantle and core; (2) the mechanism which produced the distribution of elements and isotopes; (3) on the basis of (1) and (2), the present structure and evolution of the earth. Many researchers have carried out chemical analyses and isotope measurements of terrestrial materials for this purpose. It is not difficult to collect samples representing the surface of the earth such as atmosphere, sea water and crustal rocks, and we have a large number of data about these samples. However, it is difficult to get samples representing the deep part of the earth, since even so-called "mantle materials" may be contaminated by surface materials such as crust, sea water and atmosphere during transport from the mantle. The contamination is classified into physical and chemical processes. Physical processes include variation of composition due to mixing of mantle and surface materials, due to separation of components caused by diffusion, partition and disequilibrium, or due to nuclear reaction or radioactive decay. Chemical processes produce a change in contents mainly due to chemical reactions between mantle and surface materials for example, oxidation, reduction and neutralization.

If we want to know more about the deep part of the earth

and its relation to the surface materials such as crust, ocean and atmosphere, we should first search for elements or isotopes which are not easiliy changed during the transport from the mantle. Rare gases are considered to be ideal materials among volatile elements because of their inertness. The chemical compounds of rare gases have not yet been found in nature except under the extremely severe conditions of the chemical laboratory (Bartlett, 1962; Hoppe et al., 1962; Claassen et al., 1962). Therefore rare gases in mantle materials are not affected by chemical contamination. If there are some anomalous compositions of rare gas elements and isotopes, the cause is only physical processes and explanation is easier than in the case of other volatile elements such as carbon and oxygen.

Due to their chemical inertness, the rare gases are usually greatly depleted in solid phase and enriched in gaseous phase. This suggests that the earth's atmosphere has been accumulating rare gases from the solid earth. From the low terrestrial abundances of rare gases relative to those of the solar system, Brown (1952) recognized that the atmosphere is not primary, that is, a trapped solar nebula but is secondary of degassed from the interior of the earth. Estimating the degassing rate of volatiles via volcanic gas and hot spring emanation, Rubey (1951) proposed a continuous degassing model for the formation of the atmosphere. Since then, a large number of investigations have been carried out to search for evidence of the outgassing of rare gases from

the earth. In 1968, excess ^{40}Ar was discovered in quenched basalts and volcanic xenoliths (Funkhouser and Naughton, 1968; Funkhouser et al., 1968; Dalrymple and Moore, 1968; Noble and Naughton, 1968). Based on these data, Ozima (1975) presented a catastrophic degassing model for the early stage of the earth's evolution.

Another type of evidence for the outgassing of juvenile rare gas from the mantle is Xe. The 8 % enrichment of ^{129}Xe from the decay of extinct ^{129}I was discovered in CO_2 well gas from Harding County, New Mexico (Butler et al., 1963). This well gas has been re-analyzed several times with more refined techniques and increased accuracy (Boulos and Manuel, 1971; Hennecke and Manuel, 1975; Phinney et al., 1978; Smith and Reynolds, 1981), and the result of Butler et al. was confirmed much more strongly. Excess ^{129}Xe has also been reported in a number of mantle-derived samples such as Hawaiian nodules (Hennecke and Manuel, 1975; Kaneoka and Takaoka, 1978; 1980; Kyser and Rison, 1982) and Kimberlite nodules (Kaneoka et al., 1978). Recently small enrichments of ^{129}Xe were reported for basalts from the Mid-Atlantic Ridge and the East Pacific Rise (Staudacher and Allegre, 1982). However, other groups (Ozima and Zashu 1982; Kirsten et al., 1982) did not confirm the existence of the excess ^{129}Xe in MOR-basalts. The difficulty of Xe isotope study is attributed to its low content level in basalts and its contamination by atmospheric Xe.

Among rare gases, He is a unique key to the study of the

earth's volatiles. Since it escapes from the earth's atmosphere into space by molecular diffusion (Kockarts, 1973), the concentration of atmospheric He is extremely low. Therefore He in rock and gaseous samples is not easily distorted by contamination of atmospheric He. The major part of this thesis is devoted to He isotope geochemistry.

He has two stable isotopes (mass 3 and 4) and three very short-lived radio isotopes (mass 5, 6 and 8) which have been produced artificially and are not known to occur naturally. ^{4}He is the most abundant isotope and is produced on the earth by radioactive decay of U and Th. The isotope was first discovered in the atmosphere of the sun (Jansen, 1868), and the name "Helium" was taken from that of the sun, "Helios". In 1895, Ramsey observed terrestrial He extracted from Cleveite rock, and Crookes (1895) confirmed the discovery using an emission spectrometer. ^{3}He is a very rare isotope, the terrestrial source of the nuclide is mainly attributed to the trapped component of solar nebula at the accretion of the earth. In 1939, Alvarez and Cornog discovered ^{3}He in terrestrial He with a cyclotron and showed that the $^{3}He/^{4}He$ ratio of He in a natural gas well is 10 times lower than that in the atmosphere. Aldrich and Nier (1948), using a newly developed mass spectrometer, confirmed that wide variation exists in the $^{3}He/^{4}He$ ratio in natural samples. The highest ratio, 1.2×10^{-5}, was observed in the Li mineral spodumene, and the lowest ratios, less than 2×10^{-8}, in U and Th minerals. The work of Aldrich and Nier

demonstrated the production of ^{3}He by nuclear reactions in the earth: $^{6}Li(n,\alpha)^{3}H(\beta)^{3}He$. Morrison and Pine (1955) calculated that the $^{3}He/^{4}He$ ratio in crustal rock should be about 1×10^{-7}, and this value agreed well with that for natural gas wells. Since then, it has been generally accepted that the He isotopes in the crust are radiogenic.

After the study of Aldrich and Nier (1948), analysis of the terrestrial $^{3}He/^{4}He$ ratio ceased for 20 years. In 1969, Clarke et al. found in deep Pacific water a great enrichment of ^{3}He relative to the atmospheric $^{3}He/^{4}He$ ratio. They concluded that the excess ^{3}He is due to leakage into ocean water of remnants of the earth's primordial mantle ^{3}He. Simultaneously Mamyrin et al. (1969) found that the $^{3}He/^{4}He$ ratios of volcanic gases in the Southern Kurile Islands are clearly higher than that of the atmosphere. They also considered that the increment was derived from deep-seated materials.

Since then more intensive investigations have been carried out all over the world. It has been noticed that natural gases, thermal fluid and rock samples in the same geotectonic regions show quite similar $^{3}He/^{4}He$ ratios. Emission of the primordial He is commonly found in Cenozoic volcanic areas (Mid-Oceanic Ridge, hot spots and subduction zones).

The $^{3}He/^{4}He$ ratios of fresh basalt glasses obtained from the Mid-Oceanic Ridge, including the Mid-Atlantic Ridge and the East Pacific Rise, are high at almost constant values of

$(1.25+0.15)\times 10^{-5}$. This value is defined as the MOR-type He (Lupton and Craig, 1975). Subsequent studies (Craig and Lupton, 1976; Rison, 1980; Ozima and Zashu, 1982; Kirsten et al., 1982) confirmed that the averaged basalt $^3He/^4He$ ratio is generally accepted as the He signature for the upper mantle, and the constancy of this ratio is taken as evidence that the upper mantle is well mixed on a global scale.

In 1976, Craig and Lupton first reported that the fumarole gas from Kilauea volcano, Hawaii, has a significantly higher $^3He/^4He$ ratio than that of MOR-type He. This extremely high ratio is considered as evidence that the Hawaiian hot spot is now discharging earth's volatile gases which are more enriched in ^3He than the MOR-type reservoir. This elevated $^3He/^4He$ ratio was confirmed by measurements of ultramafic nodule and volcanic rocks in Hawaii (Kaneoka and Takaoka, 1978; 1980). The study of other hot spot regions such as Iceland (Polak et al., 1975; Poreda et al., 1980; Hooker et al., 1982; Torgersen and Jenkins, 1982), Yellowstone Park (Craig et al., 1978) and the Ethiopian Rift Valley (Craig and Lupton, 1978; Craig et al., 1979) supports the existance of deep mantle component distinct from MOR-type He. $^3He/^4He$ ratios of these hot spot regions vary considerably, from 2×10^{-5} to 5×10^{-5}. The fluctuation may be attributed to the mixing of MOR-type He and crustal He.

Subduction zones, including the island arc and continental margin province, are a third type of Cenozoic volcanic area. The first indication of a mantle-derived He

component in subduction zones was reported for volcanic gases from Kamchatka ($^3He/^4He = 7.9 \times 10^{-6}$) and the Kurile Islands (from 7.5×10^{-6} to 8.8×10^{-6}) by Baskov et al. (1973). Craig et al. (1978) found similar high $^3He/^4He$ ratios from circum-Pacific volcanic gases in Hakone, Japan (8.6×10^{-6}), the Marianas (7.4 and 9.7×10^{-6}) and Lassen Park (10.7 and 11.3×10^{-6}). Subsequent studies of geothermal gases in the Japanese Islands (Nagao et al., 1981) and in New Zealand (Torgersen et al., 1982) indicate that the $^3He/^4He$ ratio of subduction zones are almost uniform from 7×10^{-6} to 11×10^{-6}.

Considering the correlation between $^3He/^4He$ ratios and global tectonic enviroments, the principal purpose of this thesis is to concentrate on the following questions: (1) Is the $^3He/^4He$ ratio of Island Arc really uniform? (2) If a variation in the ratio is oberved, are there some geological and geophysical parameters which correlate positively or negatively with the $^3He/^4He$ ratio? What accounts for the variation of the $^3He/^4He$ ratio? (3) Can the $^3He/^4He$ ratio be used to study other geochemical problems such as the origin of hot springs and the source of natural gas?

In order to examine these problems, various kinds of natural gases and thermal fluids were collected at a number of sites in the Japanese Islands, and $^3He/^4He$ ratios of these samples were measured. Rare gas isotopic analyses of selected samples were made using a Quadrupole mass spectrometer. Some technical problems of $^3He/^4He$ ratio

measurement by a magnetic deflection type mass spectrometer and rare gas isotopic analysis by a Quadrupole mass spectrometer are also described in this thesis. For comparison with Japanese Island Arc samples, several gases and thermal fluids from Iceland were analyzed.

II. Experimental

2.1 Isotopic measurements of rare gases

2.1.1 Measurements of $^3He/^4He$ and $^{20}Ne/^4He$ ratios

a) Rare gas purification line

In order to purify He and Ne from original gas and water samples, an ultra-high-vacuum line was constructed (Figure 2-1). The mass spectrometer was connected to the purification line with an ultra-high-vacuum flexible tube. Because He can penetrate through glass, stainless steel 304 was used for most parts of the line except for an ionization gauge. The line consists of three-step purification parts separated by ultra-high-vacuum valves (V1, V2 and V3). The first part is composed of inlet valves V10 and V11 (the volume between these valves is about 1 cc) and an activated charcoal trap (CT-0). The second part has a copper oxide furnace (CuO), a charcoal trap (CT-1) and a Pirani vacuum gauge (P.G.). The third part includes a titanium-zirconium getter furnace (TiZr), a charcoal trap (CT-2) and an ionization vacuum gauge (I.G.). The first part was evacuated to a vacuum below 10^{-5} Torr by an oil diffusion pump (O.D.P.) with a liquid nitrogen trap. Vacuo below 2×10^{-8} Torr in an almost oil-free condition were obtained for the second and third parts by a sputter ion pump (I.P.). Metal bellow valves V8, V9 and V12 attached to the respective charcoal traps are used to keep adsorbed species. The total

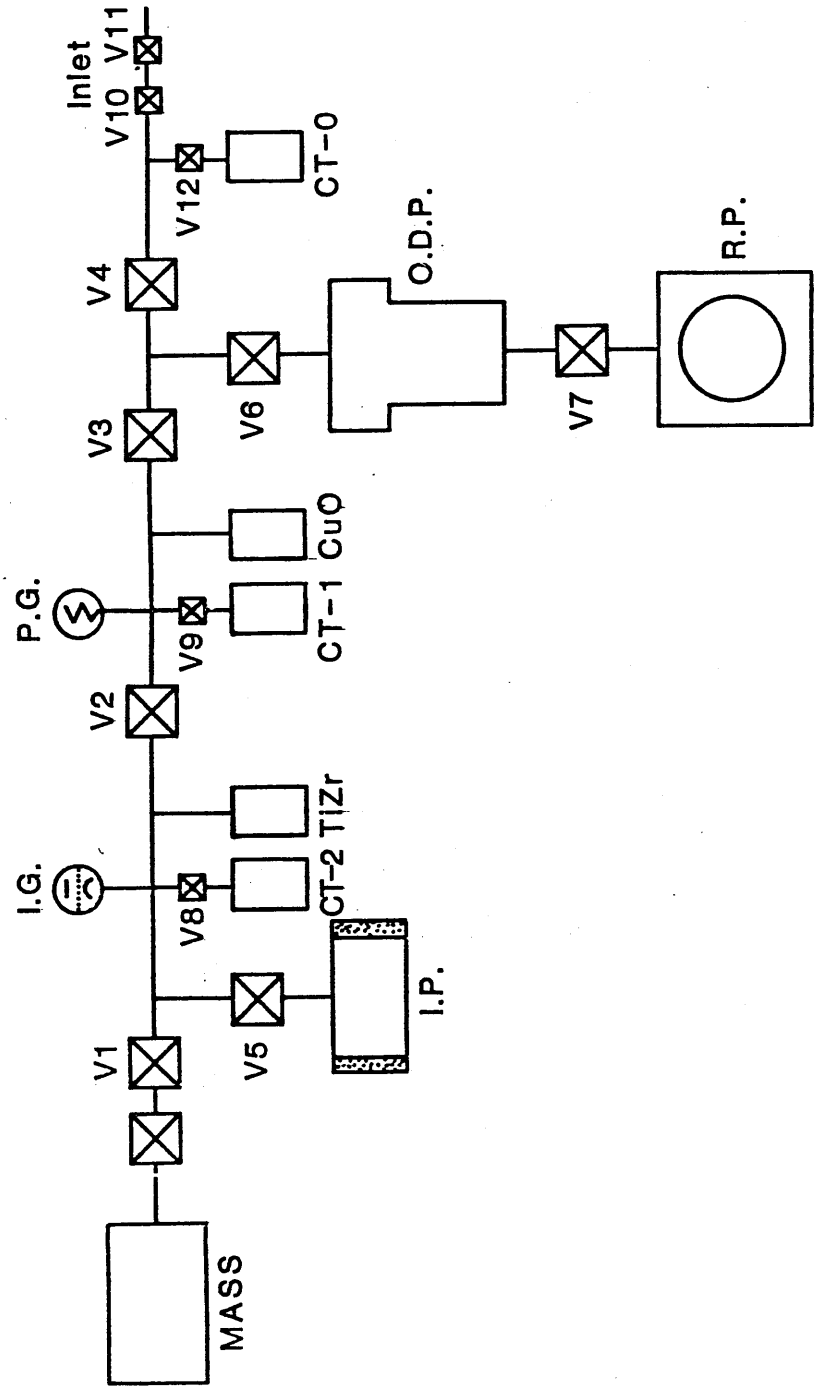

Figure 2-1. Schematic diagram of a rare gas purification line and mass spectrometer system. MASS: mass spectrometer, V: valves, I.P.: sputter ion pump, I.G.: ionization gauge, CT: charcoal trap, P.G.: pirani gauge, TiZr: titanium zirconium getter pump, CuO: copper oxide furnace, O.D.P.: oil diffusion pump and R.P.: rotary pump.

volume of the purification line is about 300 cc.

b) Preparation of a standard sample for He isotopic measurements

A standard sample for He isotopic measurement was made by mixing known amounts of pure ^{3}He and ^{4}He gases. A high vacuum line made of glass was constructed for the purpose of mixing (Figure 2-2). The line has two vacuum gauges: one is a Schulz gauge for rough measurement of the vacuum and the other a McLeod gauge for precise measurement. The vacuum below 5×10^{-6} Torr in an oil-free condition was obtained by a mercury diffusion pump with a liquid nitrogen trap. Two glass vessels with breakable seals were attached to the line in order to get some amounts of ^{3}He and ^{4}He. The smaller vessel was used for He, and its volume of 6.956 cc was precisely determined using mercury. The larger one was used for ^{4}He, and its volume, 1103.6 cc, was determined using distilled water.

The commercial ^{3}He, whose purity of ^{3}He was 99.5 % and whose ^{4}He content was less than 0.01 % was used. The volume of the ^{3}He bomb were about 1 liter, and its pressure was about 3.0 Torr. The ^{4}He was also prepared using commercial ^{4}He. The purity of ^{4}He was more than 99.9995 %, and the ^{3}He/^{4}He ratio of the commercial ^{4}He was less than 1.0×10^{-7}. The volume of ^{4}He bomb was about 1 liter and its total pressure was about 760 Torr.

First the ^{3}He bomb was connected to the inlet part of the mixing line using an O-ring high vacuum connector. Each

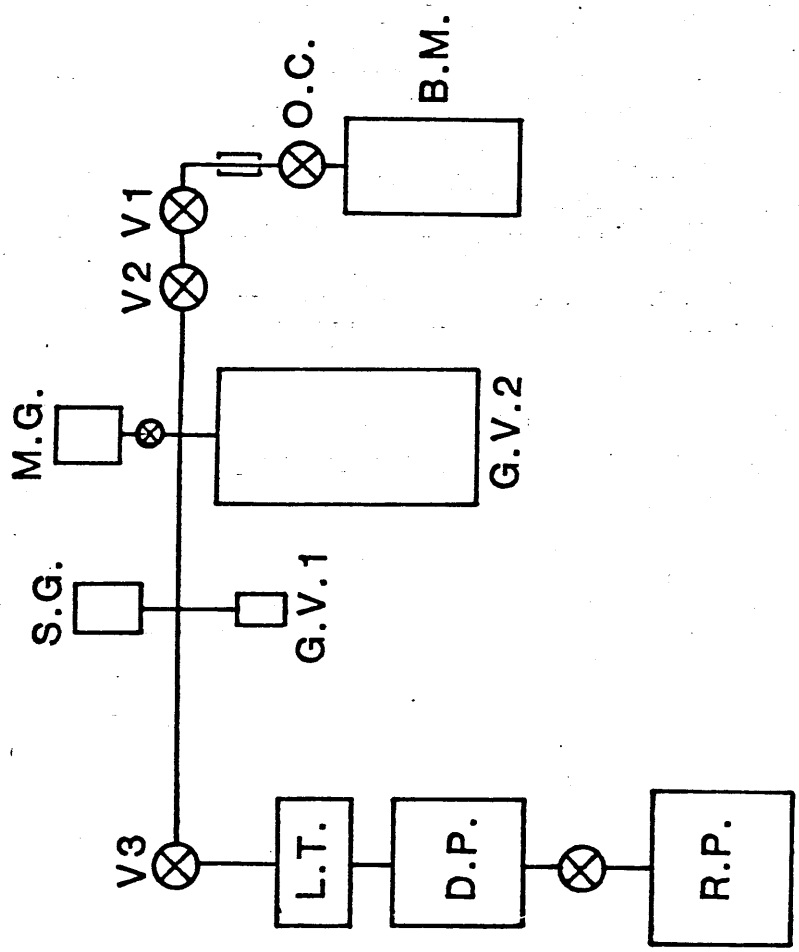

Figure 2-2. Schematic diagram of a mixing line for He standard (1). B.M.: commercial standard of pure ^{3}He or ^{4}He, O.C.: O-ring high vacuum connector, V: valve, M.G.: McLeod gauge, S.G.: Schulz gauge, L.T.: liquid nitrogen trap, D.P.: mercury diffusion pump, R.P.: rotary pump, and G.V.: glass vessel with breakable seal.

part of the line was evacuated to lower than 5×10^{-6} Torr by a mercury diffusion pump. ^{3}He from the bomb was introduced into the space between the inlet valves (V1 and V2) and transferred to the mixing line. The pressure in the line was measured precisely by the McLeod gauge, and the small glass vessel for ^{3}He was sealed off. Then the mixing line was washed by a large amount of atmospheric air to avoid contamination by a residue of ^{3}He in the line. The ^{4}He bomb was connected to the inlet part. After each part of the line was evacuated, ^{4}He from the bomb was introduced into the inlet part and transferred to the line. The pressure was measured precisely and the large glass vessel for ^{4}He was sealed off. The amounts of ^{3}He and ^{4}He in each vessel were 4.023×10^{-5} and 3.225×10^{-1} cc STP, respectively.

Both vessels were attached to the mixing line, and a metal container with metallic bellow valves for the mixed standard was also attached (Figure 2-3). Each part of the line was evacuated to below 5×10^{-6} Torr, and the valve of the metal container was closed. The breaker of the ^{3}He vessel was opened, and then that of the ^{4}He vessel. In order to avoid isotopic fractionation, 10 minutes were required to mix ^{3}He and ^{4}He sufficiently, and then the valve of the metal container was opened. After 20 mintues, the valves were closed. The mixing ratio of ^{3}He to ^{4}He was to be $(1.25 \pm 0.01) \times 10^{-4}$. Since the $^{3}He/^{4}He$ ratio in commercial ^{4}He is less than 1.0×10^{-7}, the contribution of ^{3}He from commercial ^{4}He to the mixed standard was negligibly small.

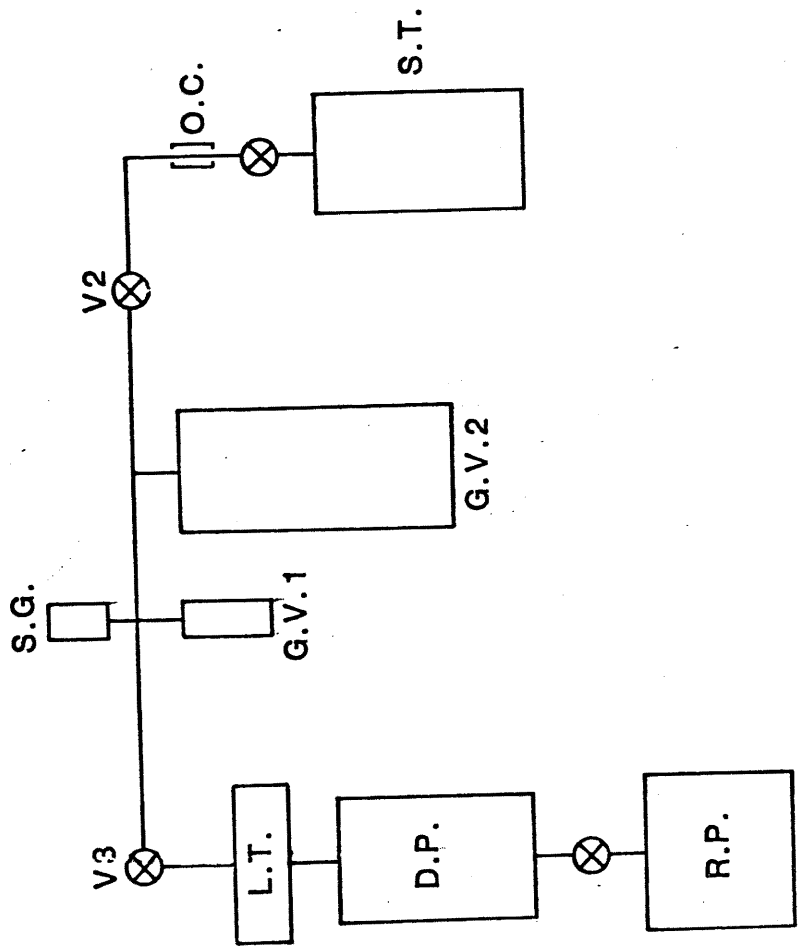

Figure 2-3. Schematic diagram of a mixing line for He standard (2). S.T.: metal container for the mixed standard, O.C.: O-ring high vacuum connector, V: valve, S.G.: Schulz gauge, L.T.: liquid nitrogen trap, D.P.: mercury diffusion pump, R.P.: rotary pump, and G.V.: glass vessel with breakable seal.

c) Extraction of He and Ne from water sample

In order to admit a gas sample to the purification line, gas dissolved in a water sample must be extracted. The sample container was connected to one end of the another new container with an O-ring high vacuum connector. The other end of the new container was attached to the sorption pump by a tygon tube (Figure 2-4). The new container and the space between it and the sample container were evacuated to below 1 x 10^{-3} Torr by a sorption pump equipped with a rotary pump. The vacuum cock between the new container and the pump was closed and the vacuum cock between the sample container and the new one was opened. The water in the sample container was transferred, to the new one but the gas dissolved in the water was left in the sample container. After 10 mintutes, to avoid elemental and isotopic fractionation, the vacuum cock between the sample container and the new one was closed.

At the equilibrium condition between gas and water, He and Ne preferentially go to the gas phase. The ratio (r) of the rare gas amount in gaseous phase to that in water phase is given by the following formula:

$$r = b \times Vw \times Pg / (Vg \times Pg) = b \times Vw / Vg$$

where, Pg, Vw, Vg, and b denote the partial pressure of the rare gas in gaseous phase, the volume of water phase, the volume of gaseous phase and the solubility of the rare gas, respectively. In this case, the volume of gaseous phase almost equals that of water, and the solubilities of He and

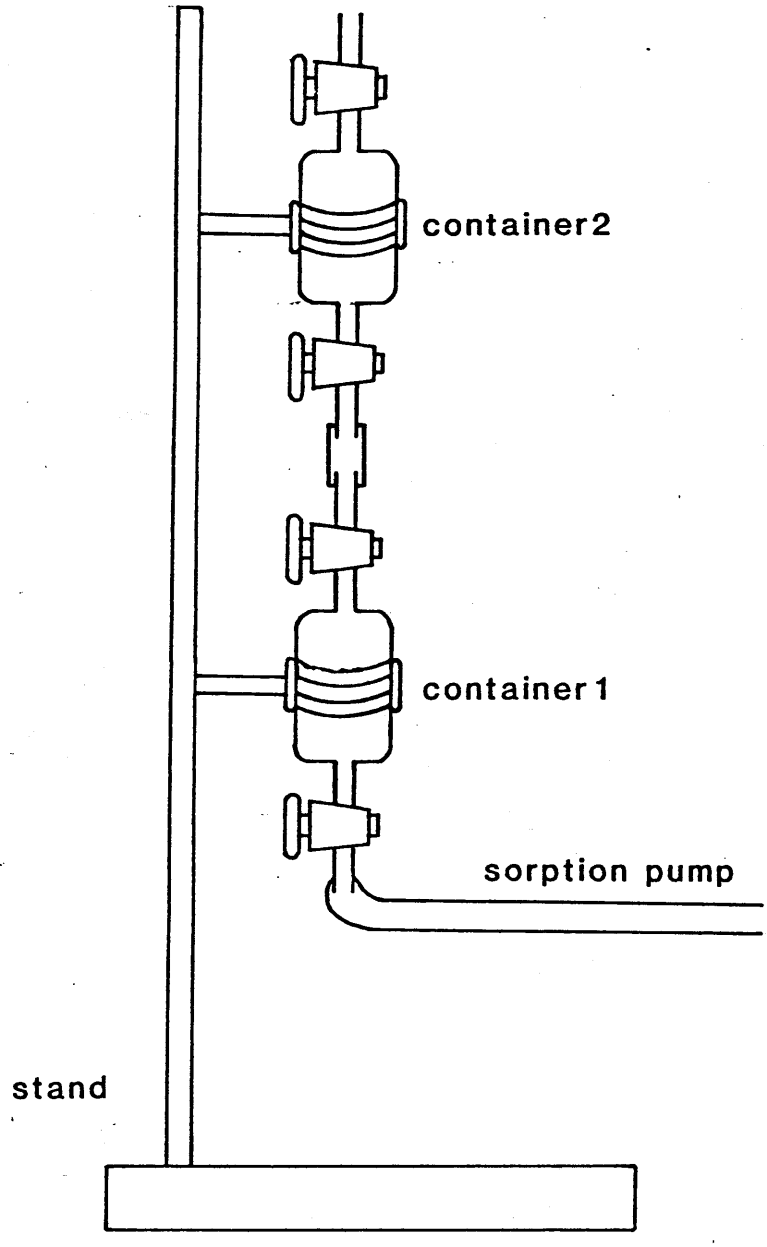

Figure 2-4. Extraction of dissolved gases in water samples. Water samples in sample container 2 are connected to container 1 with a O-ring high vacuum connector. After the system is evacuated to below 1 x 10^{-3} Torr by the sorption pump, water in container 2 is transferred to container 1. The gas dissolved in the water remains in container 2.

Ne in the water are 8.0×10^{-3} and 1.04×10^{-2} (cc/cc water.atm), respectively. Hence, more than 99 % of He and Ne in the water sample were extracted by the process.

d) Purification procedure for He and Ne

A sample container, an atmospheric air tank and an artificially mixed standard were directly connected to the inlet part using O-ring high vacuum connectors. A sample of about 1 cc STP was introduced into the space between inlet valves (V10 and V11) and was transferred to the purification line.

At first, major adsorbable components such as N_2, O_2, CH_4 and CO_2 in the sample gas were roughly removed by a charcoal trap (CT-0) kept at a temperature of - 196° C. Unadsorbed components containing He and Ne were transferred to the second part. In a copper oxide furnace maintained at 550° C, H_2 and CH_4 were oxidized to H_2O and CO_2 (for 30 min) and removed by the CT-1 kept at a temperature of -196° C. Then the purified fraction was expanded to the third part. The CT-2 kept at -196°C was used to adsorb all residual active gases and heavy rare gas (for 30 min). Finally, purified fraction containing He and Ne was introduced into a mass spectrometer. Analysis was made by a static condition. In the above process, the TiZr getter furnace was only used to obtain an oil-free ultra-high-vacuum condition before introduction of actual samples, since the TiZr getter releases significant amounts of H_2. Total purification time required for an individual sample was about two hours.

e) Mass spectrometer for $^3He/^4He$ and $^{20}Ne/^4He$ ratio measurements .

In order to measure $^3He/^4He$ ratios with a precision of 2 - 3 % at the ^3He and ^4He levels of approximately 10^{-12} cc STP and 10^{-6} cc STP, respectively, the mass spectrometer must fulfill very rigorous technical requirements such as (1) It must have a low background at peaks of mass number 3 and 4, that is, a low hydrogen and helium background. (2) High resolving power of more than 600 is necessary to separate H_3^+ plus HD^+ from $^3He^+$ ion beams. (3) Clear-cut peak shapes are required to prevent the tails of H_3^+ and HD^+ beams from contributing significantly at the $^3He^+$ position. 4) It must be sensitive enough to measure very small amounts of ^3He (as small as 10^7 atoms) in the sample.

The instrument used in this study (including the analyzer tube, ion source, collector assembly and electron multiplier) is a modified version of the Model 6-60-SGA mass spectrometer made by Nuclide Analysis Associates (Pennsylvania, U.S.A.). It is a first-order direction focussing, 60° deflection instrument having a 6" radius of curvature. The mass spectrometer is pumped by a 60 l/s sputter ion pump and a getter pump. The getter pump works even in the measurements of the isotopic ratios, since it does not pump rare gas. The ion source is based on the Nier design, and a source magnet, which produce a constant magnetic field parallel to the electron beam, was used in order to increase sensitivity . The electron accelerating

potential was 75 V. After ionization, positive ions of ^3He and ^4He are accelerated by a potential of 2.5 KV. The electromagnet is controlled by a feedback system using a Hall probe.

Ion beams of ^3He and ^4He are detected simultaneously by a double collector system. The collector slit width at the principal collector was optimized to attain a resolving power of more than 600. Ions for ^3He and other masses at the principal collector were detected using a secondary electron multiplier. THe multiplier was settled at 1.8 kV with a gain of about 6×10^5. The ion current after electron multiplication was integrated by the digital integrator. At the secondary collector, the collector slit was a fixed slit with a width sufficient to collect the ^4He beam while the ^3He beam was scanned over a small mass range. Ion beam was detected by a Farady cup, and the ion current was integrated by the digital integrator as well as by the principal collector.

f) Adjustment of the mass spectrometer and the background level

The resolving power of a mass spectrometer ($M/\Delta M$) is given by the following formula:

$$M/\Delta M = r/(S_1 + \Psi(r) + S_2)$$

where r denotes the radius of ion curvature, S_1 ~~is the~~ width of the final source slit, $\Psi(r)$ is an unavoidable aberration which is a function of the radius r and S_2 is the width of the collector slit. In order to obtain a high resolving

power, diminition of S_1 and S_2 and a smaller setting of $\Psi(r)$ are needed. The smallest value of $\Psi(r)$ was selected by adjusting the condition of the ion lens, while the geometry of the main magnet and the source magnet was kept at optimum.

The static background of the mass spectrometer, cold blank and hot blank of the measuring system were examined for ^3He, ^4He and ^{20}Ne, respectively. The cold blank indicates the static background of the whole system including the purification line. The hot blank indicates the static background after actual purification procedure is done without sample gas. The static background of the mass spectrometer and the cold blank of ^3He, ^4He and ^{20}Ne were below 7×10^{-14}, 3×10^{-10} and 9×10^{-9} cc STP, respectively. In hot blanks, ^3He and ^{20}Ne were below 1×10^{-13} and 9×10^{-9} cc STP, respectively, whereas a ^4He ion beam of 0.001 V, which was equivalent to 3×10^{-9} cc STP, was detected by the Farady cup. This amount, however, is negligibly small in the measurement of actual samples.

g) Mass discrimination factor

The Farady cup and the secondary electron multiplier were equipped with high registors of about 10^{11} and 10^9 ohm, respectively. The net gain of the multiplier over the Farady cup was measured using ^4He ion beams. About 1.6×10^{-8} cc STP of ^4He was admitted to the mass spectrometer, and the ^4He ion beam was measured by both the Farady cup and the multiplier, alternately. The net gain obtained by repeat runs was 6.00×10^3.

In order to examine the mass discrimination factor of a measuring system, one pipette of the artificially mixed He standard (^{3}He: 5.0×10^{-10} cc STP and ^{4}He: 4.0×10^{-6} cc STP) was admitted to the mass spectrometer. The observed $^3He/^4He$ ratios gave a mean value of $(9.77 \pm 0.15) \times 10^{-5}$. A mass discrimination factor (d) can be defined as follows:

$$d = (((^3He/^4He)_{obs.}/(^3He/^4He)_{cal.} - 1) \times 100$$

where $(^3He/^4He)_{obs.}$ and $(^3He/^4He)_{cal.}$ denote the observed $^3He/^4He$ ratio and calculated $^3He/^4He$ ratio, respectively. In the present case, the discrimination factor (d) is to be (21.8 ± 0.05) %.

h) Atmospheric He as a secondary standard

Since the atmospheric air is known to have a constant $^3He/^4He$ ratio of $(1.40 \pm 0.03) \times 10^{-6}$ irrespective of latitude, longitude and elevation (up to 10 km) (Mamyrin et al., 1970), it becomes an ideal standard for samples with lower $^3He/^4He$ ratios.

About 1 cc STP of air collected in Tokyo was introduced into the purification line. Purified He and Ne were measured by the mass spectrometer. A typical mass spectrum of ^{3}He and ^{4}He in Tokyo air is shown in Figure 2-5. An excellent separation between ^{3}He beams and HD plus H_3 beams was observed. A resolving power of about 600 at 1 % peak height and more than 1000 at 50 % peak height was attained. The shape of the peak is good enough to prevent the tails of HD and H_3 from contributing significantly to the ^{3}He height. The sensitivity of ^{3}He was high enough to measure one-tenth

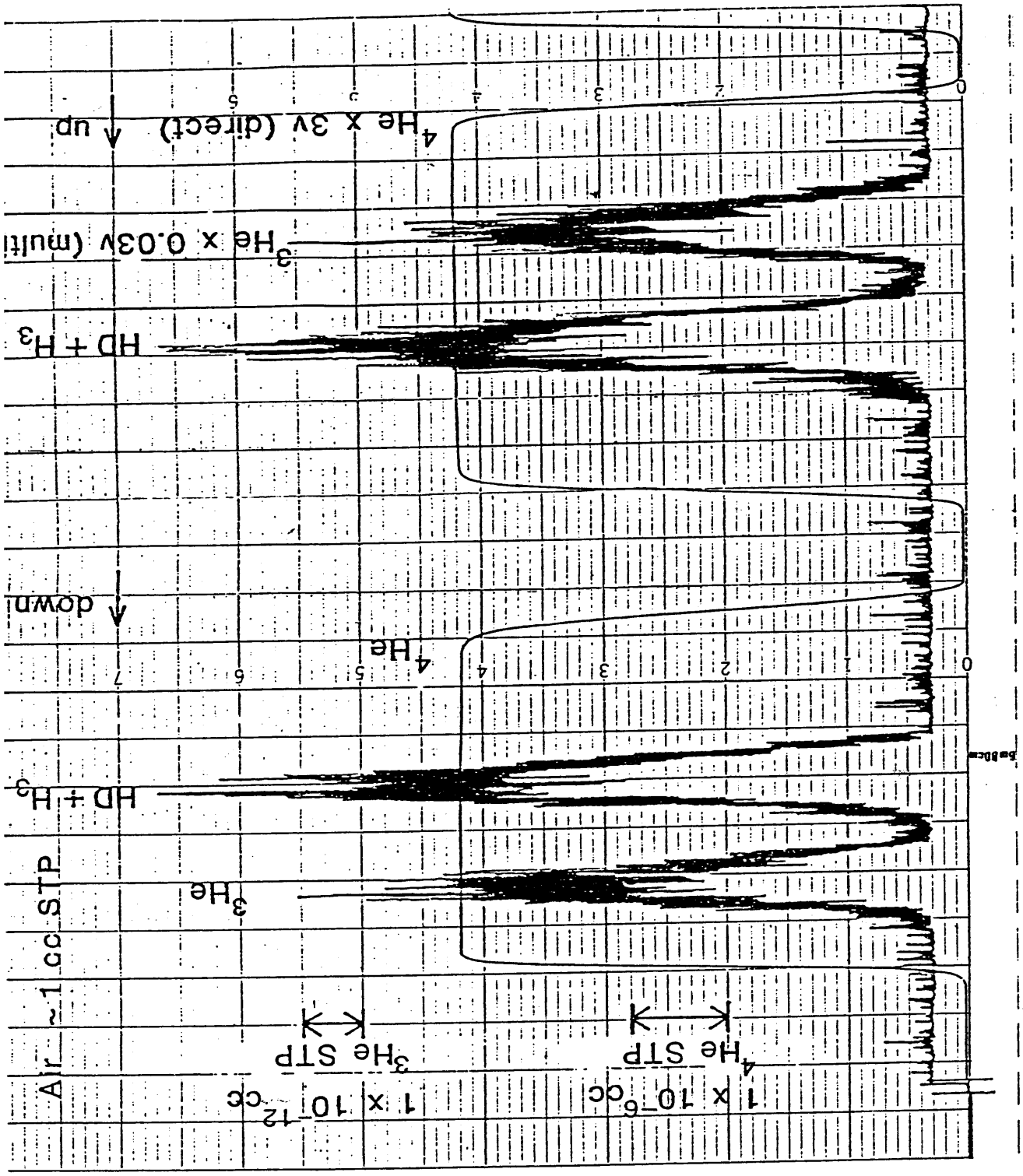

Figure 2-5. A typical mass spectrum of ^{3}He and ^{4}He in the purified He fraction from the atmospheric air of about 1 cc STP. Excellent separation between ^{3}He beams and H_3 plus HD beams is observed. A resolving power of about 600 at 1% peak height and more than 1000 at 50% peak height is attained.

of ^{3}He in the air, which corresponds to 2 x 10^7 atoms ^{3}He (7 x 10^{-13} cc STP) . Assuming the sensitivity of HD and H_3 in the mass spectrometer to be equal to that of ^{3}He, the amount of H_3 plus HD is estimated to be about 9 x 10^{-12} cc STP, which is sufficiently low in the actual measurements of ^{3}He/^{4}He ratio. The stability of the ^{4}He ion beam was less than 1 % and sufficiently good, while the ^{3}He beam was scanned over a small mass range. The statistical error of an individual run including 5 or 6 sets of scanning is about 2 % for ^{3}He/^{4}He ratio. Reproducibility of 3 % was obtained for beam intensities of both ^{3}He and ^{4}He from 7 individual runs in 2 weeks at the levels of 7 x 10^{-12} and 5 x 10^{-6} cc STP, respectively.

Correction for mass discrimination in the ^{3}He/^{4}He ratio was made by the following formula:

$$(^3\mathrm{He}/^4\mathrm{He})_{corr.} = (^3\mathrm{He}/^4\mathrm{He})_{obs.}/(1 + d/100)$$

where $(^3\mathrm{He}/^4\mathrm{He})_{corr.}$ and $(^3\mathrm{He}/^4\mathrm{He})_{obs.}$ denote the corrected ^{3}He/^{4}He and observed ^{3}He/^{4}He ratio, and d the discrimination factor of 21.8 %. Beam intensities of ^{3}He and ^{4}He are summarized in Table 2-1 together with the observed and corrected ^{3}He/^{4}He ratios. The mean value of the corrected ^{3}He/^{4}He ratio in Tokyo air is (1.43 $\pm$ 0.03) x 10^{-6}, which agrees well with the value of (1.399 $\pm$ 0.013) x 10^{-6} in Leningrad air reported by Mamyrin et al. (1970).

i) Time variation and pressure dependence of the ^{3}He/^{4}He ratio

It is well known that isotopic ratios of some rare

Table 2-1. Reproducibility of the $^3He/^4He$ measurements

No.	^3He ($\times 10^{-2}$ V)	^4He ($\times$ 1 V)	$(^3He/^4He)_{obs.}$ ($\times 10^{-6}$)	$(^3He/^4He)_{corr.}$ ($\times 10^{-6}$)
1	1.06	1.64	1.08	1.38±0.03
2	1.01	1.50	1.12	1.43±0.03
3	1.07	1.58	1.14	1.46±0.04
4	1.13	1.65	1.14	1.46±0.02
5	1.08	1.65	1.10	1.41±0.02
6	1.10	1.65	1.11	1.42±0.03
7	1.13	1.68	1.12	1.43±0.04
av.	1.08	1.62	1.12	1.43±0.03

gases, such as $^{40}Ar/^{36}Ar$ ratio, often vary with time during measurement due to the memory effects and the pumping effects of ion source in a mass spectrometer. In this study, even when the ion accelerating voltage is settled, the observed intensities of ^{3}He and ^{4}He ion beams vary with time. Figure 2-6 and Table 2-2 show the time dependence of the $^{3}He/^{4}He$ ratio of atmospheric air during the period between the starting time, when the ion-accelerating voltage was set at 2.5 kV, and 100 minutes later. As seen in the figure, $^{3}He/^{4}He$ ratio is almost constant for the first 30 minutes, but after 30 minutes, it seems to increase with time. The reason may be the pumping effects of the ion source, as indicated by the decreasing of ^{4}He ion beams. Practically, $^{3}He/^{4}He$ ratio measurements for the actual sample terminate within the first 30 minutes, so that this effect is not serious in the measured $^{3}He/^{4}He$ ratios.

Figure 2-7 and Table 2-3 show the relation between the $^{3}He/^{4}He$ ratio of the atmosphere and total pressure in the mass spectrometer. The pressure differed by almost 2 orders of magnitude, ranging from 3.2×10^{-6} Torr to 4.2×10^{-8} Torr. In the pressure range lower than 1×10^{-6}, the $^{3}He/^{4}He$ ratio was almost constant. On the other hand, a remarkable increase in the $^{3}He/^{4}He$ ratio (about 15 %) was observed in the pressure range higher than 1×10^{-6} Torr. This is attributed to the sensitivity depression of ^{4}He ion beam in the mutual electrostatic repulsion of $^{3}He^{+}$ ions due to the space charge effect. In actual measurements of samples, the

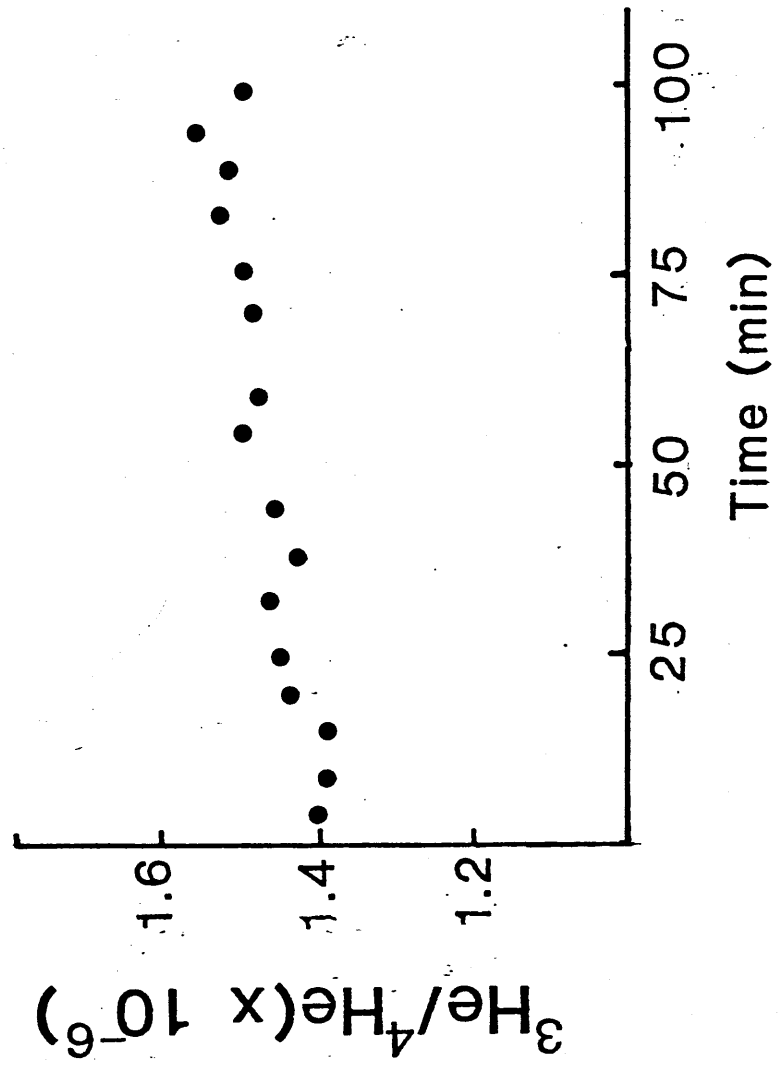

Figure 2-6. Time dependence of the $^3He/^4He$ ratios of atmospheric air during the period between the starting time and 100 minutes in the mass spectrometer. Though the 3He/4He ratio is almost constant for the first 30 minutes, the ratio seems to increase with time.

Table 2-2. Time variations in the $^{3}He/^{4}He$ ratios

No.	Time (min)	$^{3}He/^{4}He$ ($\times 10^{-6}$)
1	4	1.41
2	8	1.39
3	15	1.39
4	20	1.44
5	25	1.45
6	32	1.47
7	38	1.43
8	44	1.46
9	54	1.50
10	59	1.48
11	70	1.49
12	75	1.50
13	83	1.53
14	89	1.52
15	94	1.56
16	99	1.50

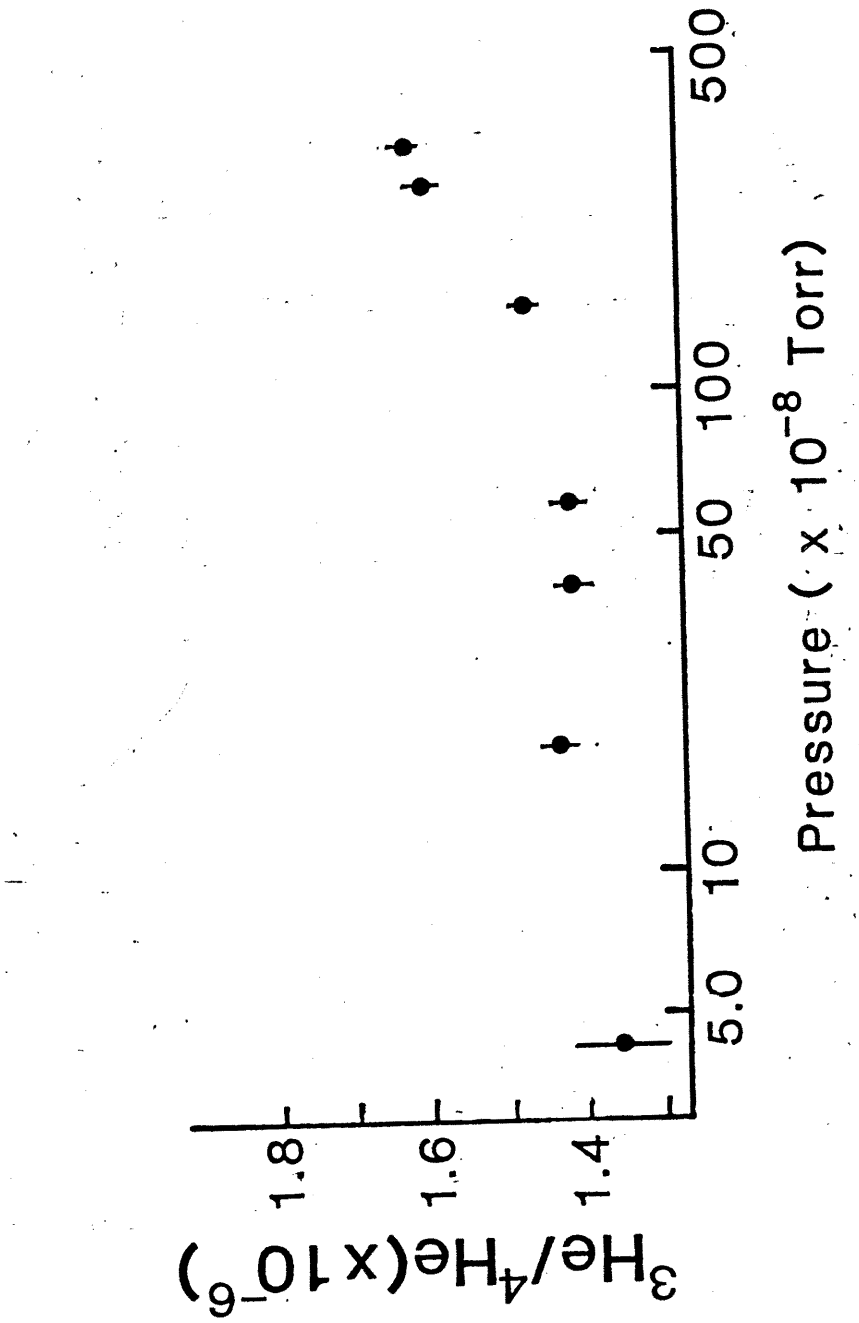

Figure 2-7. Pressure dependence of the atmospheric $^3He/^4He$ ratios in the mass spectrometer. In the pressure range lower than $1x10^{-6}$, the $^3He/^4He$ ratio is almost constant, whereas in the range higher than $1x10^{-6}$ Torr, a remarkable increase in $^3He/^4He$ ratio is observed.

Table 2-3. Pressure dependence of the $^3He/^4He$ ratio

No.	Pressure ($\times 10^{-8}$ Torr)	$^3He/^4He$ ($\times 10^{-6}$)
1	4.3	1.36±0.25
2	18	1.43±0.17
3	39	1.41±0.09
4	58	1.41±0.03
5	150	1.46±0.04
6	270	1.59±0.03
7	330	1.62±0.04

total pressure of the He and Ne fractions in the mass spectrometer was controlled to lower than 1.0×10^{-6} Torr.

To summarize: a measuring method for $^{3}He/^{4}He$ and $^{20}Ne/^{4}He$ ratios in gas and water samples was established. The accuracy and precision of measurements were examined by analyzing atmospheric air in Tokyo. The results indicate that the present method can be applicable to a routine analysis of the $^{3}He/^{4}He$ ratio in gas and water samples.

2.1.2 Rare gas isotopic measurements with a Quadrupole mass spectrometer

a) Purification procedure for all rare gases

Elemental abundances and isotopic ratios of He, Ne, Ar, Kr and Xe (except for ^{3}He, ^{78}Kr, ^{124}Xe and ^{126}Xe) in natural samples were measured with a conventional quadrupole mass spectrometer (QMS) equipped with a secondary electron multiplier. The QMS was connected to a metallic purification line with an ultra-high-vacuum flexible tube (Fig. 2-8). All parts of the line were heated to about 150°C for outgassing and evacuated with an oil diffusion pump (O.D.P) and a sputter ion pump (I.P.) prior to individual analysis. The pressure range in the purification line was about 1×10^{-8} Torr.

The purification procedures of rare gases in gas samples

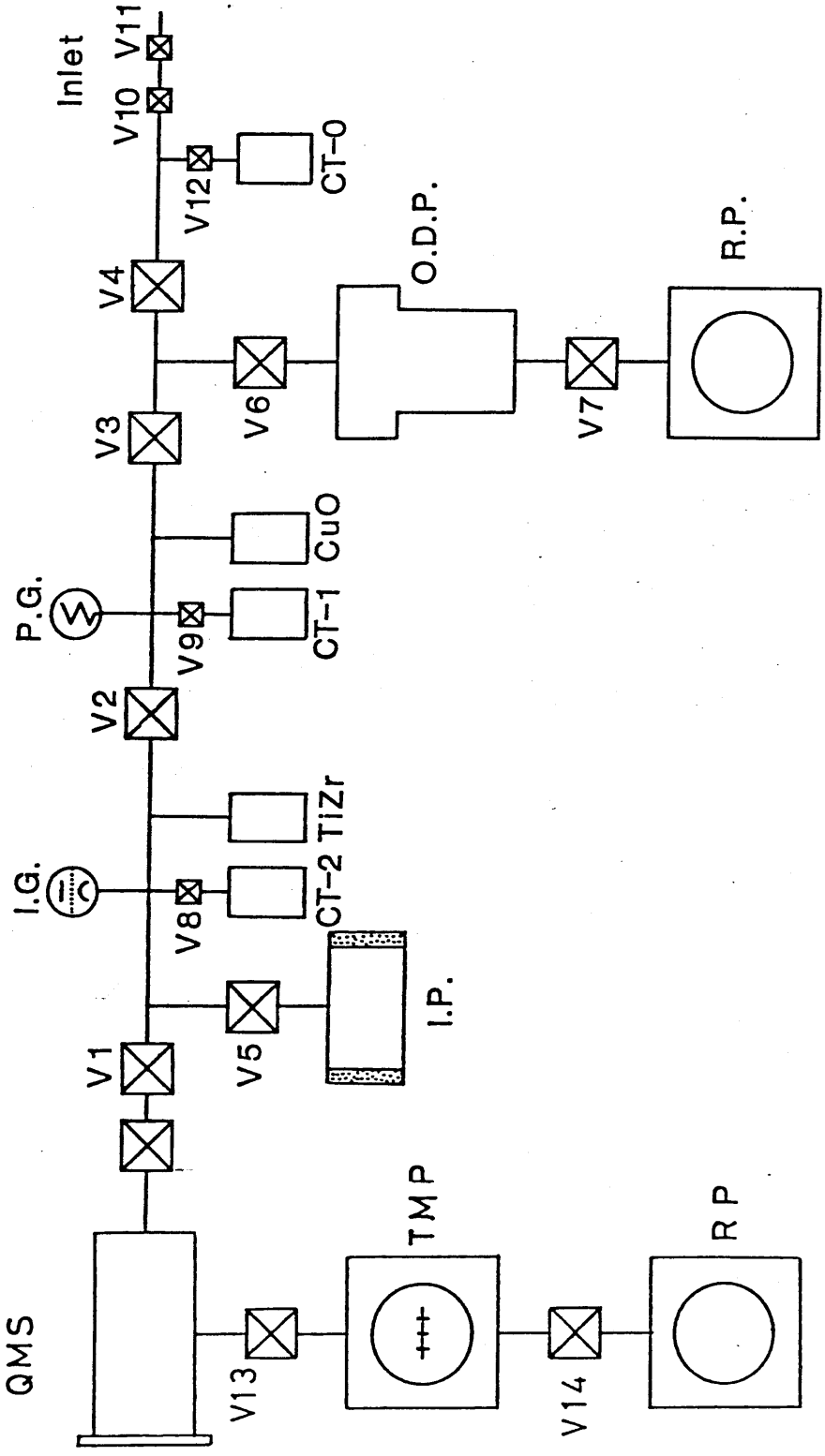

Figure 2-8. Schematic diagram of a rare gas purification line and QMS system. V: valves, ODP: oil diffusion pump, RP: rotary pump, CuO: copper oxide furnace, CT: charcoal trap, P.G.: pirani gauge, TiZr: titanium zirconium getter, I.G.: ionization gauge, I.P.: sputter ion pump, QMS: quadrupole mass spectrometer, and TMP: turbo-molecular pump.

were as follows. During the experimental procedure, a valve (V12) was closed, and charcoal trap (CT-0) was not used. Sample gas introduced into the inlet pipette (volume between valves V10 and V11) was expanded to the region 1. In order to decompose H_2, CH_4 and other hydrocarbons in the original samples, a CuO furnace (CuO) was heated up to 450°C. For CH_4-rich samples, complete combustion was attained by increasing the temperature of the furnace to 600°C. During the combustion, charcoal trap (CT-1) was cooled by liquid N_2 to adsorb N_2, O_2, H_2O, H_2S and heavier rare gases such as Ar, Kr and Xe. After the pressure had reached the range below 0.003 Torr, V9 was closed to keep gases in the trap. Non-adsorbed gases, including He, Ne and small portion of active gases, were transferred to region 2. Similar purification was repeated using charcoal trap (CT-2). Then the purified He and Ne fraction was admitted to the QMS. During the measurement of elemental abundances of ^4He and ^{20}Ne and Ne isotopic ratios of $^{20}Ne/^{22}Ne$ and $^{21}Ne/^{22}Ne$, valves V1, V8 and V13 were kept opened and CT-2 was working to adsorb accidently produced Ar and CO_2 as the memory of the QMS.

After the measurements, He and Ne fractions was evacuated, and CT-1 and CT-2 were heated at about 100°C to release adsorbed gases; a TiZr getter furnace (TiZr) was simultaneously heated to approximately 850°C for 50 minutes to adsorb active species. While the TiZr was cooled, Ar was separated from Kr and Xe by cooling traps CT-1 and CT-2 in

dry ice alcohol baths. Then Ar fraction was admitted to the QMS and the amount of ^{36}Ar and the isotopic ratios of $^{38}Ar/^{36}Ar$ and $^{40}Ar/^{36}Ar$ were measured. If the total pressure of the QMS exceeded 1×10^{-5} Torr, the gas in the QMS (volume between V13 and V14) was evacuated prior to measurement. Then the gas in the space between V13 and V1 was allowed to expand to the QMS (the volumes of V1-V13 and V13-V14 are about 30 and 1000 cc, respectively).

After the Ar measurement, Kr and Xe were released from traps CT-1 and CT-2 by heating them at 100°C. At that time the TiZr furnace was heated to approximately 850°C for 30 minutes to adsorb the remaining active gases. Then the fraction containing Kr and Xe was admitted to the QMS. CT-1 and CT-2 were kept at a temperature of about 100°C while the amounts of ^{84}Kr and ^{132}Xe and isotopic ratios of Kr and Xe were measured. The total time required for the purification and measurement of a single sample was about 6 hours.

b) Quadrupole mass spectrometer for rare gas analysis

A Quadrupole mass spectrometer (QMS) has many advantages over a magnetic deflection mass spectrometer in gas analysis. Some of those are simplicity of operation and maintenance of the instrument, a high scanning rate covering a wide range of mass numbers and a low price. Since the first development of QMS in 1953 (Paul and Steinwedel, 1953), there have not been many papers reporting rare gas measurements because of the lower sensitivity and inferior reproducibility of the QMS. The work of Matsubayashi et al.

(1978) was one of the few studies of elemental abundances of rare gases and isotopic ratios of Ar in fumarolic gases. Practically no attempt has been made to use a QMS for measurements of isotopic ratios of rare gases, including Kr and Xe. In this study a method using a QMS was established to determine both elemental and isotopic abundances of rare gases in terrestrial natural gases.

The spectrometer assembly, including the ion source, quadrupole electrode and secondary electron multiplier, was a conventional version of the Nihon Shinku Gijutsu Company (Kanagawa, Japan) model MSQ-150A quadrupole mass spectrometer. The mass spectrometer was evacuated by a 100 l/s turbo molecular pump equipped with a rotary pump as a fore pump (Figure 2-8). The pressure in the spectrometer was about 3×10^{-9} Torr in dynamic condition.

The ion source was a Pierce type using electron bombardment with no source magnet. The electron accelerating potential was 70 V. After ionization, positive ions of rare gases were removed from the source region and accelerated by a potential of 12 V in the ion lens system. The quadrupole electrode part corresponded to the analyzer tube of the magnetic deflection mass spectrometer. In step four electrodes of column shapes were arranged parallel to each other. The facing two electrodes were connected and the voltage of them were piling up alternatively. Ions in the space between the electrodes were vibrating depending on their mass; the limited ions with special vibration were

permitted to pass through the quadrupole electrode part while other ions were colliding with the electrode and could not pass through. The ion beam was generally detected by using the secondary electron multiplier. When the ion current was sufficiently large, the first electrode of the multiplier was used as a direct collector. These detectors were connected to a D.C. amplifier. The secondary electron multiplier was used at 2 kV, and the total gain of the multiplier over the Farady cup was 5.5×10^5.

c) Data collection and processing

The output of the D.C. amplifier system was displayed on an oscilloscope, a chart recorder and simultaneously fed to a digital voltmeter (Hewlett-Packard Model 3456A). The digital data were transferred to a desktop computer (Hewlett-Packard Model 9825A) by GP-IB (IEEE-488) and accumulated in its memory. The data were continuously collected during the scan of mass number, and about 100 data by one mass number were obtained for all rare gases. In order to cover mass numbers from 124 to 136, 1200 data were collected for Xe. Although the flat peak-top could not be obtained mainly due to the characteristics of the QMS, about 10 digital data were obtained at the peak position of each mass. After taking the running average of the data for smoothing, numerical differentiation was made. The peak height of each mass number was searched for using polar values and accumulated in the memory. An individual run included ten sets of scanning. About 6 minutes was required

to complete a run for Ne and about 24 minute for Xe. These times were short enough to avoid the memory effect of the measuring system and the pumping effect of the ion source.

d) Atmospheric rare gas as a secondary standard

In order to examine the reproducibility and sensitivity of the measurements, one pipette of atmospheric air of about 1 cc STP was introduced into the purification line. The purified and separated rare gases were repeatedly measured by the QMS. The results are shown in Table 2-4. The 8 repeat runs in three weeks demonstrate the reproducibility of measurements as 10 - 20 % for ^{4}He, ^{20}Ne, ^{36}Ar, ^{84}Kr and ^{132}Xe. Sensitivities for ^{4}He, ^{20}Ne, ^{36}Ar, ^{84}Kr and ^{132}Xe were 0.21, 0.41, 2.1, 1.3 and 0.62 A/cc STP, respectively. The apparent lower sensitivity of ^{36}Ar is attributed to the different detection conditions: ion currents of ^{4}He, ^{20}Ne, ^{84}Kr and ^{132}Xe were measured by a secondary electron multiplier, whereas that of ^{36}Ar was by a Farady cup.

Isotopic ratios of Ne and Ar observed in the atmospheric air are shown in Table 2-5 together with literature values (Eberhardt et al., 1965; Nier, 1950). Discrepancies of about 4 % and 2 % are observed for $^{20}Ne/^{22}Ne$ and $^{21}Ne/^{22}Ne$ ratios, respectively. On measurement of mass numbers 20 and 22, interferences from double charged ions of $^{44}CO_2^{++}$ and $^{40}Ar^{++}$ produced by contaminants should be taken into account, and the possible appearance of $^{20}H_2O^{+}$ ion should also be considered. However, intensities of ion currents of $^{44}CO_2^{+}$ and $^{40}Ar^{+}$ were less than 1 % of $^{20}Ne^{+}$ and $^{22}Ne^{+}$ in the

Table 2-4. Reproducibility of rare gas measurements by a QMS

No.	^{4}He ($\times10^{-6}$A)	^{20}Ne ($\times10^{-6}$A)	^{36}Ar ($\times10^{-5}$A)	^{84}Kr ($\times10^{-6}$A)	^{132}Xe ($\times10^{-8}$A)
1	1.0	8.5	3.2	1.5	3.0
2	0.96	6.6	2.6	2.2	4.1
3	0.94	6.2	2.9	1.7	3.3
4	0.92	6.2	3.0	1.8	2.9
5	0.88	5.0	2.7	1.7	3.1
6	0.94	5.3	2.9	1.8	4.0
7	1.1	6.1	3.3	1.8	3.5
8	1.0	5.7	2.6	1.9	3.5
av.	0.97±0.06	6.2±1.1	2.9±0.3	1.8±0.2	3.4±0.4

Table 2-5. Isotopic ratios of atmospheric Ne and Ar by a QMS

	obs.	ref.	accuracy (%)	precision (%)
$^{20}Ne/^{22}Ne$	10.07±0.03	9.80	+2.8	±0.3
$^{21}Ne/^{22}Ne$	0.0295±0.0004	0.0290	+1.6	±1.4
$^{38}Ar/^{36}Ar$	0.188±0.001	0.187	+0.5	±0.5
$^{40}Ar/^{36}Ar$	291.0±2.1	295.6	-1.6	±0.7

Table 2-6. Isotopic ratios of atmospheric Kr by a QMS

	obs.	ref.	accuracy (%)	precision (%)
$^{78}Kr/^{84}Kr$	0.735±0.005	0.609	+21	±0.7
$^{80}Kr/^{84}Kr$	4.04±0.08	3.96	+0.5	±2.0
$^{82}Kr/^{84}Kr$	20.4±0.1	20.22	+0.6	±0.5
$^{83}Kr/^{84}Kr$	20.2±0.1	20.16	+0.2	±0.5
$^{86}Kr/^{84}Kr$	29.8±0.1	30.55	-2.5	±0.3

Table 2-7. Isotopic ratios of atmospheric Xe by a QMS

	obs.	ref.	accuracy (%)	precision (%)
$^{128}Xe/^{132}Xe$	7.42±0.20	7.14	+3.9	±2.7
$^{129}Xe/^{132}Xe$	99.5±0.7	98.32	+1.2	±0.7
$^{130}Xe/^{132}Xe$	15.7±0.4	15.14	+3.6	±2.2
$^{131}Xe/^{132}Xe$	79.7±0.4	78.90	+1.0	±0.5
$^{134}Xe/^{132}Xe$	39.3±0.3	38.79	+1.3	±0.8
$^{136}Xe/^{132}Xe$	32.2±0.5	32.93	-1.9	±1.5

present measurement. Judging from the low production rates of observed $^{40}Ar^{++}/^{40}Ar^{+}$ and $^{44}CO_2^{++}/^{44}CO_2^{+}$ in a cold blank (less than 5 % and 1 %, respectively) and the low ratio of $^{20}H_2O^{+}/^{18}H_2O^{+}$ (about 0.2 %) in the measurement, the above-mentioned interference is inferred to be negligibly small. Therefore, no correction was made for ^{20}Ne and ^{22}Ne measurements. The observed $^{21}Ne/^{22}Ne$ ratio coincides with the literature value within the two sigma value of experimental error, but the $^{20}Ne/^{22}Ne$ ratio is outside the recommended values. The discrepancy may be attributed to a mass discrimination effect in the secondary electron multiplier.

On ^{36}Ar and ^{38}Ar measurements, possible interference due to the filament material has to be considered. Ion currents of mass numbers 36 and 38 in the static background were less than 0.1 % of those for the actual sample, so that such contribution can be neglected in the actual sample analysis. The observed $^{40}Ar/^{36}Ar$ and $^{38}Ar/^{36}Ar$ ratios coincide well with literature values within experimental margins of error.

Mass spectra of purified Kr and Xe in the atmospheric air are shown in Figures 2-9 and 2-10, respectively. As seen in these figures, desirable peak shapes with flat peak-tops could not be obtained, mainly due to a characteristic of the QMS. However, sensitivity was high enough to detect all stable isotopes of Kr, including ^{78}Kr, ^{80}Kr, ^{82}Kr, ^{83}Kr, ^{84}Kr and ^{86}Kr, using 1 cc STP of atmospheric air. Xe has nine stable isotpes: ^{124}Xe, ^{126}Xe, ^{128}Xe, ^{129}Xe, ^{130}Xe, ^{131}Xe,

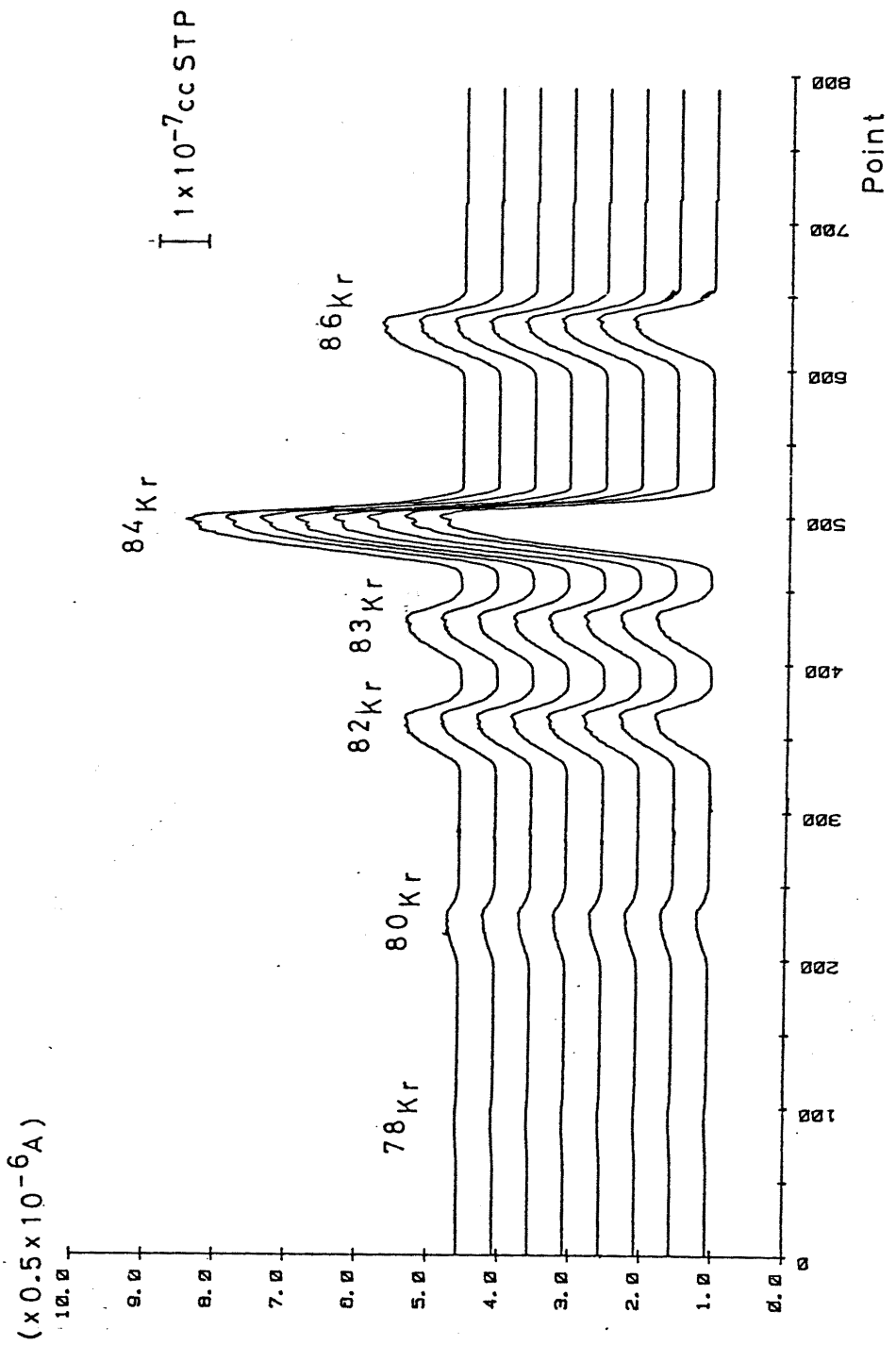

Figure 2-9. Mass spectrum of about 1 cc STP of purified Kr of the atmospheric air. Desirable peak shapes with flat peak-top cannot be obtained mainly due to a characteristic of the QMS; however, all stable isotopes of Kr, including ^{78}Kr, ^{80}Kr, ^{82}Kr, ^{83}Kr, ^{84}Kr and ^{86}Kr, are observed. All the isotopes are detected in the range of $5x10^{-7}$ A.

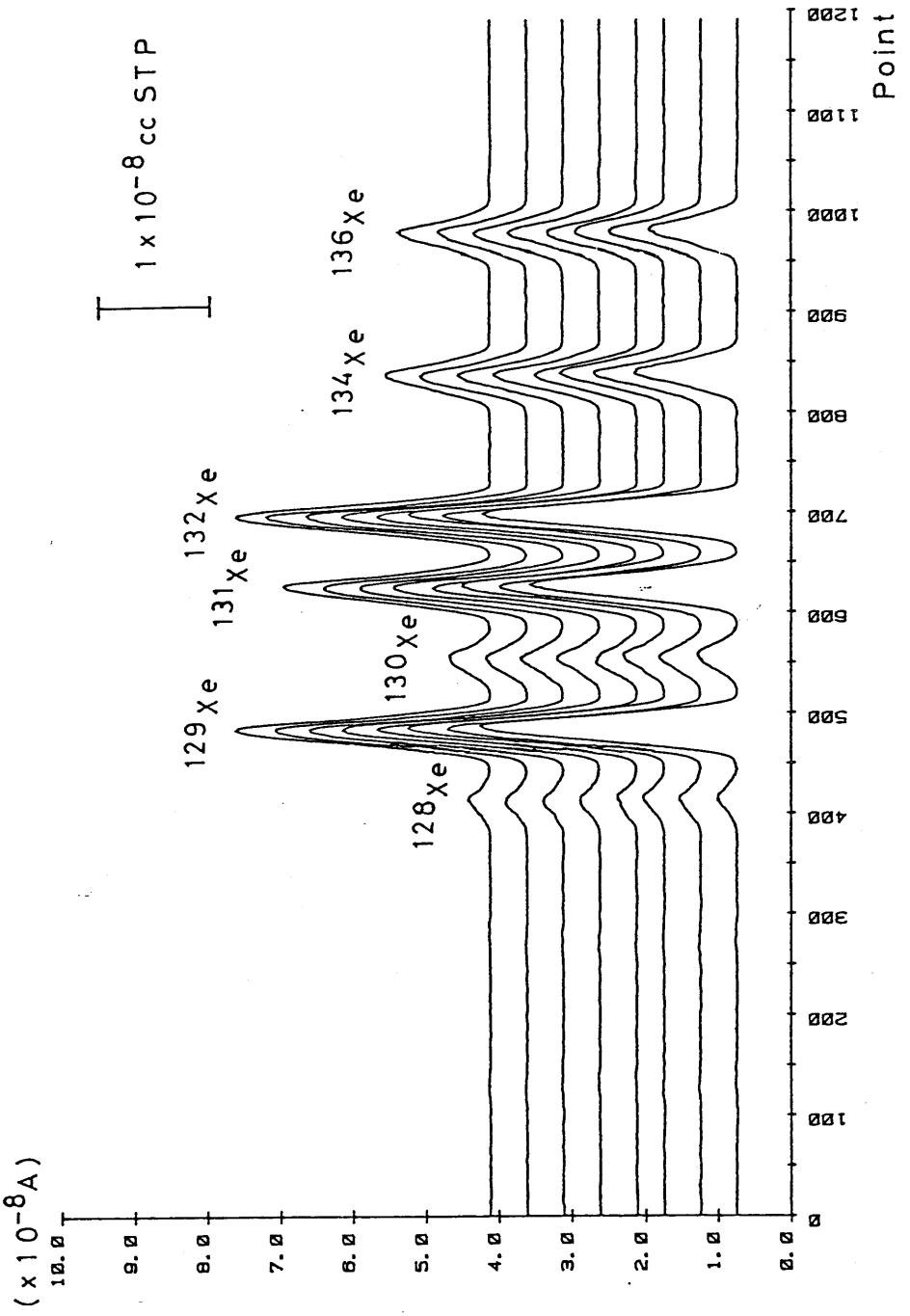

Figure 2-10. Mass spectrum of about 1 cc STP of purified Xe of the atmospheric air. The running average of the digital data is taken for smoothing. Seven stable isotopes of Xe, including ^{128}Xe, ^{129}Xe, ^{130}Xe, ^{131}Xe, ^{132}Xe, ^{134}Xe and ^{136}Xe, are observed. ^{124}Xe and ^{126}Xe are not detected in the spectrum in the present system, owing to their low abundances. All the isotopes are detected in the range of 1×10^{-8} A.

^{132}Xe, ^{134}Xe and ^{136}Xe. Of these, ^{124}Xe and ^{126}Xe were not detected in the spectrum (Fig. 2-10) owing to their relatively low abundances.

Isotopic ratios of Kr and Xe observed in the atmospheric air are shown in Table 2-6 and 2-7 together with the literature values (Eugster et al., 1967; Basford et al., 1973). In general observed isotopic ratios agree with literature values within experimental error margins. The $^{78}Kr/^{84}Kr$ ratio in this work is clearly higher than that in the literature, probably due to interference from hydrocarbon with mass number 78.

Consequently, elemental abundances and isotopic ratios of rare gases in gaseous samples can be measured by the present QMS system with experimental errors of about 2 % (except for $^{78}Kr/^{84}Kr$, $^{124}Xe/^{132}Xe$ and $^{126}Xe/^{132}Xe$), if sufficient amounts of rare gases corresponding to 1 cc STP atmospheric air are available in a sample gas.

2.2 Natural gas and thermal water

2.2.1 Sample collection method

Various kinds of gases which emerged from the interior of the earth into the atmosphere were collected for rare gas isotopic analysis. They include bubble gases in hot springs, mineral springs, lakes, ponds, rivers and water wells; methane-rich natural gases in gas fields, petroleum gas in oil fields,volcanic fumaroles and others. Several kinds of collection methods were used, varying with the features of gas discharge. A water sample was also collected. Each method of sample collection is described below.

a) Volcanic fumaroles

A sample container with vacuum cocks on both ends was used for the collection of volcanic fumaroles. The container was made of pyrex glass, and the inside volume was about 100 cc. A manual pump, pyrex glass tube and thick wall tygon tubes were prepared. At a sampling site, one end of the container was connected to a manual pump the other end to the pyrex glass tube using tygon tubes. The sampling system is shown in Figure 2-11. The end of the glass tube was put into the source of fumarole and the container was purged of air by passing fumarolic gas through it for several minutes using a manual pump. Then both ends of the container were closed with the cocks.

b) Bubble gas in hot springs

A sample container with a vacuum cock on one end was

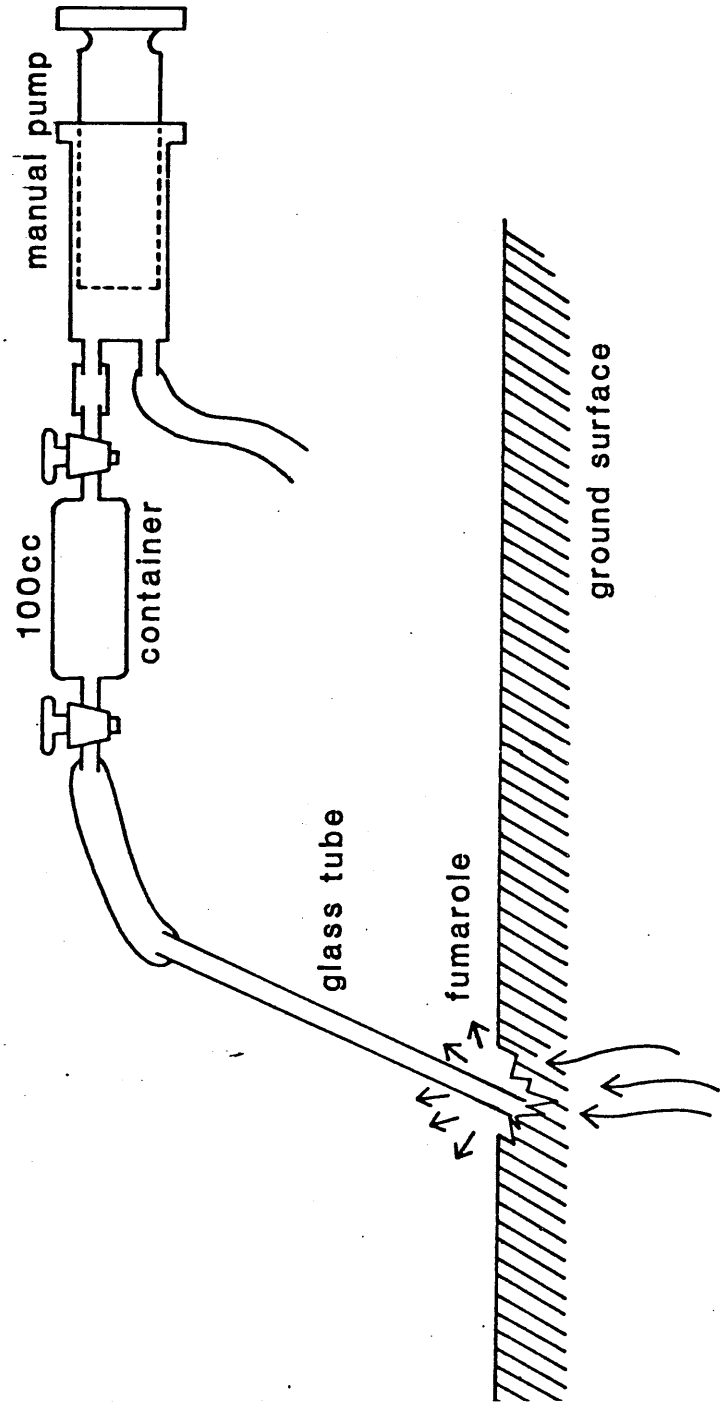

Figure 2-11. A schematic diagram of volcanic fumarole collection. The end of a glass tube is put into the vent of a fumaroles, and air in the container is purged out by passing fumarolic gas using a manual pump.

used for the collection of bubble gas from a hot spring. The container was made of lead glass and the inside volume was about 50 cc. Prior to gas collection in the field, the container was evacuated in the laboratory by a rotary pump and then a sorption pump. The pressure of the container is less than 1×10^{-3} Torr, and the residual gas is negligibly small compared to the actual sample. A funnel made of pyrex glass, a rubber tube and a stainless stand were prepared. At the sampling site, an inverted funnel was connected to the container using a rubber tube. Both container and funnel were fixed by a stainless stand using a metal clamp as shown in Figure 2-12. First the inside of the rubber tube and funnel were filled with spring water and the inverted funnel was placed on the bubbling position in the spring. After the water in the inverted funnel was replaced by gas, the cock of the container was opened. Gas in the funnel was transferred to the container, and when the equilibrium condition was attained, the cock was closed.

c) Bubble gas in mineral springs and water wells

Most samples from mineral springs and water wells were collected by the same method as that used for the collection of hot spring gas. A few samples were collected by another method, in which a sample container with vacuum cocks on both ends was used. The container was made of pyrex glass and the inside volume was about 20 cc. A funnel, manual pump and tygon tube were prepared. At the sampling site, one end of the container was connected to an inverted funnel and the

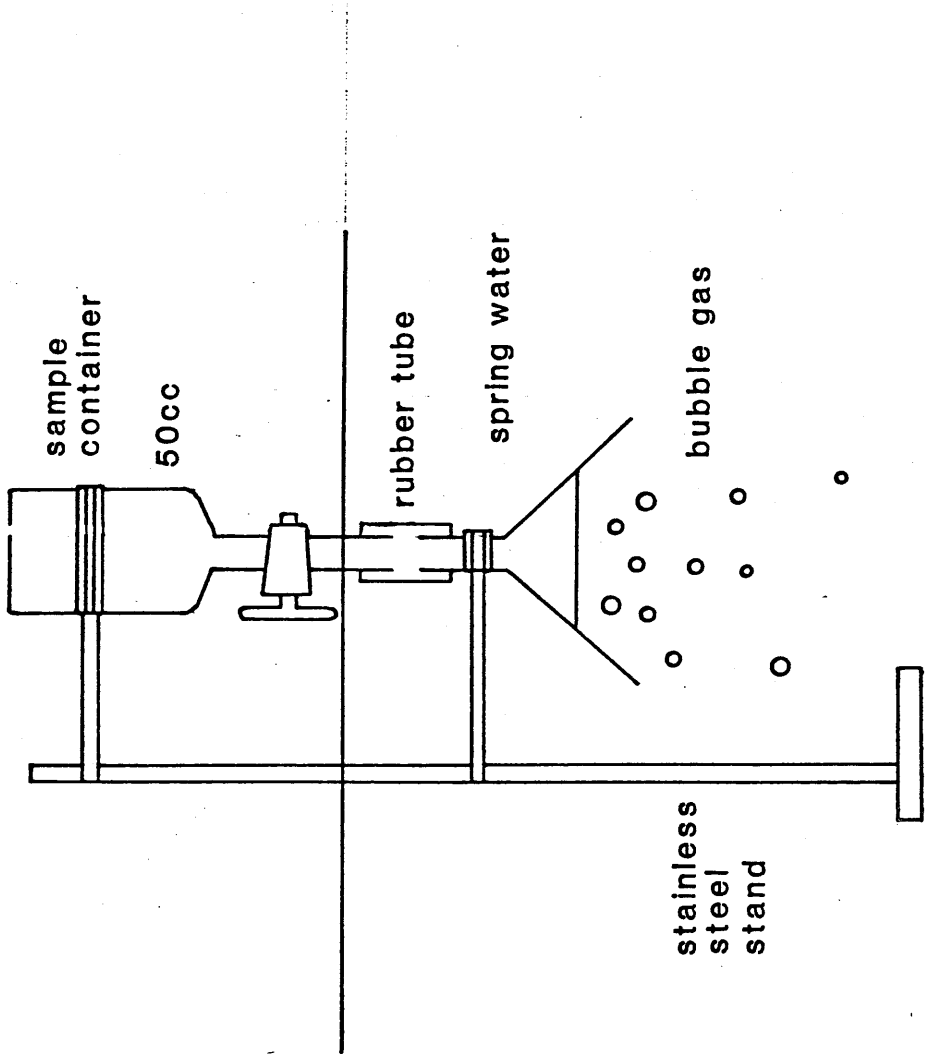

Figure 2-12. The collection of hot spring gases. An inverted funnel connected with a evacuated container is placed on the bubbling position in the spring. Gas in the inverted funnel is introduced into the container.

other end to a manual pump using tygon tubes as shown in Figure 2-13. First the inverted funnel was put into the spring water and the container and tygon tubes were filled with spring water through it using a manual pump. Then the funnel was placed on the bubbling position of the spring. After the water in the funnel was replaced by the gas, the gas in the inverted funnel was transferred into the container by using a manual pump. The inside of the container was flushed several times by passing sample gas through it in order to avoid the atmospheric contamination. Then both ends of the container were closed with the cocks.

d) Fuel gas from oil and gas fields

A sample container with vacuum cocks on both ends was used for the collection of fuel gas from oil and gas fields. The container was made of pyrex glass and the inside volume was about 50 cc. At the sampling site, the container was put into water in a bucket and the inside of the container was filled with water. One end of the container was connected to the gas source using a tygon tube. The valve of the gas source was opened and the water in the container was replaced by natural gas. The container was purged for several minutes by passing the natural gas through it as shown in Figure 2-14. First the outlet cock of the container was closed, then the cock to the gas source. This method of collecting natural gas is almost the same as that used for hot spring gas.

e) Spring water

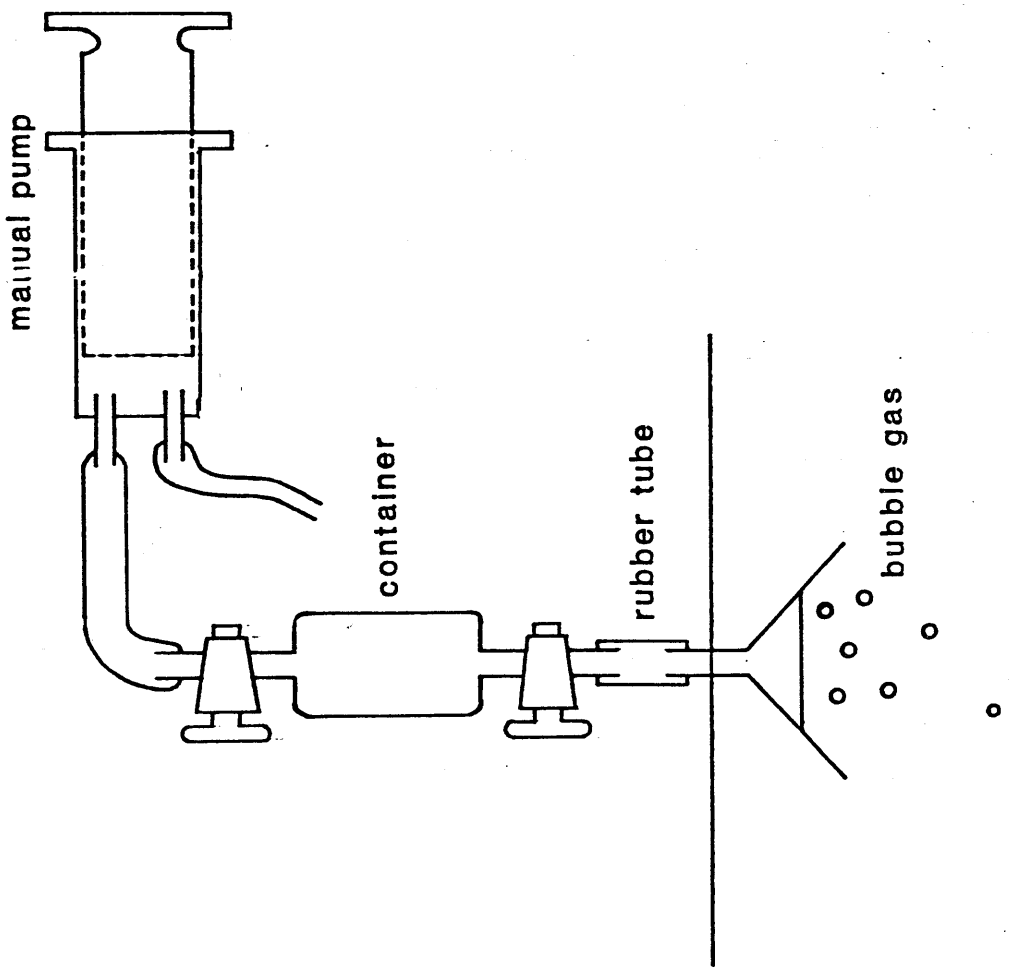

Figure 2-13. The collection of mineral spring and water well gases. Gas in an inverted funnel is transferred into a container using a manual pump. The container is flushed several times by passing sample gas through it to avoid atmospheric contamination.

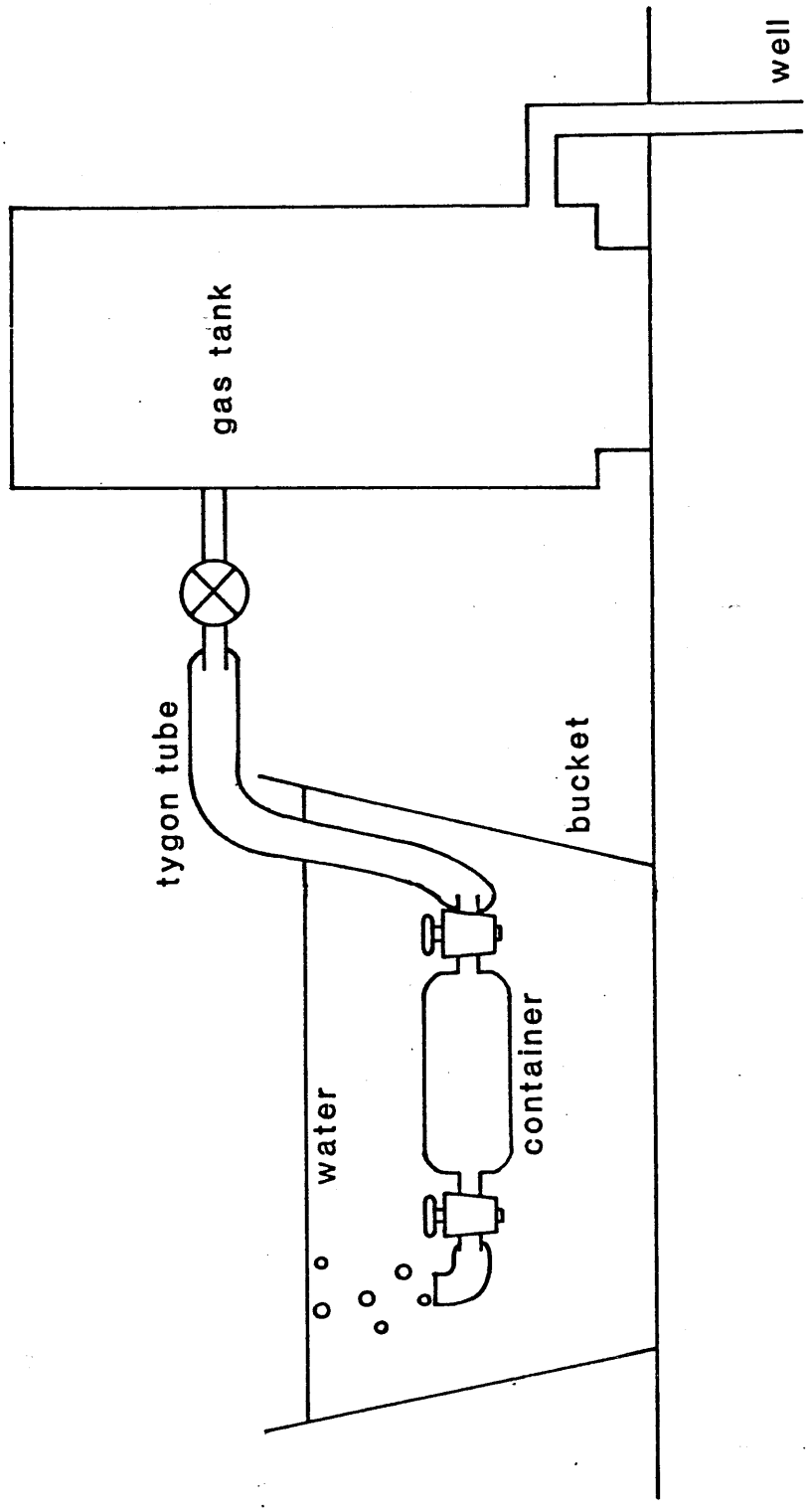

Figure 2-14. The collection of fuel gases from oil and gas fields. One end of the container is connected to the gas source using a tygon tube. The valves are opened for several minutes to purge the content of the container by passing the natural gas.

Collection of a water sample from a spring was limited to self-spouting springs, since in a spring where the water is artificially pumped, the water is generally affected by atmospheric contamination. The same type of sample container as that used for volcanic fumaroles was used for water samples. At the sampling site, one end of the container was connected to a manual pump and the other end to the long tygon tube. The end of the long tube was put as deep into the water of the spring as possible. The container was purged of air by passing spring water through it for several minutes using a manual pump. Then both cocks of the container were closed.

2.2.2 Sampling sites and samples

144 samples, including various kind of gaseous and water samples, were collected at 100 locations in Japan and 10 in Iceland. In order to examine the temporal variation and the spatial distribution of $^3He/^4He$ ratios in a short range of about some 100 m, several samples were collected in a single location but at different sites. The concentration of major chemical components such as CO_2, N_2 and CH_4 in these samples varied significantly from 0 to nearly 100 %. Based on the features of gas emission, water temperature and chemical composition, collected gas samples in Japan were classified into six groups as follows: a) volcanic fumarole, b) hot spring gas, c) mineral spring gas, d) water well gas, e)

methane-rich natural gas from gas fields and f) methane-rich petroleum gas from oil fields.

Sampling locations in the Japanese Islands are shown in Figure 2-15 through Figure 2-21. The sample numbers, codes, and classifications are indicated in Table 2-8. The water temperatures and major chemical components are also listed and referred to by Urabe (1982).

Thermal fluids and geothermal gases in Iceland were collected by Drs Sakai and Chiba using the same methods as those employed in Japan. Locations of sampling sites in Iceland are shown in Figure 2-22. The sample numbers, codes and classifications are listed in Table 2-9 together with the water temperatures.

a) Volcanic fumaroles

Nearly 200 Quaternary volcanoes exist in Japan, and about 30 % of them are active. It is difficult to collect the magmatic gases emitted directly from a volcanic crater. Therefore, fumaroles from smaller gas vents in places where the activity is less violent were collected. Even at a fumarole, the collection of samples uncontaminated by air is impossible. Only few samples of fumarolic gases were collected.

b) Hot spring gas

A hot spring is defined as hot water issuing from underground at a temperature of more than 25° C and containing mineral components. In this study bubble gases in hot springs were collected at over thirty locations. The

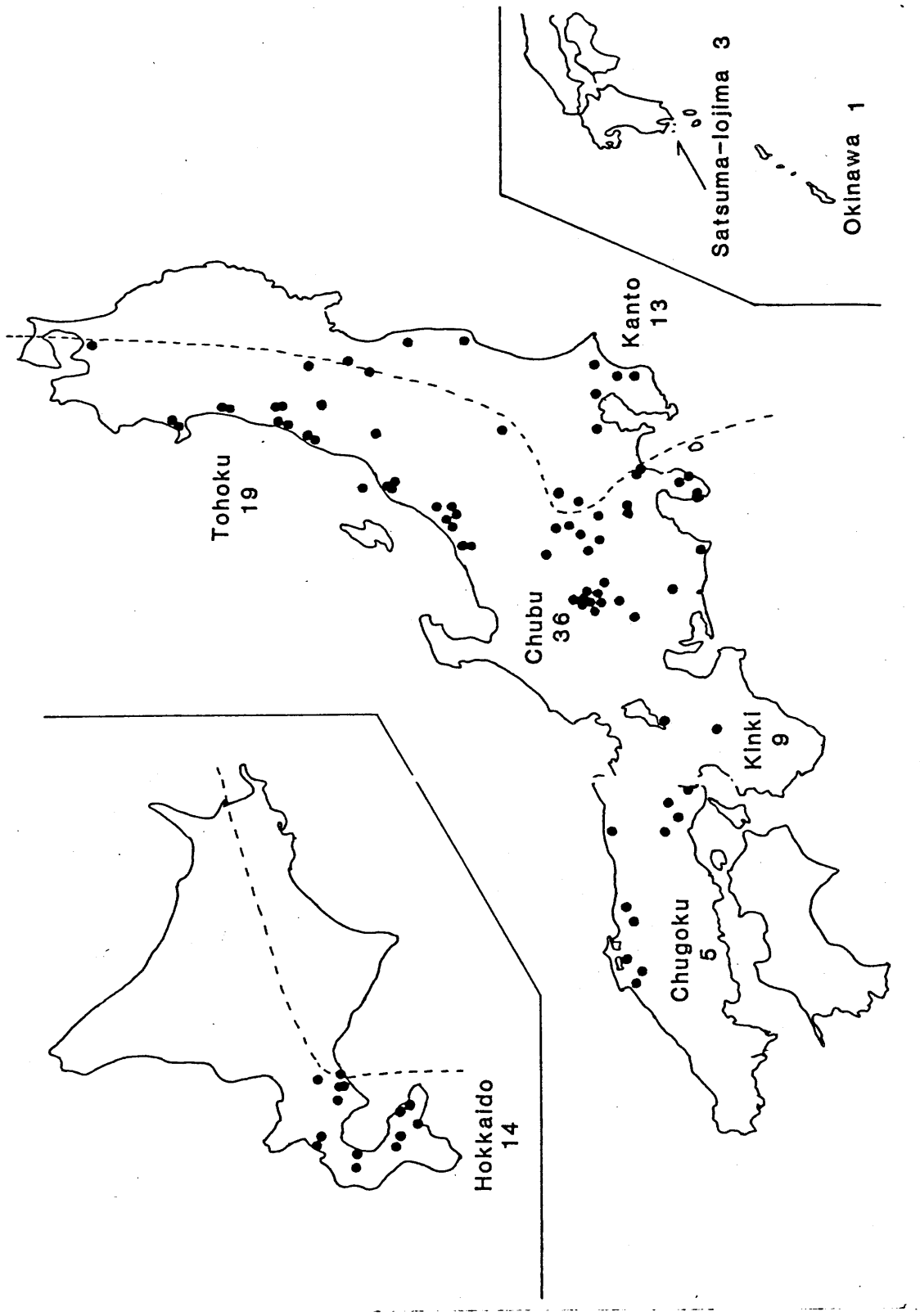

Figure 2-15. Sampling locations in the Japanese Islands. Numerals are numbers of samples.

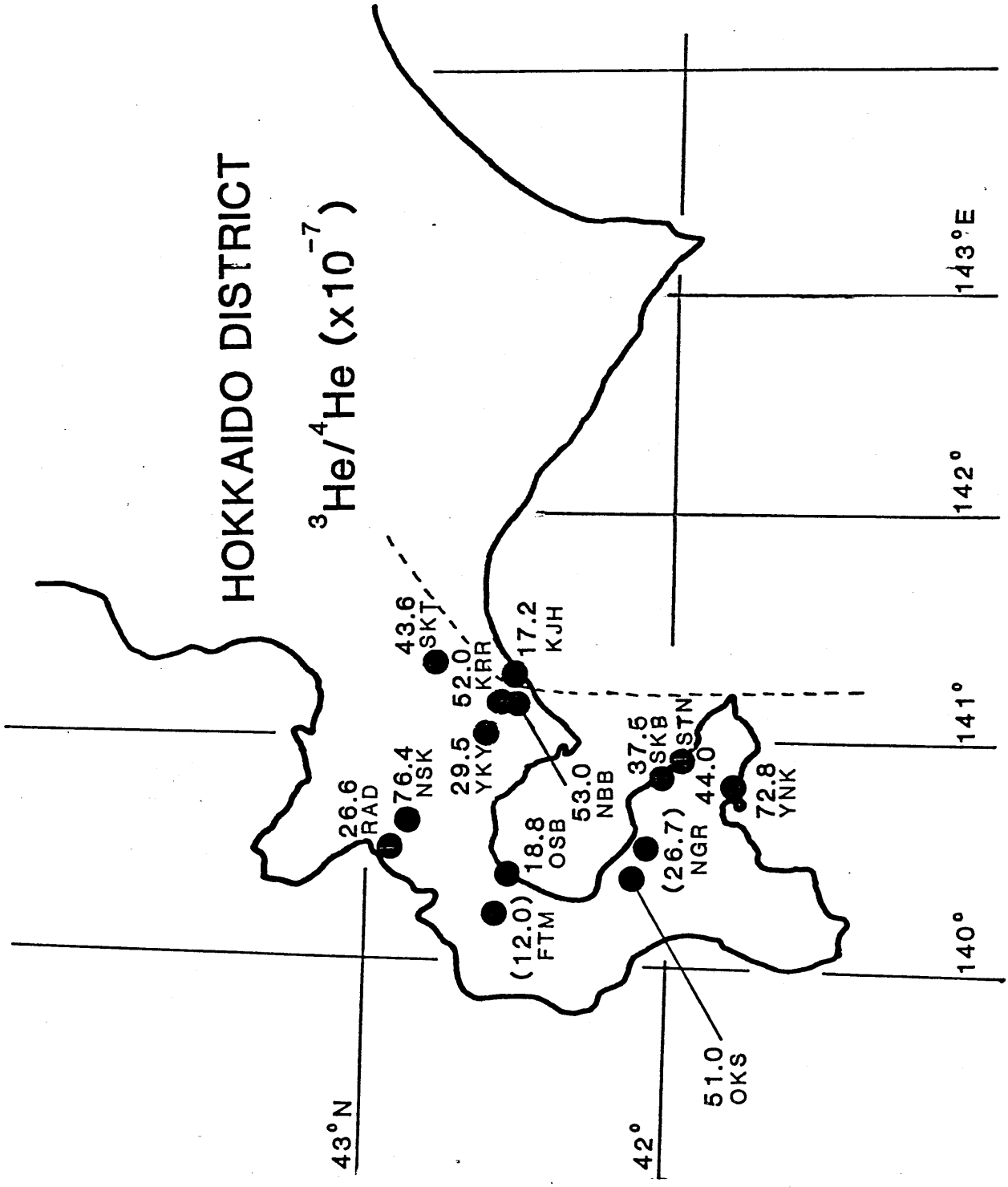

Figure 2-16. Locations of sampling sites in the Hokkaido district and observed $^3He/^4He$ ratios with code names. The unit of the $^3He/^4He$ ratio is expressed as 10^{-7}. Significantly air-contaminated samples are indicated by parentheses around the values.

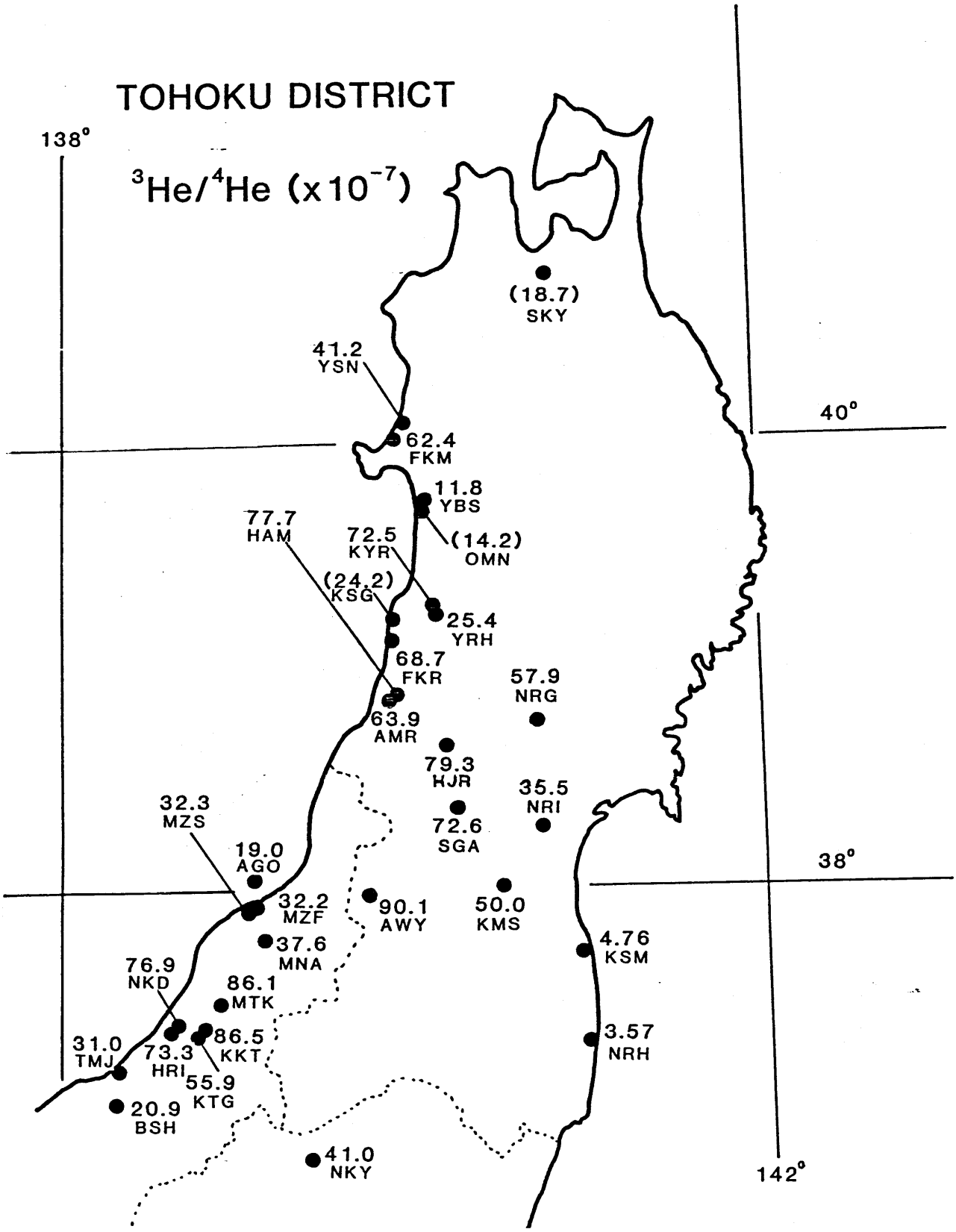

Figure 2-17. Locations of sampling sites in the Tohoku district and observed $^3He/^4He$ ratios with code names. The unit of the $^3H/^4He$ ratio is expressed as 10^{-7}. Siginificantly air-contaminated samples are indicated by parentheses around the values.

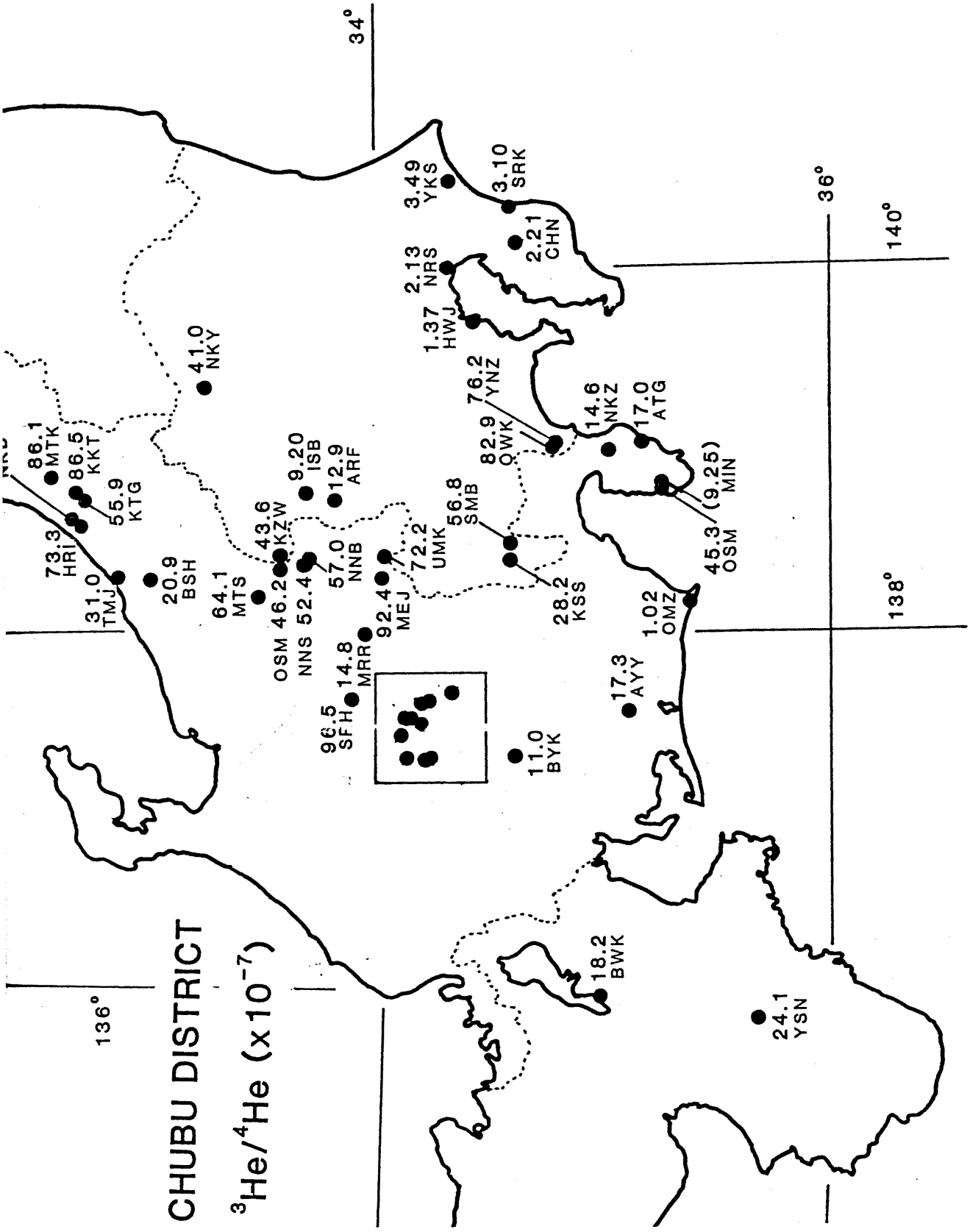

Figure 2-18. Locations of sampling sites in the Kanto and Chubu districts and observed $^3He/^4He$ ratios with code names. The unit of the $^3He/^4He$ ratio is expressed as 10^{-7}. Significantly air-contaminated samples are indicated by parentheses around the values. The $^3He/^4He$ ratios of sites in the area shown in the square are referred to Figure 2-9.

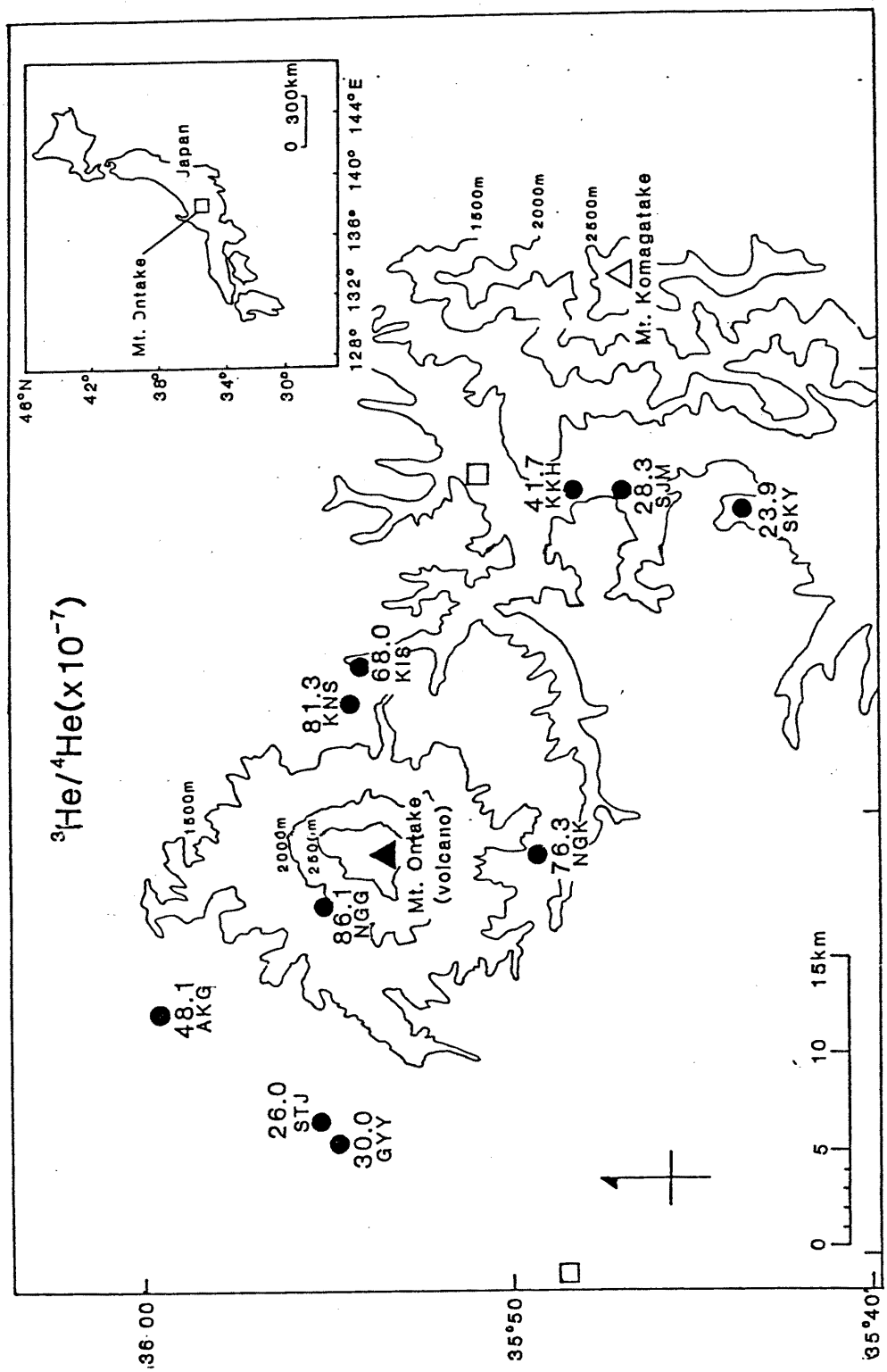

Figure 2-19. Locations of sampling sites around Mt. Ontake and observed $^3He/^4He$ ratios with code names. The unit of the $^3He/^4He$ ratio is expressed as 10^{-7}.

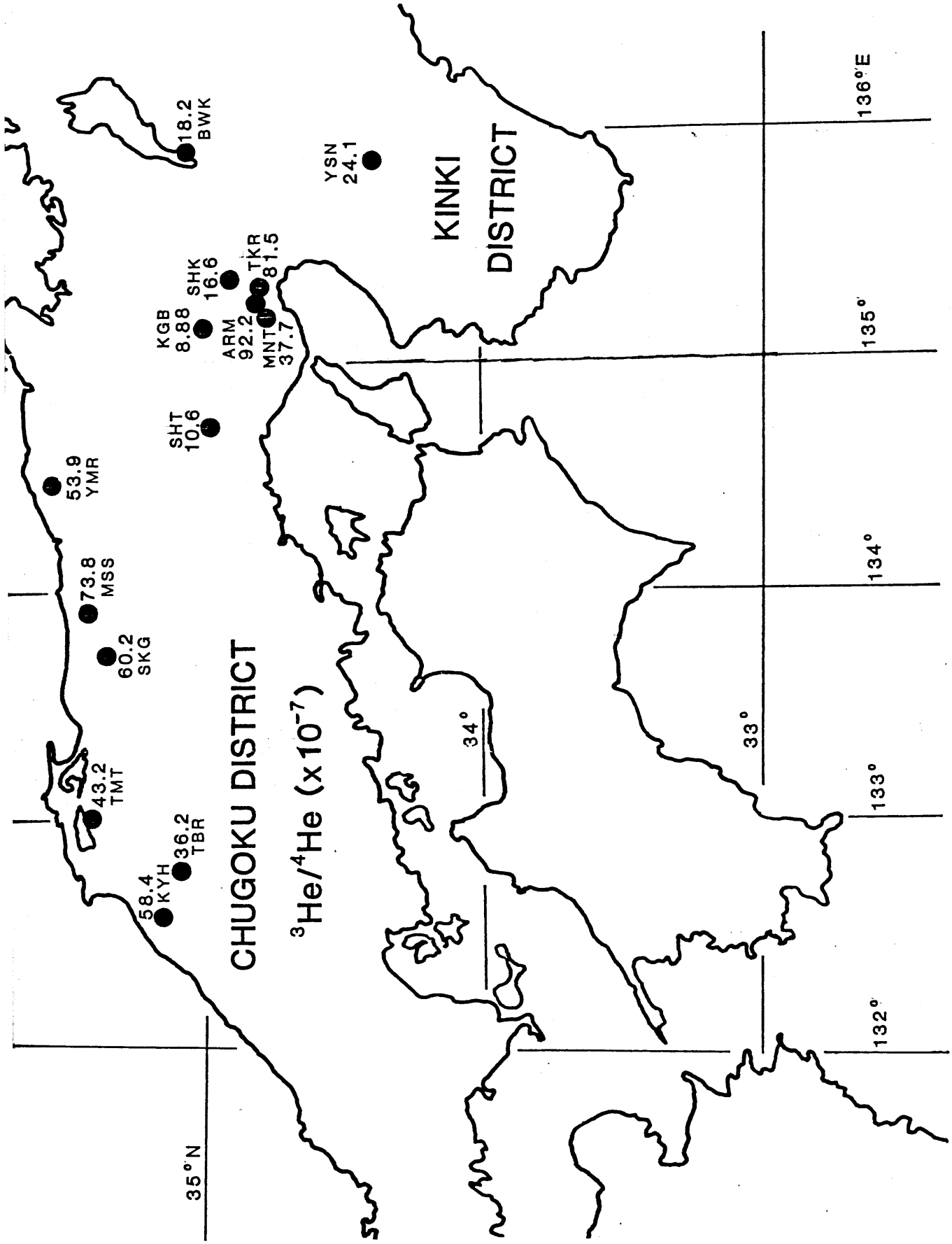

Figure 2-20. Locations of sampling sites in the Kinki and Chugoku districts and observed $^3He/^4He$ ratios with their code names. The unit of the $^3He/^4He$ ratio is expressed as 10^{-7}.

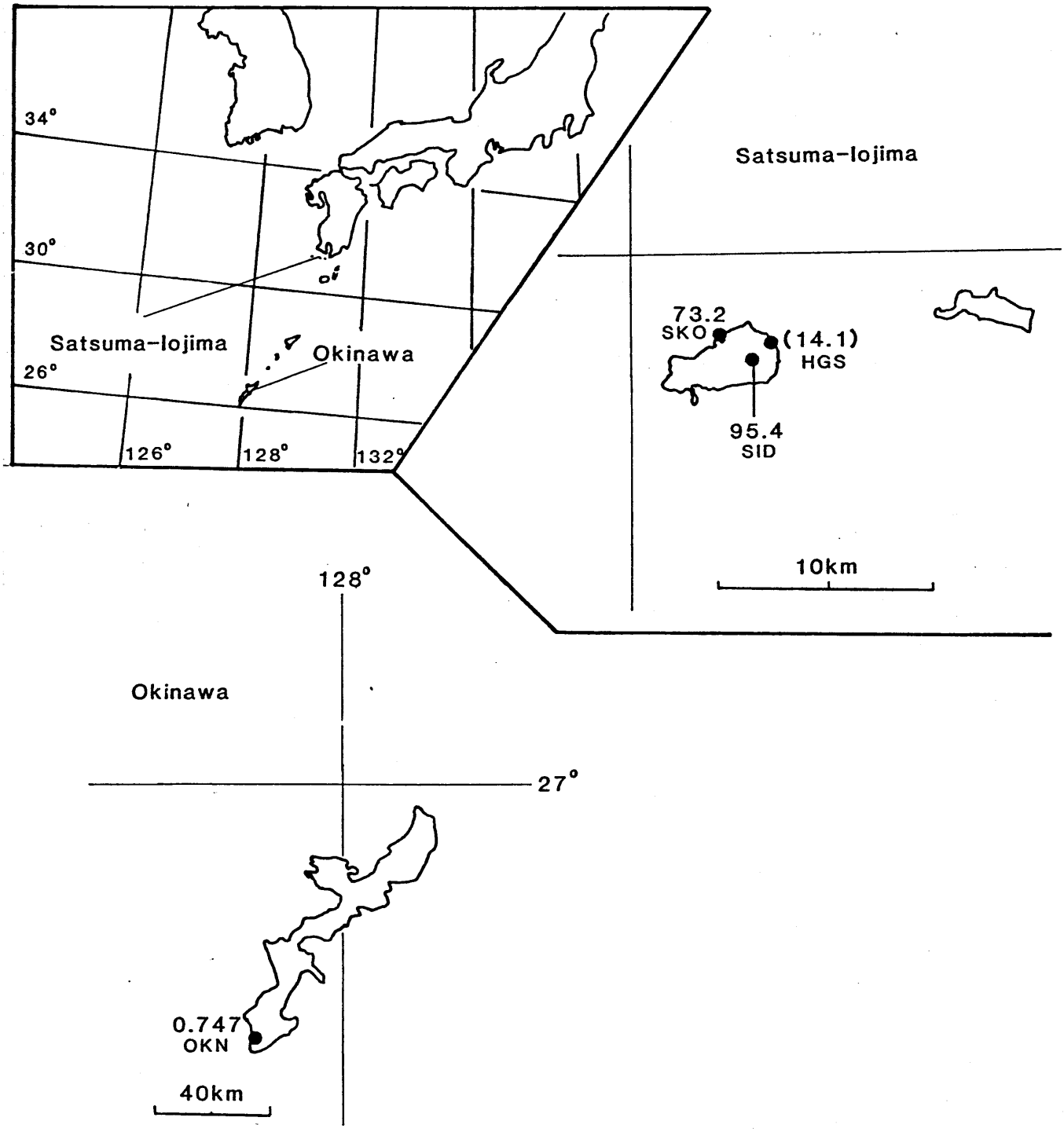

Figure 2-21. Locations of sampling sites in the Satsumaiojima and Okinawa Islands and observed $^{3}He/^{4}He$ ratios with their code names. The unit of the $^{3}He/^{4}He$ ratio is expressed as 10^{-7}. Significantly air-contaminated samples are indicated by parentheses around the values.

Table 2-8. Description of samples from the Japanese Islands

No.	Code	Name	Prefecture	Temp. (°C)	Feature	Location (° ′N, ° ′E)				Date
Hokkaido District										
1	NBB	Jigokudani, Noboribetsu	Hokkaido	85	HS	42	29	141	9	6/ 8/82
2	KRR	Karurusu, Noboribetsu	Hokkaido	62	HS	42	30	141	7	6/ 8/82
3	YKY	Yokoyama, Otaki, Usu	Hokkaido	89	HS	42	37	141	2	6/ 8/82
4	NSK	Niseko-Yumoto	Hokkaido	68	HS	42	52	140	38	6/ 9/82
5	STN	Shitanoyu, Kayabe	Hokkaido	70	HS	41	57	140	50	6/10/82
6	NGR	Nigorikawa, Mori	Hokkaido	57	HS	42	7	140	26	6/10/82
7	SKB	Yoshinoyu, Shikabe	Hokkaido	75	HS	42	1	140	49	6/10/82
8	YNK	Yunokawa, Hakodate	Hokkaido	60	HS	41	46	140	47	6/10/82
9	OTS	Otoshibe, Yakumo	Hokkaido	74	HS	42	8	141	13	6/10/82
10	RAD	Raiden, Iwanami	Hokkaido	45	HS	42	54	140	25	6/ 9/82
11	FTM	Futamata, Oshamanbe	Hokkaido	47	HS	42	34	140	14	6/ 9/82
12	OSB	Oshamanbe	Hokkaido	<20	NG	42	30	140	22	6/ 9/82
13	SKT	Marukoma, Shikotsuko	Hokkaido	45	SW	42	46	141	17	6/ 8/82
14	KJH	Kojo, Shiraoi	Hokkaido	20	SW	42	27	141	13	6/ 8/82
Tohoku District										
15	SKY	Sukayu, Hakkoda	Aomori	64	HS	40	38	140	51	8/23/82
16	YSN	Yoshino, Oga	Akita	-	PG	40	1	139	54	3/19/82
17	FKM	Fukumezawa, Oga	Akita	-	PG	39	56	139	59	3/19/82
18	YBS	Yabase, Akita	Akita	-	PG	39	44	140	5	3/19/82
19	OMN	Omonogawa, Akita	Akita	-	PG	39	41	140	6	3/19/82
20	KSG	Kisagata	Akita	-	PG	39	14	139	55	3/19/82
21	YRH	Yurihara, Yuri	Akita	-	PG	39	14	140	5	*
22	KYR	Kita-Yurihara, Yuri	Akita	-	PG	39	15	140	5	*
23	NRG	Narugo	Miyagi	94	HS	38	44	140	43	10/17/81
24	KMS	Kamasaki, Shiraishi	Miyagi	39.5	HS	38	1	140	34	10/19/81
25	NRI	Nariai, Miyagi	Miyagi	23.5	MS	38	18	140	47	10/19/81
26	HJR	Hijiori, Mogami	Yamagata	88	HS	38	36	140	10	10/17/81
27	SGA	Sagae	Yamagata	46	HS	38	22	140	16	10/18/81
28	AWY	Awanoyu, Oguni	Yamagata	40.5	HS	37	56	139	42	10/18/81
29	FKR	Fukura	Yamagata	-	HS	39	4	139	54	3/18/82
30	AMR	Amarume	Yamagata	-	PG	38	51	139	54	3/18/82
31	HAM	Higashi-Amarume	Yamagata	-	PG	38	51	139	56	3/18/82
32	KSM	Kashima	Fukushima	13	WW	37	42	140	54	*
33	NRH	Naraha	Fukushima	17	WW	37	15	140	54	*
Kanto District										
34	NKY	Nikko-Yumoto	Tochigi	61	HS	36	48	139	25	*
35	KZW	Kazawa	Gunma	36	HS	36	26	138	25	5/ 2/81
36	ISB	Isobe, Annaka	Gunma	17	MS	36	17	138	50	7/ 9/81
37	ARF	Arafune, Shimonita	Gunma	15	MS	36	13	138	44	5/ 1/81
38	NRS	Narashino	Chiba	-	NG	35	41	140	02	7/ 7/81
39	YKS	Yokoshiba	Chiba	-	NG	35	37	140	30	7/ 7/81
40	SRK	Shirako	Chiba	-	NG	35	22	140	21	7/ 7/81
41	CHN	Chonan	Chiba	<20	NG	35	22	140	17	7/ 7/81
42	HWJ	Heiwajima	Tokyo	36	HG	35	35	139	45	12/25/81

Table 2-8 (continued)

No.	Code	Name	Prefecture	Temp. (°C)	Feature	Location (° ′N	° ′E)	Date
43	SMB	Shimobe	Yamanashi	30	HS	35 25	138 29	7/ 9/82
44	KSS	Kusashio, Minobe	Yamanashi	21	NG	35 26	138 20	7/ 9/82
45	OWK	Owakudani, Hakone	Kanagawa	81	VF	35 14	139 1	11/17/82
46	YNZ	Yunohanazawa, Hakone	Kanagawa	100	VF	35 13	139 2	11/17/82
Chubu District								
47	MTS	Matsushiro	Nagano	45	HS	36 34	138 12	5/ 2/81
48	NNS	Nunoshita, Komoro	Nagano	36	HS	36 20	138 22	11/12/81
49	NNB	Nunobiki, Komoro	Nagano	41	HS	36 20	138 23	*
50	OSM	Osamura, Saku	Nagano	25	HS	36 29	138 23	5/ 2/81
51	UMN	Uminokuchi, Saku	Nagano	34	HS	36 1	138 30	*
52	SRH	Shirahone, Azumi	Nagano	49	HS	36 9	137 38	7/ 9/82
53	MEJ	Meiji, Tateshina	Nagano	25	HS	36 2	138 18	*
54	MDR	Midoriko, Shiojiri	Nagano	18	MS	36 6	138 1	*
55	KNS	Kanose, Kiso	Nagano	28	HS	35 54	137 34	11/23/81
56	NGK	Nigorikawa, Kiso	Nagano	47	HS	35 50	137 28	11/17/81
57	KIS	Kiso, Kiso	Nagano	9	MS	35 54	137 35	*
58	KKH	Kakehashi, Kiso	Nagano	11	MS	35 48	137 41	11/23/81
59	SJM	Shojima, Kiso	Nagano	11	MS	35 48	137 43	12/18/81
60	SKY	Shikanoyu, Kiso	Nagano	20	MS	35 43	137 41	5/ 4/81
61	NKZ	Nakaizu	Shizuoka	25	HS	35 56	139 2	*
62	ATG	Atagawa, Izu	Shizuoka	96	SW	34 48	139 4	6/ 6/82
63	MIN	Mine, Izu	Shizuoka	87	SW	34 45	138 58	6/ 6/82
64	OSW	Ohsawa, Izu	Shizuoka	47	SW	34 45	138 50	6/ 6/82
65	OMZ	Omaezaki	Shizuoka	19	WW	34 36	138 14	11/22/81
66	TMJ	Meiji, Kubiki	Niigata	-	PG	37 12	138 20	3/17/82
67	MNA	Minami-aga	Niigata	-	PG	37 45	139 8	3/15/82
68	AGO	Aga-oki	Niigata	-	PG	38 6	139 7	3/15/82
69	MZF	Matsuzaki 1, Niigata	Niigata	-	PG	37 57	139 11	3/18/82
70	MZS	Matsuzaki 2, Niigata	Niigata	-	PG	37 55	139 6	3/18/82
71	KTG	Katagai	Niigata	43	PG	37 22	138 47	6/16/82
72	KKT	Kita-Katagai	Niigata	184	PG	37 23	138 47	6/16/82
73	BSH	Besho, Takada	Niigata	-	PG	37 2	138 20	3/17/82
74	HRI	Hirai, Kashiwazaki	Niigata	-	PG	37 22	138 37	3/17/82
75	NKD	Nakadori, Kashiwazaki	Niigata	-	PG	37 23	138 39	3/17/82
76	MTK	Mitsuke	Niigata	-	PG	37 31	138 51	9/ 9/82
77	NGG	Nigorigo, Masuda	Gifu	54	HS	35 55	137 27	*
78	SHJ	Shitajima, Masuda	Gifu	18	MS	35 55	137 20	11/22/81
79	GYY	Yuya, Masuda	Gifu	13	MS	35 55	137 20	11/22/81
80	AKG	Akigami, Ohno	Gifu	17	MS	36 00	137 24	*
81	BYK	Byakko, Mizunami	Gifu	24	MS	35 24	137 17	8/ 1/81
82	AYY	Yuya, Shidara	Aichi	30	HS	34 58	137 37	8/ 1/81
Kinki District								
83	BWK	Biwako	Shiga	35.2	WW	35 7	135 57	10/ 9/81
84	YSN	Miyataki, Yoshino	Nara	15	MS	34 24	135 55	6/19/81

Table 2-8 (continued)

No.	Code	Name	Prefecture	Temp. (°C)	Feature	Location (° ′N, ° ′E)				Date
85	ARM	Arima	Hyogo	98	HS	34	48	135	15	6/21/81
86	MNT	Minatoyama, Kobe	Hyogo	27.5	HS	34	41	135	10	10/ 8/81
87	TKR	Takarazuka	Hyogo	30	HS	34	48	135	21	6/21/81
88	KGB	Kagobo, Taki	Hyogo	10	MS	35	2	135	20	*
89	SHT	Shiota, Shikama	Hyogo	16	MS	34	51	134	42	6/21/81
90	SHK	Shikano, Inagawa	Hyogo	11	MS	34	55	134	53	10/ 8/81
91	YMR	Yumura, Mikata	Hyogo	43	HS	35	33	134	29	5/ 2/82
Chugoku District										
92	MSS	Misasa	Tottori	76	HS	35	24	133	53	5/ 1/82
93	SKG	Sekigane	Tottori	-	SW	35	21	133	46	5/ 1/82
94	KYH	Koyahara, Ohta	Shimane	38	HS	35	9	132	35	4/30/82
95	TBR	Tonbara, Iishi	Shimane	15	MS	35	4	132	48	4/30/82
96	TMT	Tamatsukuri	Shimane	-	SW	35	24	133	1	5/ 1/82
Kyushu										
97	SKO	Sakamoto, Satsuma-io	Kagoshima	-	HS	30	47	130	17	7/21/82
98	SID	Satsuma-iodake	Kagoshima	100	VF	30	47	130	19	7/22/82
99	HGS	Higashi, Satsuma-io	Kagoshima	-	HS	30	46	130	18	7/21/82
100	OKN	Itoman, Okinawa	Okinawa	-	NG	26	7	127	40	10/25/82

*: Collected at several times.
HS: hot spring gas
MS: mineral spring gas
WW: water well gas
PG: petroleum gas
NG: natural gas
VF: volcanic fumarole

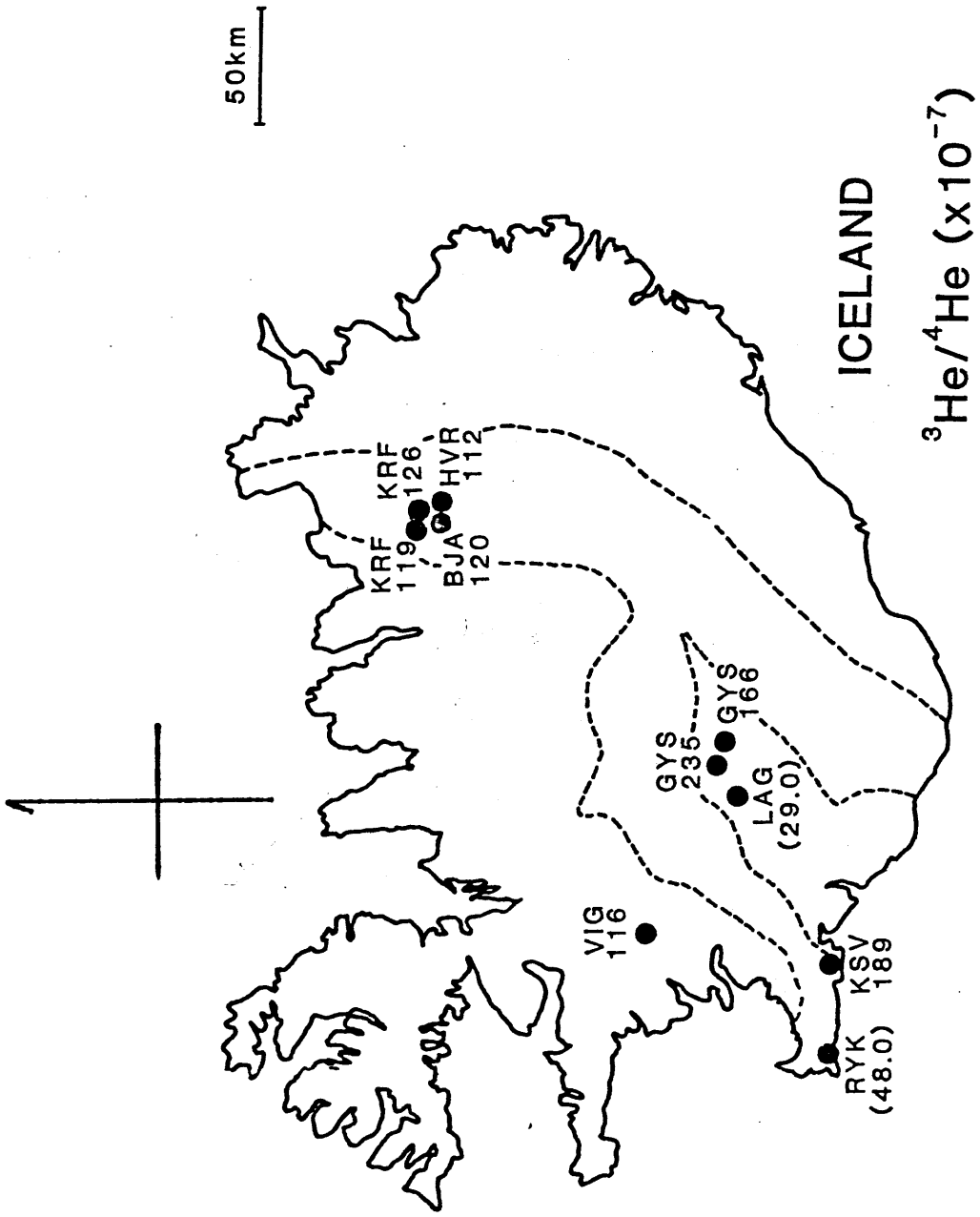

Figure 2-22. Locations of sampling sites in Iceland and observed $^3He/^4He$ ratios with code names. The unit of the $^3He/^4He$ ratio is expressed as 10^{-7}. Significantly air-contaminated samples are indicated by parentheses around the values.

Table 2-9. Description of samples from Iceland

No.	Code	Name	Class	Temp. (°C)	Date
101	KRF	Krafla #15	GG	-	8/ 6/1982
102	KRF	Krafla #8	GG	145	8/ 6/1982
103	HVR	Hveragirdi G3	GG	100	8/ 6/1982
104	BJA	Bjarharflag #12	GG	195	8/ 7/1982
105	VIA	Vidigerdi	TF	101	8/ 4/1982
106	GYS	Geysir 1	TF	100	8/14/1982
107	GYS	Geysir 2	GG	101	8/14/1982
108	LAG	Laugarvatu	TF	100	8/14/1982
109	RKG	Reykjanes Geysir	TF	97	8/ 2/1982
110	KSV	Krisuvik	GG	88	8/ 2/1982
111	RYK	Reykjanes 1	GG	103	8/ 2/1982
112	RYK	Reykjanes 2	GG	103	8/ 2/1982

GG: geothermal gas
TF: thermal fluid

temperature of water varied from 25° C to about 100° C. The major chemical constituents were CO_2 and N_2. Water discharging rates varied siginificantly from several 100 cc/min to over 100 l/min, whereas gas emitting rates were usually small, about 100 cc/min at maximum.

In Japan, hot springs are used commercially as baths called Onsen, and many bore holes have been drilled for the purpose of getting hot water. There are more than 2200 hot springs in Japan, and their locations generally have a close relation to Tertiary and Quaternary volcanic activity.

c) Mineral spring gas

A mineral spring is defined as cold water issuing from underground at a temperature lower than 24° C and containing mineral species such as CO_2, Fe, H_2S, Rn and others. The difference between a hot spring and a mineral spring is only the temperature of the discharging water. In this study, bubble gases from mineral springs were collected at eighteen locations. The temperature of the water varied from 9° C to 24° C. The major chemical constituent were CO_2 and N_2. Gas emitting rates are almost the same as those of hot spring gases.

d) Water well gas

Water wells investigated in this study were drilled for the purpose of earthquake prediction and environmental survey. Water discharging rates of wells were smaller than those of hot springs and mineral springs, whereas their gas emitting rate was almost the same. The water temperatures

are ranged from 13°C to 31°C. Bubble gases in water wells were collected at four different locations. The major chemical constituents were N_2 and CH_4.

e) Methane-rich natural gas from gas fields

Samples of this group are fuel gases from gas fields with thick Quaternary and Tertiary sedimentary layers. Several bore holes were drilled at a single site, and large-scale artificial pumping of ground water was carried out to obtain the fuel gas soluble in water. In order to get natural gas from the water, a gas-liquid separater was used. The discharging rates of gases are greater than 5000 m^3/d. The dominant chemical constituent is CH_4. The temperature of water varied from 15° C to 38 °C. Sample gases were collected at seven different sites.

f) Methane-rich petroleum gas from oil fields

The samples in this group are fuel gases from oil fields on the coast facing the Japan Sea. Several bore holes were drilled in a single location as well as natural gas. The artificial pumping of a mixture of oil and water has been carried out to obtain petroleum. The methane-rich fuel gases are obtained as a by-product of petroleum, which is isolated by a separater. The discharging rates of gases are greater than 5000 m^3/d, of the same order as natural gas. The major chemical constituent is CH_4, and C_2H_6 is also abundant. Sample gases were collected at over twenty locations.

III. Results

3.1 $^{3}He/^{4}He$ and $^{20}Ne/^{4}He$ ratios in samples from Japan and Iceland

A total of 144 samples were collected at 100 locations in Japan (Figure 2-15), and $^{3}He/^{4}He$ and $^{20}Ne/^{4}He$ ratios of samples were measured by a magnetic deflection type mass spectrometer. Results are shown in Table 3-1 and Figure 2-15 through Figure 2-21. Several samples were collected and measured at a single sampling location in order to check the temporal variation and spatial distributions of $^{3}He/^{4}He$ and $^{20}Ne/^{4}He$ ratios in a short range (Tables 3-2 and 3-3).

Eleven samples were collected at 9 locations in Iceland, and their $^{3}He/^{4}He$ and $^{20}Ne/^{4}He$ ratios were measured. Results are indicated in Table 3-4 and Figure 2-22.

a) $^{3}He/^{4}He$ and $^{20}Ne/^{4}He$ ratios in gaseous samples in Japan

The highest $^{3}He/^{4}He$ ratio, 9.65×10^{-6}, was observed at Shirahone (#52) hot spring, Nagano Prefecture, and values higher than 9.0×10^{-6} were observed at several sites (Awanoyu (#28), Meiji (#53) and Arima (#85) hot springs and Satsuma-iodake (#98) volcano). These sites are located close to volcanic and geothermal areas. The lowest $^{3}He/^{4}He$ ratio, 7.47×10^{-8}, was observed at Itoman (#100) natural gas field, Okinawa Prefecture, and the second lowest value was

Table 3-1. *The $^3He/^4He$ and $^{20}Ne/^4He$ ratios of Japanese samples

No.	Code	Name	$^3He/^4He$ ($\times10^{-7}$)	$^{20}Ne/^4He$ ($\times10^{-3}$)	Type*	helium* (ppm)
Hokkaido District						
1	NBB	Noboribetsu	53.0±1.3	90	CO2	6.2
2	OSB	Oshamanbe	18.8±0.8	110	CH4	2.2
3	YKY	Yokoyama	29.5±0.4	400	N2	25
4	NSK	Niseko-Yumoto	76.4±1.9	51	CO2	5.1
5	STN	Shitanoyu	44.0±1.0	98	CO2	5.3
6	NGR	Nigorikawa	26.7±0.5	2600	N2-CO2	4.0
7	SKB	Shikabe	37.5±0.4	64	N2-CO2	49
8	YNK	Yunokawa	72.8±0.3	17	CO2	28
9	OTS	Otoshibe	51.0±1.7	230	CO2	34
10	KRR	Karurusu	52.0±0.3	560	N2	22
11	RAD	Raiden	26.6±0.6	920	N2	3.2
12	FTM	Futamata	12.0±0.4	2140	CO2	0.1
13	SKT	Shikotsuko	43.6±1.8	690	-	-
14	KJH	Kojo	17.2±0.5	83	-	-
Tohoku						
15	SKY	Sukayu	18.7±0.4	3380	CO2	4.2
16	YSN	Yoshino	41.2±0.3	14	CH4	11.2
17	FKM	Fukumezawa	62.4±0.7	20	CH4	4.3
18	YBS	Yabase	11.8±0.4	110	CH4	2.1
19	OMN	Omonogawa	14.2±0.8	3210	CH4	2.1
20	KSG	Kisagata	24.2±0.3	2370	CH4	4.2
21	YRH	Yurihara	25.4±0.8	11	CH4	3.3
22	KYR	Kita-Yurihara	72.5±1.3	1.9	CH4	6.8
23	NRG	Narugo	57.9±1.5	78	CO2	1.9
24	KMS	Kamasaki	50.0±0.8	41	N2	260
25	NRI	Nariai	35.5±0.4	56	N2-CO2	70
26	HJR	Hijiori	79.3±2.0	260	CO2	3.2
27	SGA	Sagae	72.6±0.7	50	N2-CH4	100
28	AWY	Awanoyu	90.1±0.9	5.9	CO2	1.4
29	FKR	Fukura	68.7±1.7	520	CH4-CO2	29.5
30	AMR	Amarume	63.9±1.3	23	CH4	2.3
31	HAM	Higashi-Amarume	77.7±1.5	2.5	CH4	47.3
32	KSM	Kashima	4.76±0.16	1.8	N2	6900
33	NRH	Naraha	3.57±0.23	37	N2-CH4	140
Kanto District						
34	NKY	Nikko-Yumoto	41.0±0.8	160	CO2	11.2
35	KZW	Kazawa	43.6±0.7	530	CH4-CO2	0.9
36	ISB	Isobe	9.20±0.37	1.6	CO2-N2-CH4	96
37	ARF	Arafune	12.9±1.3	110	CO2	<0.5
38	NRS	Narashino	2.13±0.6	20	CH4	<0.5
39	YKS	Yokoshiba	3.49±0.11	71	CH4	1.1
40	SRK	Shirako	3.10±0.05	210	CH4	0.68
41	CHN	Chonan	2.21±0.10	240	CH4	<0.5
42	HWJ	Heiwajima	1.37±0.10	10	CH4	3.3

Table 3-1 (continued)

No.	Code	Name	$^3He/^4He$ ($\times10^{-7}$)	$^{20}Ne/^4He$ ($\times10^{-3}$)	Type*	helium* (ppm)
43	SMB	Shimobe	56.8±2.3	97	N2	110
44	KSS	Kusashio	28.2±1.0	10	CH4	36.8
45	OWK	Owakudana	82.9±2.0	61	-	3.4
46	YNZ	Yunohanazawa	76.2±0.7	140	-	-
Chubu District						
47	MTS	Matsushiro	64.1±1.0	34	CO2	40
48	NNS	Nunoshita	52.4±0.17	-	N2	110
49	NNB	Nunobiki	57.0±0.4	110	N2-CH4	33
50	OSM	Osamura	46.2±0.9	190	CH4-CO2	3.6
51	UMN	Uminokuchi	72.2±1.5	16	N2-CO2	130
52	SRH	Shirahone	96.5±2.8	62	N2-CO2	11
53	MEJ	Meiji	92.4±0.7	83	N2-CO2	89
54	MRR	Midoriko	14.8±0.3	34	CO2-N2-CH4	107
55	KNS	Kanose	81.3±2.7	-	CO2	4.5
56	NGK	Nigorikawa	76.3±1.8	230	CO2	1.3
57	KIS	Kiso	68.0±0.7	6.7	CO2	53
58	KKH	Kakehashi	41.7±0.6	14	CO2	14
59	SJM	Shojima	28.3±1.0	-	CO2	6.6
60	SKY	Shikanoyu	23.9±0.4	14	CO2	3.3
61	NKZ	Nakaizu	14.6±0.4	3100	N2	5.7
62	ATG	Atagawa	17.0±0.9	1490	-	-
63	MIN	Mine	9.25±0.17	1540	-	-
64	OSM	Ohsawa	45.3±1.5	1360	-	-
65	OMZ	Omaezaki	1.02±0.04	150	CH4	6.9
66	TMJ	Meiji	31.0±0.6	8.7	CH4	4.7
67	MNA	Minami-aga	37.6±0.8	16	CH4	4.4
68	AGO	Aga-oki	19.0±0.2	7.0	CH4	2.1
69	MZF	Matsuzaki 1	32.2±0.9	11	CH4	3.4
70	MZS	Matsuzaki 2	32.3±0.3	13	CH4	3.6
71	KTG	Katagai	55.9±0.8	13	CH4	9.5
72	KKT	Kita-Katagai	86.5±0.8	4.1	CH4	30.7
73	BSH	Besho	20.9±0.8	16	CH4	5.7
74	HRI	Hirai	73.3±0.9	0.88	CH4	51
75	NKD	Nakadori	76.9±0.8	1.7	CH4	5.3
76	MTK	Mitsuke	86.1±2.9	0.99	CH4	-
77	NGG	Nigorigo	86.1±1.1	31	N2-CO2	89
78	STJ	Shitajima	26.0±1.6	1300	CO2	<0.5
79	GYY	Yuya	30.1±1.5	27	CO2	1.7
80	AKG	Akigami	48.1±1.8	400	N2-CO2	45
81	BYK	Byakko	11.0±0.3	17	N2	750
82	AYY	Yuya	17.3±0.4	10	N2	320
Kinki District						
83	BWK	Biwako	18.2±1.0	22	N2-CH4	150
84	YSN	Yoshino	24.1±1.1	160	CO2	3.9

Table 3-1 (continued)

No.	Code	Name	$^{3}He/^{4}He$ ($\times10^{-7}$)	$^{20}Ne/^{4}He$ ($\times10^{-3}$)	Type*	helium* (ppm)
85	ARM	Arima	92.2±1.1	27	CO2	16
86	MNT	Minatoyama	37.7±0.6	23	N2-CO2	200
87	TKR	Takarazuka	81.5±2.1	24	CO2	6.3
88	KGB	Kagobo	8.88±0.41	120	CO2	4.2
89	SHT	Shoita	10.6±0.4	53	CO2	1.3
90	SHK	Shikano	16.6±0.3	9.4	N2-CH4	1200
91	YMR	Yumura	53.9±1.0	17	N2-CO2	230
Chugoku District						
92	MSS	Misasa	73.8±0.2	160	N2	830
93	SKG	Sekigane	60.2±0.8	33	-	-
94	KYH	Koyahara	58.4±0.5	17	CO2	3.3
95	TBR	Tonbara	36.2±0.8	57	CO2	11
96	TMT	Tamatsukuri	43.2±0.4	34	-	-
Kyushu District						
97	SKO	Sakamoto	73.2±2.3	320	CO2	3.2
98	SID	Satsuma-iodake	95.4±2.8	59	N2	2.8
99	HGS	Higashi	14.1±0.4	2200	-	-
100	OKN	Itoman	0.747±0.033	2.9	CH4	-

*: Urabe (1982)
CO2: CO_2-rich gas
CH4: CH_4-rich gas
N2 : N_2-rich gas
N2-CO2: N_2-CO_2 mixture
N2-CH4: N_2-CH_2 mixture
CH4-CO2: CH_4-CO_2 mixture
CO2-N2-CH4: CO_2-N_2-CH_4 mixture

Table 3-2. Spacial distribution of the $^3He/^4He$ ratios in a short distance

No.	Name		$^3He/^4He$ ($\times10^{-7}$)	$^{20}Ne/^4He$ ($\times10^{-3}$)	N_2* (%)	CH_4* (%)	CO_2* (%)	He* (ppm)
6	Nigorikawa	A	26.7±0.5	2600	35.0	0.31	55.2	4.0
		B	20.4±1.5	2730	11.0	0.15	79.7	2.5
11	Raiden	A	26.6±0.6	920	98.3	0.50	0.11	3.2
		B	13.3±0.1	4490	79.0	0.06	0.25	<0.5
17	Fukumezawa	A	62.4±0.7	20	0.37	68.3	1.31	4.3
		B	59.6±1.2	21	0.46	73.2	1.04	4.3
34	Nikko-Yumoto	A	41.0±0.8	160	13.0	0.19	79.4	11.2
		B	40.9±1.1	144	32.0	0.35	57.4	26.7
44	Kusashio	A	26.6±0.5	19	14.1	86.4	0.51	30.9
		B	27.4±0.5	18	29.9	67.8	1.1	91.0
		C	28.2±1.0	10	14.8	89.9	0.51	36.8
52	Shirahone	A	81.1±3.2	120	44.1	0.93	42.8	11.3
		B	96.5±2.8	62	38.0	4.82	54.6	55.7
57	Kiso	A	68.0±0.7	6.7	5.51	0.10	84.5	26.4
		B	38.4±1.0	1600	0.427	0.02	91.9	1.3
		C	62.2±1.7	66	6.21	0.08	89.7	28.0
77	Nigorigo	A	84.2±0.7	35	38.3	0.38	55.5	107
		B	79.7±1.3	38	10.3	0.25	86	27.0
85	Arima	A	88.8±0.8	6.5	0.59	0.14	94	9.0
		B	92.2±1.1	27	2.35	0.63	90	95.9
100	Okinawa	A	2.98±0.12	520	-	-	-	-
		B	0.747±0.033	2.9	-	-	-	-

*: Urabe (1982)

Table 3-3. Temporal variations in the $^{3}He/^{4}He$ and $^{20}Ne/^{4}He$ ratios

No.	Name		Date	$^{3}He/^{4}He$ ($\times10^{-7}$)	$^{20}Ne/^{4}He$ ($\times10^{-3}$)
21	Yurihara	1	5/10/82	24.5±0.5	1.3
		2	6/24/82	23.9±0.4	9.3
22	Kita-Yurihara	1	5/10/82	72.5±1.3	1.9
		2	6/24/82	71.3±0.8	9.3
32	Kashima	1	8/ 1/79	4.73±0.14	8.7
		2	7/ 8/80	4.71±0.15	1.8
		3	3/15/81	4.69±0.15	2.0
		4	7/26/81	5.03±0.15	1.0
		5	10/20/81	4.55±0.18	2.3
		6	12/22/81	4.84±0.16	1.8
		7	8/10/82	4.76±0.15	1.1
33	Naraha	1	3/15/81	3.34±0.08	44
		2	7/26/81	3.80±0.10	30
		3	12/22/81	3.53±0.07	39
		4	8/10/82	3.56±0.09	41
34	Nikko-Yumoto	1	3/30/82	40.9±1.1	144
		2	6/30/82	40.9±0.9	133
49	Nunobiki	1	8/17/82	57.1±0.4	110
		2	11/12/82	49.7±2.2	82
51	Uminokuchi	1	5/ 4/81	72.2±1.5	16
		2	11/12/81	69.6±1.8	18
		3	7/10/82	69.1±1.0	14
		4	8/22/82	73.9±1.7	23
52	Shirahone	1	8/20/81	50.7±0.8	970
		2	7/ 9/82	81.1±3.2	120
53	Meiji	1	8/20/81	92.4±0.7	83
		2	7/18/82	88.7±1.0	84
54	Midoriko	1	8/21/81	14.8±0.3	34
		2	11/12/81	14.0±0.3	19
57	Kiso	1	11/23/81	59.5±1.2	4.5
		2	12/18/81	68.0±0.7	6.7
61	Nakaizu	1	10/13/81	14.6±0.4	3100
		2	12/19/81	14.4±0.5	3150
77	Nigorigo	1	9/21/81	86.1±1.1	31
		2	11/22/81	84.1±0.7	35
80	Akigami	1	11/ 2/79	46.0±1.5	19
		2	9/21/81	48.1±1.8	400
88	Kagobo	1	6/20/81	8.88±0.41	120
		2	10/ 7/81	12.8±0.3	2100

Table 3-4. The $^{3}He/^{4}He$ and $^{20}Ne/^{4}He$ ratios of Iceland samples

No.	Code	Name	$^{3}He/^{4}He$ ($\times 10^{-7}$)	$^{20}Ne/^{4}He$ ($\times 10^{-3}$)
101	KRF	Krafla #15	1.26 ± 0.04	49
102	KRF	Krafla #8	1.19 ± 0.03	58
103	HVR	Hveragirdi G3	1.12 ± 0.02	9.2
104	BJA	Bjarharflag #12	1.20 ± 0.03	28
105	VIG	Vidigerdi	1.16 ± 0.02	260
106	GYS	Geysir 1	1.66 ± 0.03	250
107	GYS	Geysir 2	2.35 ± 0.03	170
108	LAG	Laugarvatu	0.294± 0.007	1260
109	RKG	Reykjanes Geysir	0.513± 0.009	1420
110	KSV	Krisuvik	1.89 ± 0.04	33
111	RYK	Reykjanes 1	0.480± 0.015	2050

1.02×10^{-7} in water well gas at Omaezaki (#65), Shizuoka Prefecture. Lower $^{3}He/^{4}He$ ratios were observed in samples collected from places which have thick sedimentary layers and old basements. The highest $^{20}Ne/^{4}He$ ratio, 4.49, was observed at Raiden (#11) hot spring, Hokkaido; this is higher than the atmospheric value of 3.15. The lowest ratio, 8.8×10^{-4}, was observed for a petroleum well at Hirai (#74). There is no correlation between $^{3}He/^{4}He$ ratios and $^{20}Ne/^{4}He$ ratios.

b) $^{3}He/^{4}He$ and $^{20}Ne/^{4}He$ ratios in samples from Iceland

The highest $^{3}He/^{4}He$ ratio, 2.35×10^{-5}, was observed at Geysir 2 (#107) geothermal well, and the second highest value was, 1.89×10^{-5} for a geothermal gas at Krisuvik (#110). These sites are located on the southern part of the island. Values lower than 1.0×10^{-5} were observed at Laugarvatu (#108), Reykjanes 1 (#111) and Reykjanes Geysir (#109) geothermal wells. The $^{20}Ne/^{4}He$ ratios vary significantly from 9.2×10^{-3} to 2.05. The $^{3}He/^{4}He$ ratios of Icelandic samples increase when the $^{20}Ne/^{4}He$ ratios increase.

c) Spatial distribution of $^{3}He/^{4}He$ and $^{20}Ne/^{4}He$ ratios within a short distance

There have not been many papers dealing with spatial distribution in $^{3}He/^{4}He$ and $^{20}Ne/^{4}He$ ratios of gaseous samples collected in a small area (Torgersen and Jenkins, 1982). Most published data are based on a single sample collection in a single location. In a hot spring region in Japan, numerous bore holes have usually been drilled for the

purpose of getting hot water, and/or several self-flowing springs exist at one location. Chemical compositions of gases accompanied by hot water usually change at different sites even in the same hot spring region. Contents of He also vary significantly. How can we expect constancy of isotopic ratios ? In order to obtain basic knowledge on spatial variations in $^{3}He/^{4}He$ and $^{20}Ne/^{4}He$ ratios, gaseous samples were collected at two or three different sites in ten locations. Observed $^{3}He/^{4}He$ and $^{20}Ne/^{4}He$ ratios are listed in Table 3-2 with chemical compositions referred from Urabe (1982). The distances between sampling sites in a location range from several hundred meters at Raiden hot spring to a few meters at Kiso mineral spring.

Chemical compositions and $^{3}He/^{4}He$ and $^{20}Ne/^{4}He$ ratios of two gas samples obtained from different bore holes in Fukumezawa oil field agree well. Irrespective of significant discrepancies in chemical compositions and concentrations of He, $^{3}He/^{4}He$ ratios of different sites agree well in three locations (Nikko-Yumoto (#34), Nigorigo (#77), Arima hot spring (#85)). However, $^{20}Ne/^{4}He$ ratios at Arima (#85) hot spring show a large variation. In Kusashio (#44) natural gas field, three gaseous samples were collected at different situations. One sample is directly from the source of the well, and the second is bubble gas in the rice field near the well. The third one is fuel gas separated from water and accumulated in the gas tank. The chemical compositions of the first and third ones are almost the same but differ from

that of the second one. However, $^{3}He/^{4}He$ and $^{20}Ne/^{4}He$ ratios agree well among the three samples.

Relatively large variations of $^{3}He/^{4}He$ ratios were shown in Nigorikawa (#6), Shirahone (#52) and Raiden (#11) hot springs, Kiso (#57) mineral spring and Okinawa (#100) natural gas. The variations in Nigorikawa (#6) and Raiden (#11) hot springs and Okinawa (#100) natural gas should be attributed to the mixing of atmospheric He and the original He as is described below. At Kiso (#57) mineral spring, gas bubbles were observed in the surface of a wide water pool covering several tens of meters. Gaseous samples were collected at three positions, the distance between them being about 10 m. Observed $^{3}He/^{4}He$ and $^{20}Ne/^{4}He$ ratios fluctuated; the difference in the $^{3}He/^{4}He$ ratio was up to 43.5 % of the highest ratio. However, there were close relations between $^{3}He/^{4}He$ and $^{20}Ne/^{4}He$ ratios. The higher the $^{3}He/^{4}He$ ratio was, the lower the $^{20}Ne/^{4}He$ ratio became. This tendency suggests that the observed variation of $^{3}He/^{4}He$ ratio was attributable to the mixing of atmospheric He with the hot spring He at Nigorikawa (#6) and Raiden (#11) hot springs as well. At Shirahone hot spring, the $^{3}He/^{4}He$ ratios differed by 16 % at two bore holes, and the difference exceeded the experimental error (4 %). The cause of the difference is not well understood.

Generally, the fluctuation of $^{3}He/^{4}He$ ratios in a single location was small irrespective of large variations in chemical compositions and features of gas discharging.

Hence, at present, the value of even a single measurement at a location may be assigned as an approximate value for the location.

c) Temporal variations of $^{3}He/^{4}He$ and $^{20}Ne/^{4}He$ ratios

Only a few papers have reported temporal variations in $^{3}He/^{4}He$ and $^{20}Ne/^{4}He$ ratios of gaseous samples or spatial variations within a short distance (Nagao et al., 1980). In order to discuss the relationships between the $^{3}He/^{4}He$ ratios and the geotectonic enviornment, the constancy of the isotopic ratio over time must be proved. However, most published data are based on a single sample collection. In order to better understand temporal variations in $^{3}He/^{4}He$ ratios, gaseous samples were collected at several different times at fifteen sites.

Recently, continuous measurement of chemical composition of volcanic gases and bubble gases in deep water well has been undertaken for the purpose of predicting volcanic eruptions and large earthquakes. Anomalous changes in chemical compositions have been observed prior to these natural disasters. Continuous measurement of the isotopic ratio will provide useful knowledge on the disaster predition research.

Collection of gaseous samples has been repeated at fifteen sites, as many as possible. Results obtained to date are shown in Table 3-3. At twelve sites (Nikko-Yumoto (#34), Nunobiki (#49), Nigorigo (#77), Nakaizu (#61), Midoriko (#54), Akigami (#80), Kiso (#57), Kagobo (#88),

Shirahone (#52), Meiji (#53), Yurihara (#21) and Kita-Yurihara (#22)), samples were collected at two different times. The intervals of sampling ranged from about two years (Akigami (#78)) to a few months (Kiso (#57) and Nakaizu (#61)).

At most sampling sites, observed $^{3}He/^{4}He$ and $^{20}Ne/^{4}He$ ratios agree well over time within margins of experimental errors; the exceptions are Akigami (#80), Kiso (#57), Kagobo (#88) and Shirahone (#52). At Akigami hot spring (#80), observed $^{3}He/^{4}He$ ratios at two different dates show similar values but $^{20}Ne/^{4}He$ ratios are apparently different. About 14 km away from the spring is an active volcano (Mt. Ontake). The first eruption of the volcano in historical time took place on October 28 - 29, 1979. The first sample from Akigami hot spring was collected on November 2, a few days after the eruption, and the second sample was collected about 23 months later. A large variation in chemical composition of the two samples was found (Urabe, 1982). The first samples was a N_2 and CO_2 mixture, whereas the second was a CO_2-rich gas. The concentration of He also changed significantly. The observed variation in the $^{20}Ne/^{4}He$ ratio may be attributed to the volcanic activity as well to chemical composition. However, the $^{3}He/^{4}He$ ratios of these samples showed little variation. This implies that the isotopic ratio was not easily affected by the eruption of the volcano.

At Kagobo (#88) and Shirahone (#52) hot springs, the

$^{3}He/^{4}He$ and $^{20}Ne/^{4}He$ ratios of gas samples changed. The later sample had higher $^{3}He/^{4}He$ and $^{20}Ne/^{4}He$ ratios than the earlier at Kagobo (#88). On the other hand, at Shirahone (#52) the $^{3}He/^{4}He$ ratio of the later sample was higher than the earlier but the $^{20}Ne/^{4}He$ ratio was lower. In this case, the difference may be attributed to the different degrees of contamination by atmospheric He. For Kiso (#57) mineral spring, $^{20}Ne/^{4}He$ ratios had a similar values but $^{3}He/^{4}He$ ratios were apparently different. The cause of this variation (by about 13 %) is not well understood.

At Uminokuchi (#51) hot spring and the Naraha (#33) water well, samples were collected at four different times within two years (Figure 3-1). These samples from two locations are representaive of higher and lower $^{3}He/^{4}He$ ratios. The $^{3}He/^{4}He$ ratios agreed well within the the margin of experimental error. No seasonal variations were observed. Although the $^{20}Ne/^{4}He$ ratio seems to fluctuate slightly, the variation is within the range of the reproducibility of measurement.

At the Kashima (#32) water well, seven samples were collected over a period of nearly three years (Figure 3-1). The $^{3}He/^{4}He$ ratios were almost constant within the margin of experimental error. The $^{20}Ne/^{4}He$ ratios showed no variation, except for the first sample. This higher $^{20}Ne/^{4}He$ ratio may be attributed either to a change in the degassing rates of the two elements or to permeation of ^{4}He from the glass container over a long storage period.

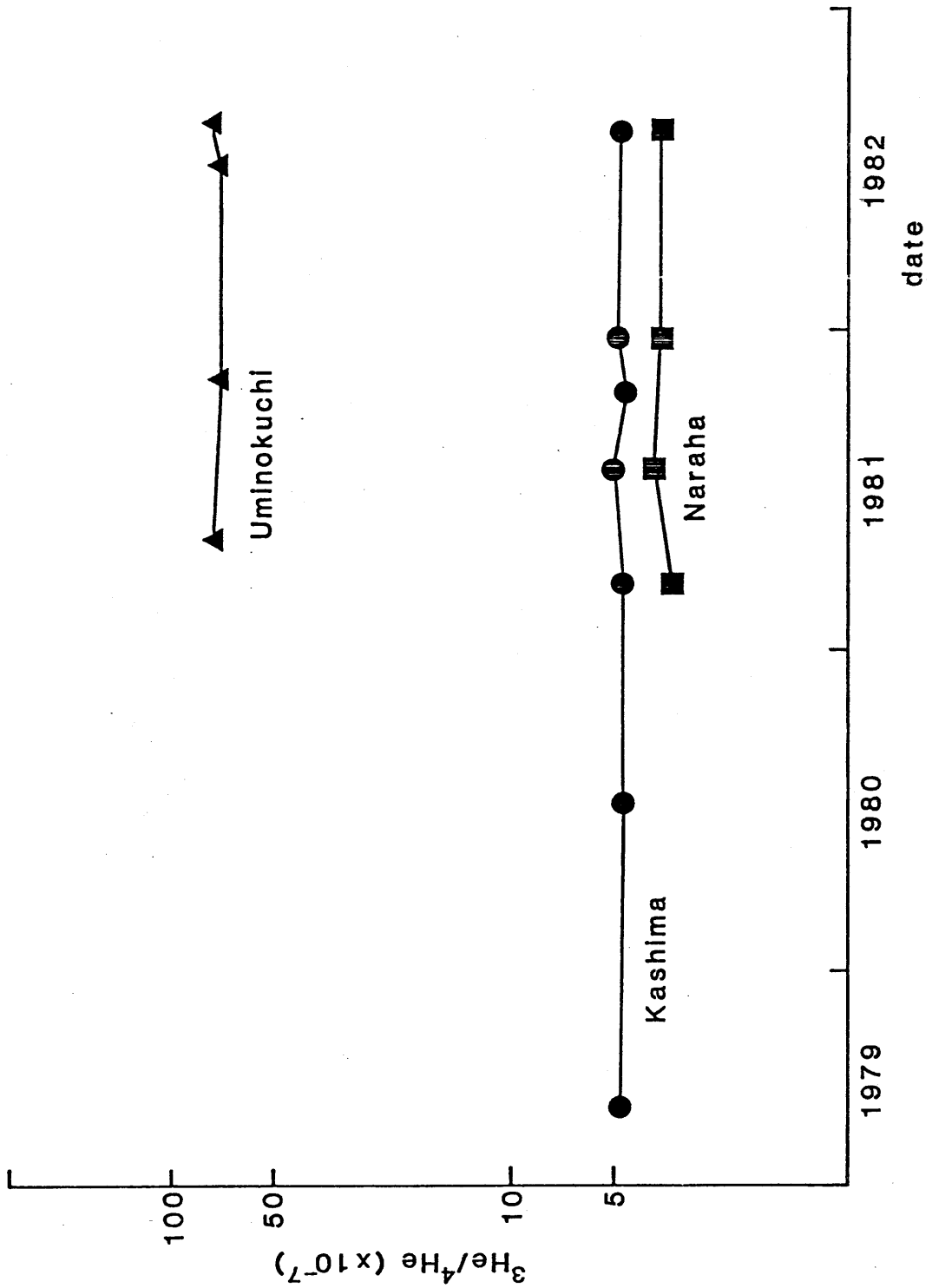

Figure 3-1. Temporal variations in $^3He/^4He$ ratios observed at three sampling sites. At Uminokuchi hot spring and Naraha water well, samples were collected at four different times within two years. At Kashima water well, seven samples were collected during a period of nearly three years. These are selected as representative samples with higher and lower $^3He/^4He$ ratios.

Consequently, even a single measurement performed at a location may be assigned as an approximate value for the site, irrespective of spatial distribution and temporal variation, as far as hot spring and water well gases are concerned.

d) $^{3}He/^{4}He$ and $^{20}Ne/^{4}He$ ratios in water samples

In order to clarify the relation between $^{3}He/^{4}He$ ratios and geological and geophysical parameters, it is necessary in the future to collect at least one sample in every 25 km^2 of area, since the $^{3}He/^{4}He$ ratios change over this large an area. However, there are not many locations where gases are being discharged. For example, most of the hot spring in Japan are not accompanied by bubbling gas. Hence, if water samples are available for $^{3}He/^{4}He$ ratio measurement, they are very useful for discussion of the spatial distribution of the ratios. In this study, measurements of $^{3}He/^{4}He$ and $^{20}Ne/^{4}He$ ratios in water samples were made.

At first, fresh water saturated with atmospheric air in the laboratory was tested. The observed $^{3}He/^{4}He$ and $^{20}Ne/^{4}He$ ratios were $(1.27 \pm 0.13) \times 10^{-6}$ and 3.57, respectively. The $^{3}He/^{4}He$ ratio agrees well with the value of atmospheric air (1.40×10^{-6}) within the margin of experimental error. This implies that there is no significant isotopic fractionation between air and water. The $^{20}Ne/^{4}He$ ratio shows an agreement with the calculated $^{20}Ne/^{4}He$ ratio in water. The value of 3.72 is based on the difference in the solubilities of He and Ne (Weiss, 1971).

To check the validity of the measurement of water samples, several samples of hot spring and mineral spring water were collected in locations where gaseous samples were also collected. Some sample pairs were collected at the same bore holes, and others at different holes. Observed $^{3}He/^{4}He$ and $^{20}Ne/^{4}He$ ratios of water samples are shown, together with the data on gaseous samples from the same locations, in Table 3-5. At Uminokuchi (#51), Nunoshita (#48) hot springs, observed $^{3}He/^{4}He$ and $^{20}Ne/^{4}He$ ratios of water samples agreed well with those of gaseous samples. At Nunobiki (#49) and Yumura (#94) hot springs, $^{3}He/^{4}He$ ratios of water samples were slightly lower than those of gaseous samples, and the $^{20}Ne/^{4}He$ ratios slightly higher. This may be attributed to the dilution of original He by the atmospheric He dissolved in water. The difference in $^{3}He/^{4}He$ ratios between gas and water at the Omaezaki (#65) well is significantly large. However, it can also be explained by the dilution of the atmospheric He.

3.2 Isotopic abundances of rare gases in Japan and in Iceland

Isotopic abundances of rare gases in collected samples in Japan were measured by a Quadrupole mass spectrometer (QMS). Numbers and types of measured samples in Japan are as follows: 1) Rare gas elemental abundance: eight, 2) Ne

Table 3-5. Observed $^{3}He/^{4}He$ ratios of water and gaseous samples obtained at same sampling sites

No.	Name	Feature	$^{3}He/^{4}He$ ($\times 10^{-7}$)	$^{20}Ne/^{4}He$ ($\times 10^{-3}$)
48	Nunoshita	water	54.3±0.8	130
		gas	52.4±1.7	-
49	Nunobiki	water	49.0±1.1	620
		gas	57.0±0.4	110
51	Uminokuchi	water	69.9±0.9	27
		gas	72.2±1.5	16
65	Omaezaki	water	2.23±0.13	560
		gas	1.02±0.04	150
92	Sekigane	water A	60.2±0.8	33
		water B	56.4±1.1	14
94	Yumura	water	46.9±1.2	100
		gas	53.9±1.0	17
96	Tamatsukuri	water A	60.2±0.8	33
		water B	56.4±1.1	14
	Atmosphere	water	12.7±1.3	3.57
		gas	14.2±0.4	3.15

isotopic analysis: thirteen, 3) Ar isotopic analysis: twenty, 3) Kr and Xe isotopic analysis: four.

Isotopic compositions of Ne and Ar in eight Iceland samples were made using a Nuclide mass spectrometer. Observed Ne and Ar isotopic ratios are listed in Table 3-9.

3.2.1 Isotopic compositions of rare gases in Japan

a) Elemental abundance patterns of rare gases

In order to verify the applicability of the QMS method, rare gas measurements were made for some typical samples in Japan. The elemental abundances of rare gases relative to 36Ar in eight gaseous samples are shown in Table 3-6 together with the chemical compositions of major constituents. Four samples (Matsushiro (#47), Osamura (#50), Arafune (#37) and Shikanoyu (#60) hot spring gases) are CO_2-rich gases from different sites in central Japan. Osamura (#50) spring gas contained about 20 % CH_4. Three samples (Kashima (#32) water well and Yuya (#82) and Byakko (#81) hot springs) are N_2-rich gases obtained at three sites, one in the eastern part of the Tohoku district and two from the central Japan. Yuya (#82) and Byakko (#81) spring gases contained 6 and 13 % CH_4, respectively. Naraha water well gas, from in the eastern part of the Tohoku district, was also analyzed; it was composed almost entirely of CH_4.

An overall similarity is found between the data obtained by the QMS in this study and those by Nagao et al., (1981)

Table 3-6. Elemental abundances of rare gases

No.	Name	$^{4}He/^{36}Ar$ (x 1)	$^{20}Ne/^{36}Ar$ (x 1)	$^{84}Kr/^{36}Ar$ ($\times10^{-2}$)	$^{132}Xe/^{36}Ar$ ($\times10^{-3}$)	CO_2* (%)	N_2* (%)	CH_4* (%)
32	Kashima	130	0.031	1.9	1.2	0.01	97.5	0.01
33	Naraha	35	0.52	2.4	1.2	0.19	34.0	65.8
37	Arafune	0.45	0.32	7.9	2.8	99.9	1.42	0.01
47	Matsushiro	16	0.27	4.5	1.1	79.4	17.0	0.02
50	Osamura	1.3	0.050	6.8	1.3	74.4	7.28	22.6
60	Shikanoyu	21	0.11	6.2	1.9	97.0	2.42	0.87
81	Byakko	0.87	0.21	2.6	1.1	0.06	84.4	13.1
82	Yuya	9.2	0.037	2.2	1.2	0.17	89.0	6.10

*: Urabe (1982)

who obtained data via a magnetic deflection mass spectrometer. Elemental abundance patterns of rare gases in CO_2-rich gases, N_2-rich gases and one CH_4-rich gas are shown in Figures 3-2 and 3-3, respectively. The rare gas fractionation factor is defined by Henneke and Mauel (1975) as

$$^mF = (^mX/^{36}Ar)_s/(^mX/^{36}Ar)_{atm}$$

where ^mX and subscript "atm" represent a rare gas element X with mass m and the atmospheric composition, respectively. The patterns in these figures are characterized by a significant enrichment in the $^4He/^{36}Ar$ and by depletion in the $^{20}Ne/^{36}Ar$ relative to the atmospheric composition. The relative $^4He/^{36}Ar$ ratios vary over two orders of magnitude. ^{20}Ne depletions are more siginificant in N_2-rich and CH_4-rich gas samples. Although apparent enrichment in $^{84}Kr/^{36}Ar$ and $^{132}Xe/^{36}Ar$ is seen in all samples, more significant enrichment is observed in CO_2-rich gases. An overall similarity exists between the observed patterns and the "Type 1" pattern defined by Ozima and Alexander (1976). The pattern is thought to be produced by the solubility of atmospheric rare gases into water at low temperature.

b) Isotopic composition of Ar

Isotopic analysis of Ar were made by a Nuclide mass spectrometer for twenty samples in Japan. $^{38}Ar/^{36}Ar$ and $^{40}Ar/^{36}Ar$ ratios are shown in Table 3-7 together with Ar concentrations and major chemical compositions. The $^{38}Ar/^{36}Ar$ ratios for all samples agree well with the

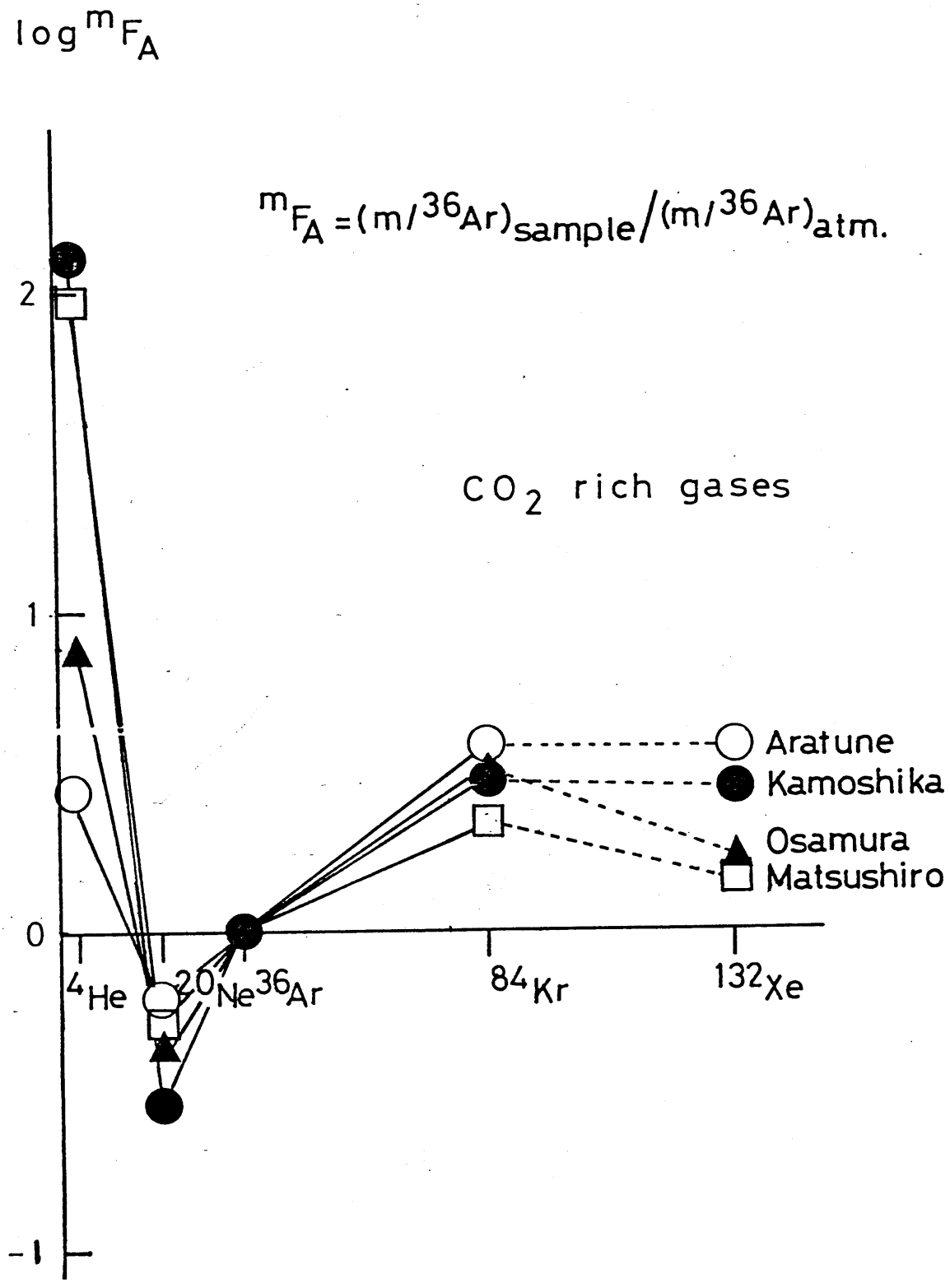

Figure 3-2. Rare gas elemental abundance patterns of CO_2-rich gases in Japan. Significant enrichment in ^{4}He, ^{84}Kr and ^{132}Xe, and depletion in ^{20}Ne relative to ^{36}Ar are observed. An overall similarity exists between the observed patterns and the "Type 1" pattern defined by Ozima and Alexander (1976).

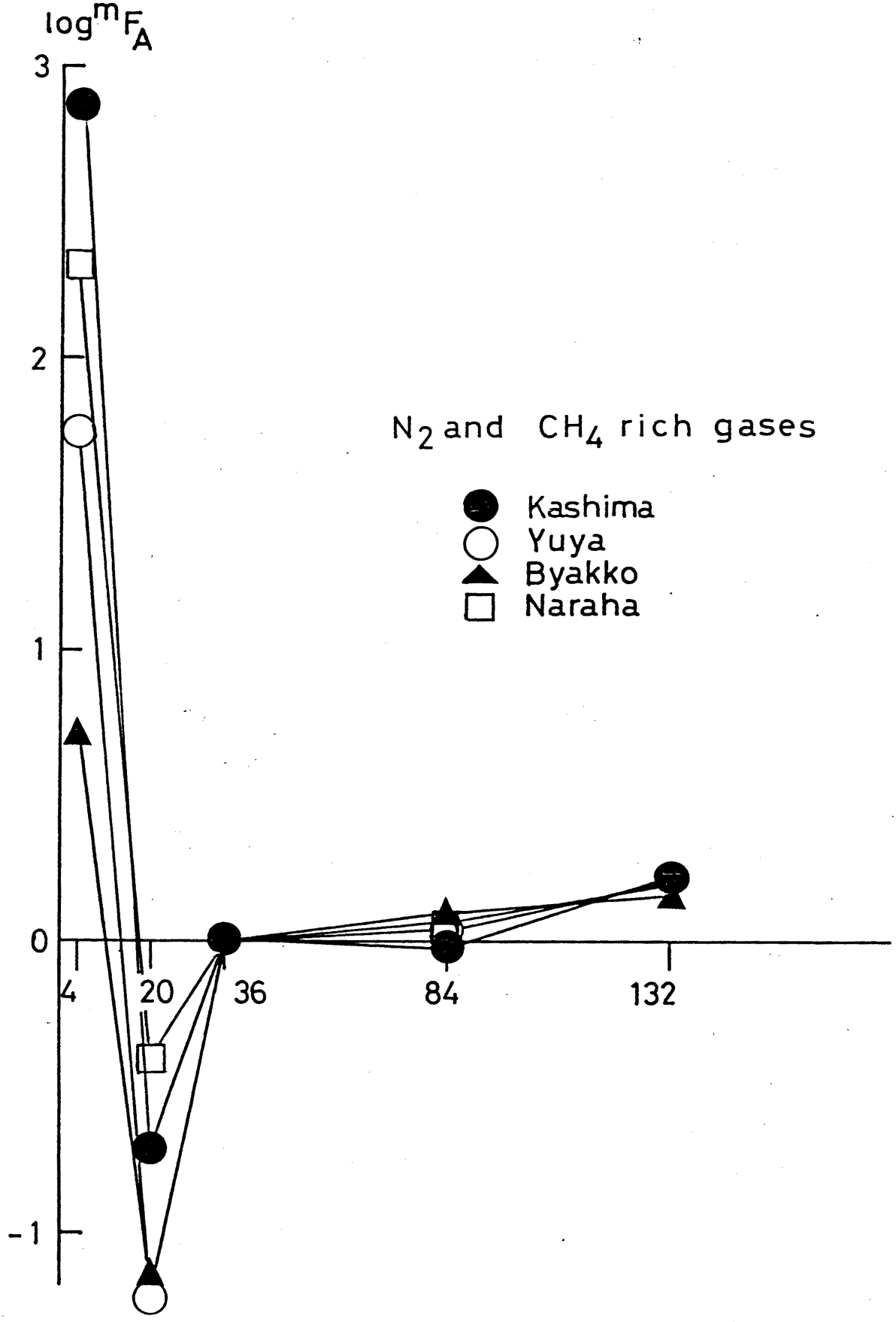

Figure 3-3. Rare gas elemental abundance patterns for N_2-rich gases and CH_4-rich gas in Japan. ^{20}Ne depletion is more significant in N_2-rich and CH_4-rich gases than in CO_2-rich gases. Enrichment in ^{84}Kr and ^{132}Xe relative to ^{36}Ar is slight.

Table 3-7. Ar isotopic compositions of Japanese samples

No.	Name	$^{38}Ar/^{36}Ar$ ($\times10^{-1}$)	$^{40}Ar/^{36}Ar$ ($\times 1$)	Ar^{*} (ppm)	CO_2* (%)	N_2* (%)	CH_4* (%)
18	Yabase	1.84±0.05	285.7±1.9	<20	0.01	0.24	66.1
21	Yurihara	1.89±0.02	299.2±1.2	-	-	-	-
22	Kita-Yurihara	1.87±0.04	300.6±3.0	-	-	-	-
24	Kamasaki	1.90±0.01	303.9±1.2	10300	9.3	89.6	0.08
28	Awanoyu	1.95±0.04	290.6±3.2	28	99.0	0.1	0.56
32	Kashima	1.84±0.01	321.0±1.7	6490	0.01	97.5	0.01
33	Naraha	1.87±0.01	299.2±1.5	5350	0.19	34.0	65.8
34	Nikko-Yumoto	1.86±0.01	290.4±1.2	2780	79.4	13.0	0.19
37	Arafune	1.93±0.05	302.7±2.0	380	99.9	1.42	0.01
38	Narashino	1.84±0.01	289.4±0.9	50	1.47	0.14	99.6
42	Heiwajima	1.88±0.01	301.1±2.1	277	1.17	1.12	95.6
47	Matsushiro	1.85±0.02	315.1±1.8	740	79.4	17.0	0.02
50	Osamura	1.82±0.03	301.6±2.2	1230	74.4	7.28	22.6
60	Shikanoyu	1.90±0.03	316.9±2.4	300	97.0	2.42	0.87
68	Agaoki	1.86±0.01	294.9±0.4	<20	0.70	0.15	102
72	Kita-Katagai	1.86±0.04	289.5±1.1	<20	6.1	2.8	80.9
75	Nakadori	1.87±0.02	310.2±5.8	<20	0.50	0.72	76.8
81	Byakko	1.90±0.02	291.7±1.5	7050	0.06	84.4	13.1
82	Yuya	1.87±0.03	294.0±1.6	8150	0.17	89.0	6.10
85	Arima	1.85±0.01	287.4±0.7	240	97.9	2.82	0.56

*: Urabe (1982)

atmospheric values within margins of experimental error. The $^{40}Ar/^{36}Ar$ ratios for most samples were higher than the atmospheric value of 295.5. This suggests possible mixing of atmospheric Ar and radiogenic ^{40}Ar. The highest $^{40}Ar/^{36}Ar$ ratio (321.0 $\pm$ 1.7) was found at Kashima (#32) water well. The value is similar to the highest $^{40}Ar/^{36}Ar$ ratio (325 at Shiramine hot spring) reported by Nagao et al. (1981). However, the geotectonic conditions at the sampling site are quite different. The Kashima (#32) water well is located on the coast of the Pacific Ocean, on the outside of the volcanic front in the Tohoku district, and there is no sign of any magmatic activity; Shiramine hot spring exists in an active volcanic area in the Chubu district. The $^{40}A/^{36}Ar$ ratio may not reflect this difference in geotectonic conditions, however. The lowest value of $^{40}Ar/^{36}Ar$ ratio (285.7 $\pm$ 1.9) at Yabase (#18) petroleum well is apparently lower than that of the atmospheric air. Since the $^{38}Ar/^{36}Ar$ ratio (0.184 $\pm$ 0.005) of the sample is slightly lower than that of the atmosphere, the lower $^{40}Ar/^{36}Ar$ ratio may be attributed to the mass fractionation of the atmospheric Ar (Figure 3-4).

C) Isotopic composition of Ne, Kr and Xe

Measurements of isotopic ratios of Ne were made by a Nuclide mass spectrometer for thirteen samples. The resulting $^{20}Ne/^{22}Ne$ and $^{21}Ne/^{22}Ne$ ratios are shown in Table 3-8. Observed $^{21}Ne/^{22}Ne$ ratios for samples almost agree with the atmospheric values within the margin of experimental

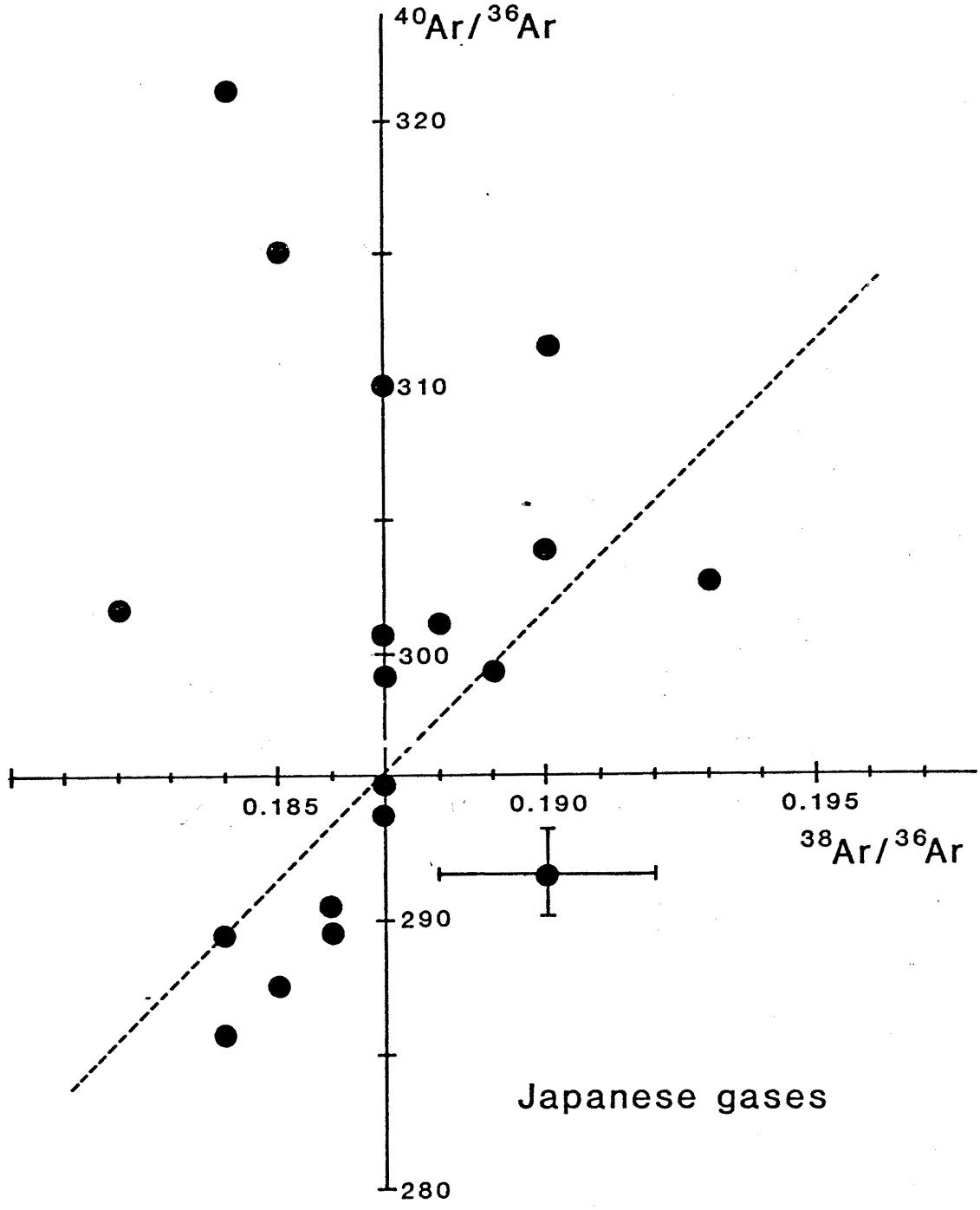

Figure 3-4. A correlation diagram of $^{38}Ar/^{36}Ar$ and $^{40}Ar/^{36}Ar$ in gaseous samples from the Japanese Islands. Some samples show small enrichment in radiogenic ^{40}Ar. The highest enrichment of ^{40}Ar is about 9% at the Kashima well. Samples with low $^{40}Ar/^{36}Ar$ and $^{38}Ar/^{36}Ar$ ratios may be attributed to the mass fractionation of the atmospheric Ar.

Table 3-8. Ne isotopic compositions of Japanese samples

No.	Name	$^{20}Ne/^{22}Ne$ (x 1)	$^{21}Ne/^{22}Ne$ ($\times 10^{-2}$)
18	Yabase	9.851±0.035	2.854±0.039
21	Yurihara	9.926±0.025	2.874±0.076
22	Kita-Yurihara	9.901±0.051	2.945±0.071
24	Kamasaki	9.880±0.009	2.943±0.047
28	Awanoyu	9.538±0.296	2.481±0.370
32	Kashima	9.760±0.178	3.043±0.950
34	Nikko-Yumoto	9.874±0.067	2.909±0.037
38	Narashino	9.924±0.023	2.870±0.056
42	Heiwajima	9.852±0.030	2.922±0.057
68	Agaoki	9.910±0.060	2.924±0.058
72	Kita-Katagai	9.878±0.039	2.902±0.075
75	Nakadori	9.977±0.029	2.922±0.028
85	Arima	9.971±0.040	2.901±0.037

error. The highest $^{21}Ne/^{22}Ne$ ratio (0.03043 $\pm$ 0.0095) at Kashima (#32)·water well is slightly higher than that of the atmosphere. However, the $^{20}Ne/^{22}Ne$ ratio of the sample (9.766 $\pm$ 0.178) is consistent with the atmospheric value. Excess ^{21}Ne may be attributed to the radiogenic origin of the isotope reported by Stroud et al. (1967). The $^{20}Ne/^{22}Ne$ ratio of almost all the samples agree with that of the atmosphere; the exceptions are Arima (#85) hot spring, Nakadori (#75) and Yurihara (#21) petroleum wells and Narashino (#38) natural gas well. Excess ^{20}Ne in these samples may be due to the mass fractionation of Ne. Since observed $^{21}Ne/^{22}Ne$ ratios have a relatively large error, these values are regarded as still on the mass fractionation line (Figure 3-5).

Isotopic analyses of Kr and Xe were made by a QMS for only four samples. Observed Kr and Xe isotopic ratios in gaseous samples were in agreement with those in the atmosphere within the margin of experimental error.

In summary: significant enrichment of heavier rare gases relative to atmospheric abundance was observed in CO_2-rich gases but not in N_2-rich and CH_4-rich gas from the Japanese Islands. Ar values from these samples are explained as admixture of the atmospheric Ar and radiogenic ^{40}Ar. On the other hand, Ne, Kr and Xe isotopic compositions of the samples approximately equal those of the atmosphere.

3.2.2 Isotopic compositions of Ne and Ar in samples from

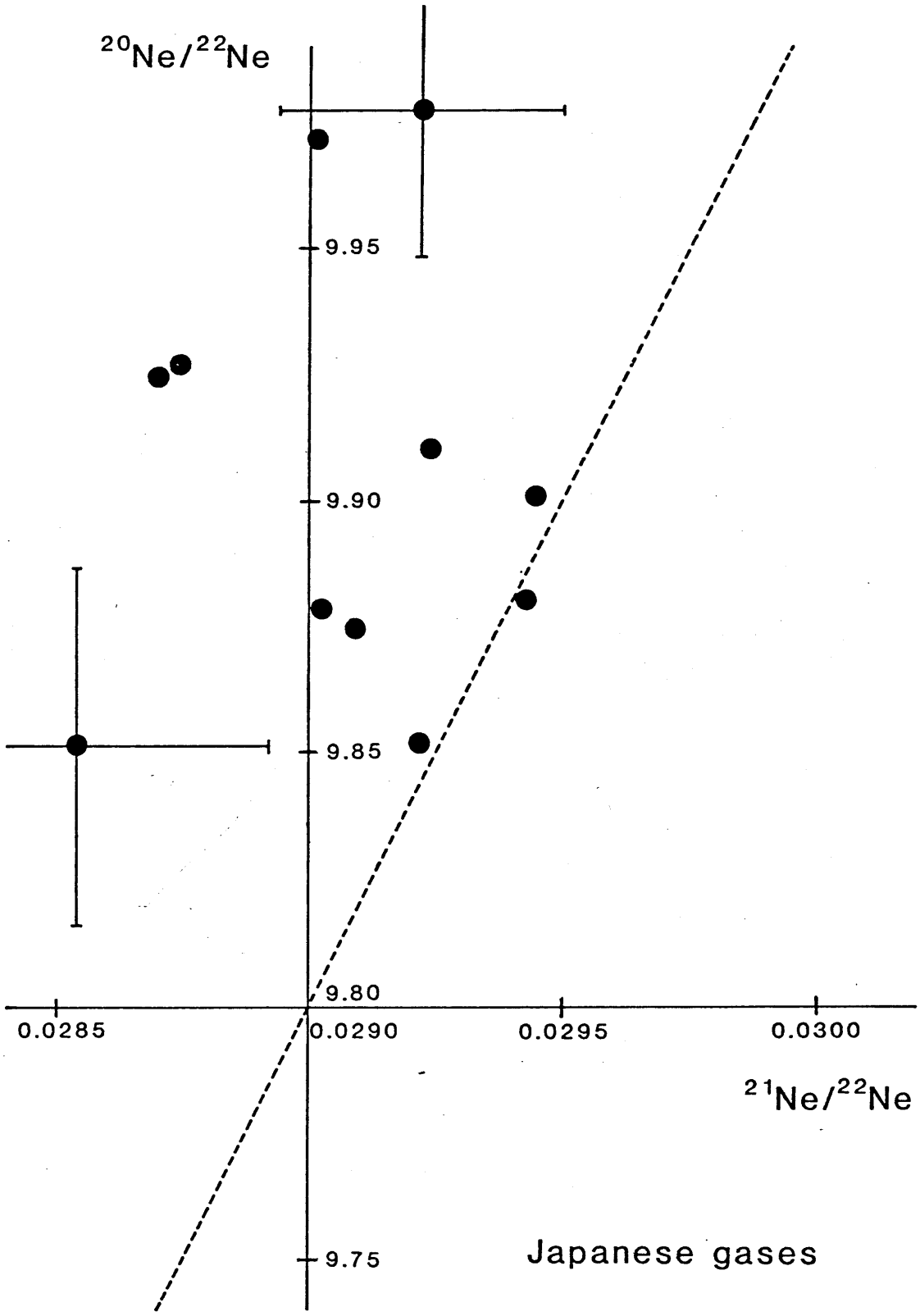

Figure 3-5. A correlation diagram of $^{20}Ne/^{22}Ne$ and $^{21}Ne/^{22}Ne$ in gaseous samples in the Japanese Islands. Some samples such as those from the Arime (hot spring) and Nakadori (petroleum well) seem to have excess ^{20}Ne. Considering relatively large error in the $^{21}Ne/^{22}Ne$, however, these samples are regarded still on the mass fractionation line.

Iceland

Though the $^{3}He/^{4}He$ ratio signature of Iceland has been well investigated, isotopic compositions of other rare gases, such as Ne and Ar are not well understood. I made Ne and Ar isotopic measurements together with $^{3}He/^{4}He$ ratio analyses for gaseous samples (Table 3-9).

Geysir 2 (#107) and Hveragirdi (#103) samples indicate slightly excess ^{20}Ne compared to the atmospheric $^{20}Ne/^{22}Ne$ ratio. However, as is shown in Figure 3-6, there are relatively large experimental error margins for $^{21}Ne/^{22}Ne$ ratios. Observed Ne isotopic compositions agree well with mass fractionated Ne from atmospheric air within a 2 sigma value of error. Figure 3-7 shows the relation between $^{40}Ar/^{36}Ar$ and $^{38}Ar/^{36}Ar$ ratios in gaseous samples. All samples, including strongly discriminated ones such as those from Krisuvik (#110) and Bjarharflag (#104), are just fitted to the mass fractionation line within experimental error margins. This implies that Ar in these samples is attributed to atmospheric Ar and that the contribution of radiogenic ^{40}Ar is small.

Consequently, Ne and Ar isotopic compositions of Icelandic gases are well explained by the fractionation of the atmospheric rare gases.

Table 3-9. Ne and Ar isotopic compositions of Icelandic samples

No.	Name	$^{20}Ne/^{22}Ne$ (x 1)	$^{21}Ne/^{22}Ne$ ($\times10^{-2}$)	$^{38}Ar/^{36}Ar$ ($\times10^{-1}$)	$^{40}Ar/^{36}Ar$ (x 1)
101	Krafla #15	9.787±0.035	2.921±0.029	1.911±0.019	304.9±2.3
102	Krafla #8	9.621±0.041	2.877±0.027	1.891±0.008	303.2±3.9
103	Hveragirdi	9.940±0.055	2.945±0.091	1.900±0.027	301.4±1.1
104	Bjarharflag	9.920±0.047	2.895±0.089	1.800±0.006	272.6±14.2
107	Geysiy 2	10.050±0.028	2.927±0.057	1.905±0.015	298.2±1.1
110	Krisuvik	9.919±0.047	2.910±0.023	1.792±0.005	277.2±4.8
111	Reykjanes 1	9.762±0.015	2.925±0.019	1.889±0.008	302.0±1.4
112	Reykjanes 2	9.815±0.017	2.905±0.034	1.856±0.005	293.4±19.3

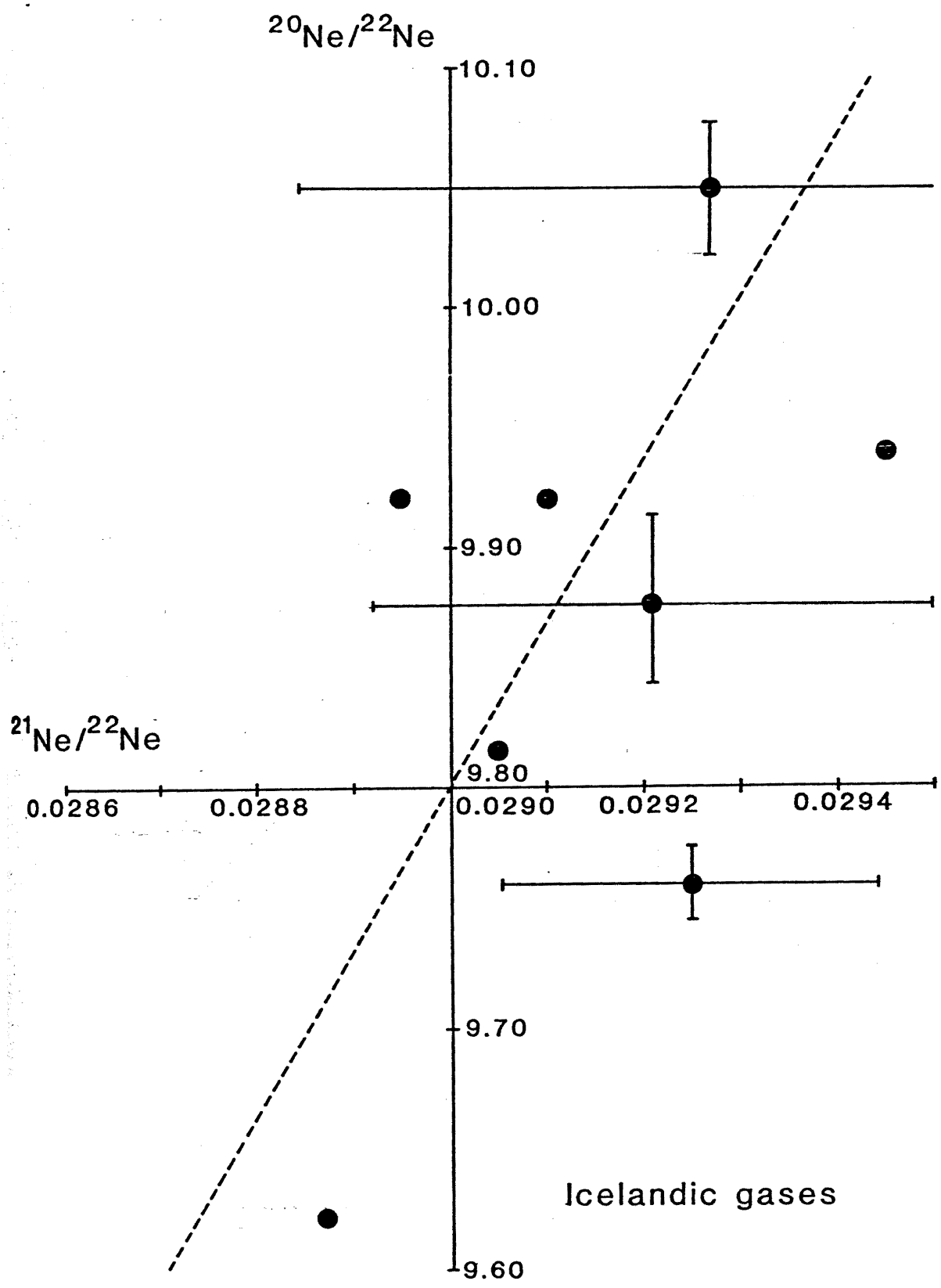

Figure 3-6. Correlation diagram of $^{20}Ne/^{22}Ne$ and $^{21}Ne/^{22}Ne$ in gaseous samples in Iceland. Some samples such as those from the Geysir and Hvergir indicate slight excess ^{20}Ne compared to the atmospheric $^{20}Ne/^{22}Ne$ ratio. However, there are relatively large experimental errors for the $^{21}Ne/^{22}Ne$ ratios, and the Ne isotopic composition agrees with mass fractionated Ne from the atmosphere.

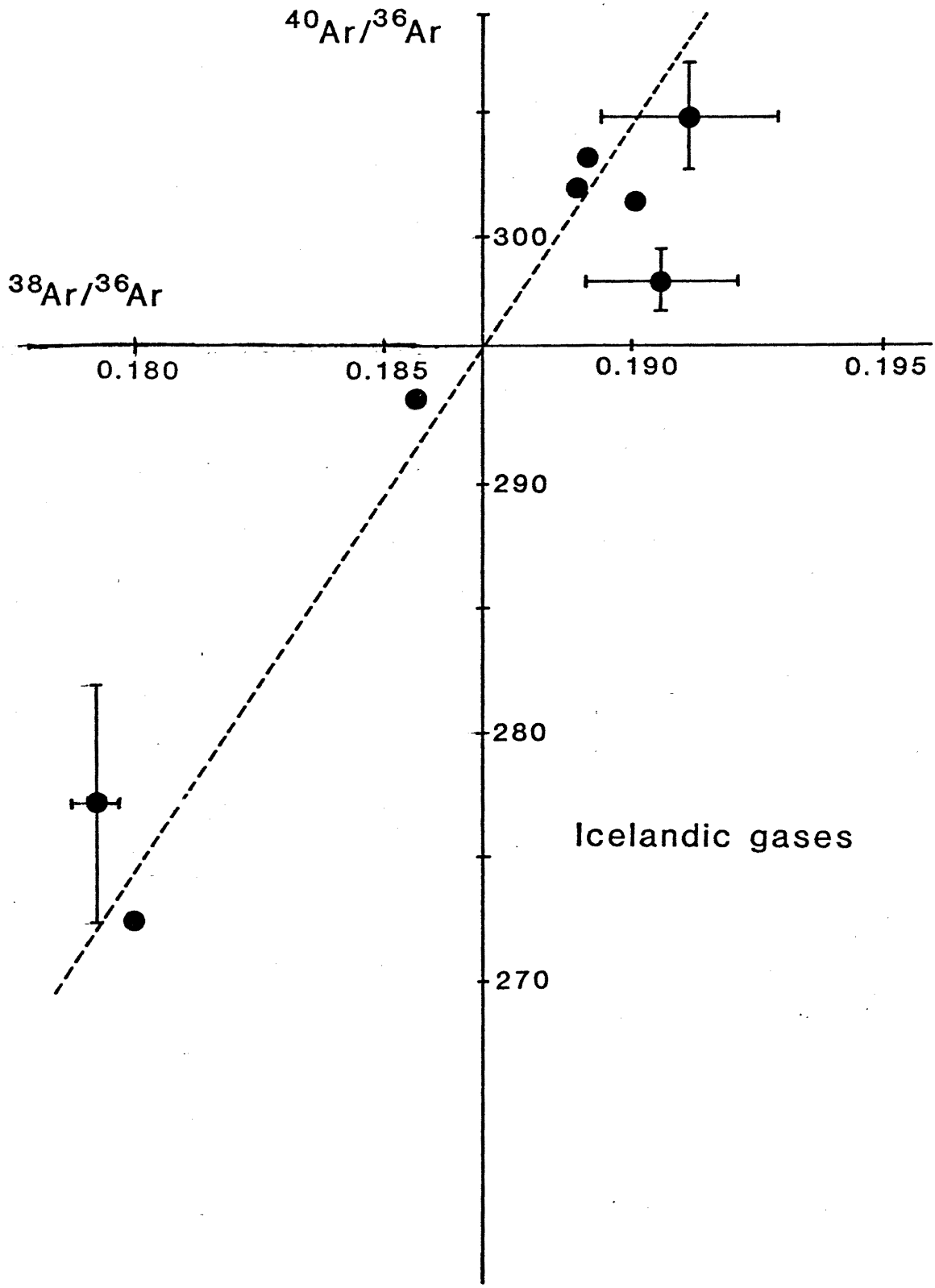

Figure 3-7. Correlation diagram of $^{38}Ar/^{36}Ar$ and $^{40}Ar/^{36}Ar$ in gaseous samples in Iceland. All samples, including strongly discriminated ones such as those from Krisuvik and Bjarharflag, are just fitted on the mass fractionation line within the experimental error.

IV. Discussion

4.1 He signatures in Japan and Iceland

4.1.1 $^{3}He/^{4}He$ and $^{20}Ne/^{4}He$ ratios of gaseous samples

a) Japanese Islands

The histogram of $^{3}He/^{4}He$ ratios observed in gaseous samples from Japan are shown in Figure 4-1. The $^{3}He/^{4}He$ ratios of natural gases of Japan reported by Nagao et al. (1981) are also included. Their data indicate that $^{3}He/^{4}He$ ratios have a log-normal distribution with a mean value of 8.0×10^{-6}, whereas those in this study have a large distribution in the mid-high ratios ($1.4 - 5.0 \times 10^{-6}$). This may reflect differences in sampling locality, features of gas discharging and geotectonic structure.

Since He has only two isotopes, we cannot identify whether it is atmospheric He or a mixture of mantle-derived and crustal He, if the observed $^{3}He/^{4}He$ ratio shows the value of about 1.4×10^{-6}. When there are more than two end members of He sources in the earth, more information will be needed to estimate the contribution of each He source. The $^{20}Ne/^{4}He$ ratio is a possible indicator for the purpose. ^{20}Ne is one of the family of rare gases, but its chemical properties resemble to those of He more closely than do other volatile elements. Among rare gases (Ne, Ar, Kr and Xe), the physical properties of ^{20}Ne are most similar to those of He because of the molecular radius. Therefore, ^{20}Ne may be

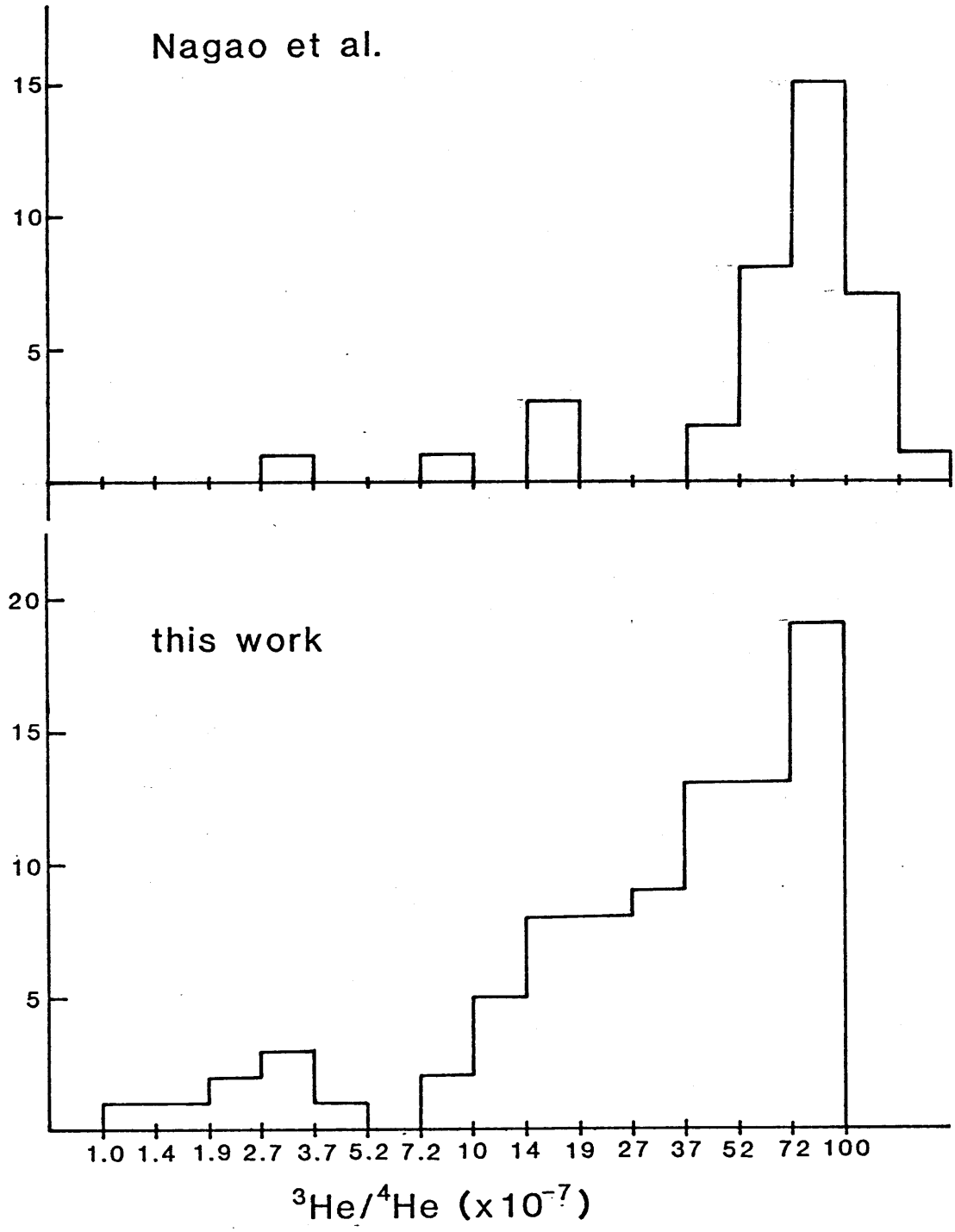

Figure 4-1. Histogram of $^3He/^4He$ ratios observed in gaseous samples in the Japanese Islands. The $^3He/^4He$ ratios reported by Nagao et al. (1981) are also shown in the upper part. Their data indicate that $^3He/^4He$ ratios have a log-normal distribution with a mean value of $8.0x10^{-6}$, whereas those of this study have a large distribution in mid-high ratios and a sharp cutoff at the highest range.

accompanied by He during transportation and is not easily fractionated by chemical and physical processes. The $^{20}Ne/^{4}He$ ratios of mantle-derived and crustal rare gases are usually smaller than that of the atmosphere, so we can easily identify the difference between the atmospheric He and a mixture of mantle He and crustal He.

Nagao et al. (1981) investigated the relation between the $^{3}He/^{4}He$ and $^{4}He/^{20}Ne$ ratios of natural gases in Japan and showed that most of the samples with high $^{4}He/^{20}Ne$ ratios contain He with high $^{3}He/^{4}He$ ratios and least contribution of crustal He. They concluded that the variations in $^{3}He/^{4}He$ ratios are mainly attributed to mixing between atmospheric He and He-rich gas with the $^{3}He/^{4}He$ ratio of 1.0×10^{-5}. In this study, such a tendency is not found between observed $^{3}He/^{4}He$ and $^{4}He/^{20}Ne$ ratios in gaseous samples.

The $^{3}He/^{4}He$ ratios for all gaseous samples from the Japanese Islands are plotted against the $^{20}Ne/^{4}He$ ratios in Figure 4-2. All data lie below the mixing line proposed by Nagao et al. (1981). Distribution of samples in the $^{3}He/^{4}He$ - $^{20}Ne/^{4}He$ diagram (Figure 4-2) shows a triangle-like shape, which suggests that there exist three end members. The first is atmospheric He with a $^{3}He/^{4}He$ ratio of 1.40×10^{-6}. The second one is mantle-derived He with $^{3}He/^{4}He$ ratios of about 1.0×10^{-5} (subduction-type He), and the third one is crustal He with a value of about 1.0×10^{-8}.

b) Iceland

In 1974, Kononov et al. carried out the extensive work

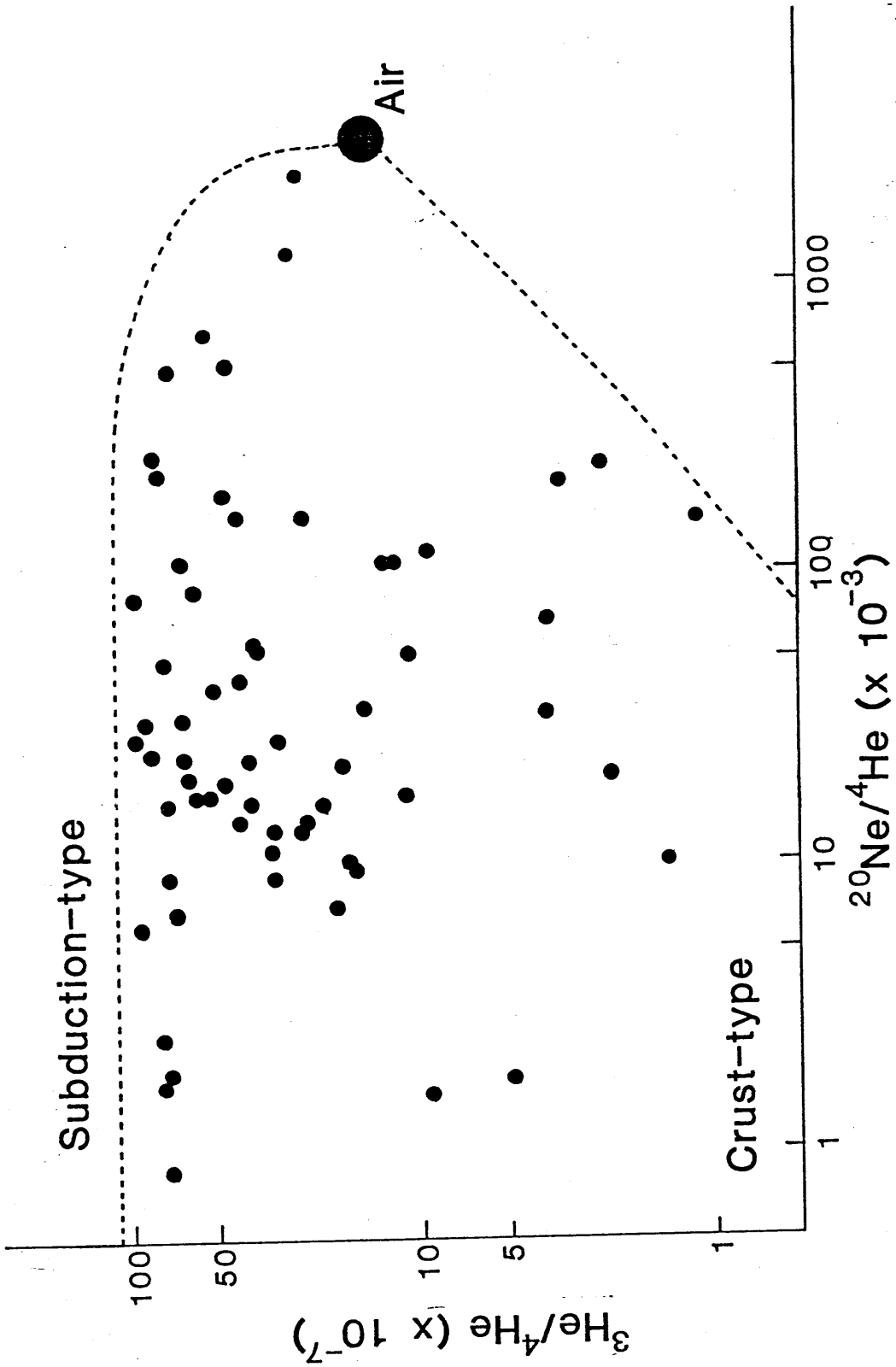

Figure 4-2. Correlation between the $^{3}He/^{4}He$ and $^{20}Ne/^{4}He$ ratios in Japanese samples. Samples are distributed in a triangle-like region. This suggests that there exist three end members: atmospheric He, subduction-type He and crust-type He. The $^{3}He/^{4}He$ ratio of subduction-type He is 1.1×10^{-5}.

of mapping the distribution of He isotopic composition in Icelandic thermal fluid. According to their results, the northeastern part of the island shows the $^3He/^4He$ ratios ranging from 1.2×10^{-5} to 1.4×10^{-5}, whereas the area surrounding the Hekla volcano, in the southern part of the island, shows apparently higher $^3He/^4He$ ratios than those of the northeastern part with values of up to 3.3×10^{-5}. Kononov et al. (1974) concluded that the earth's mantle has He with $^3He/^4He$ ratio of $(3 \pm 1) \times 10^{-5}$ and that lower values such as 1.2×10^{-5} may be explained by dilution of the crustal He.

Observed $^3He/^4He$ ratios in this study (Table 3-4) vary from 2.94×10^{-6} to 2.35×10^{-5} and agree well with the results of Kononov et al. (1974). Icelandic samples are plotted in a $^3He/^4He$ - $^{20}Ne/^4He$ diagram (Figure 4-3). They have apparently higher $^3He/^4He$ ratios than the Japanese samples and are distributed within a mixing region of three end members. The first is atmospheric He. The second is mantle-derived He (MOR-type) with a $^3He/^4He$ ratio of about 1.3×10^{-5}, the third is also mantle-derived He but distinct from MOR-type He with a $^3He/^4He$ ratio of about 5.0×10^{-5} (Plume-type).

4.1.2 Source of He in gas samples of Japan and Iceland

Two mechanisms for changing the $^3He/^4He$ ratio exist in addition to the mixing of proposed end members. One is mass

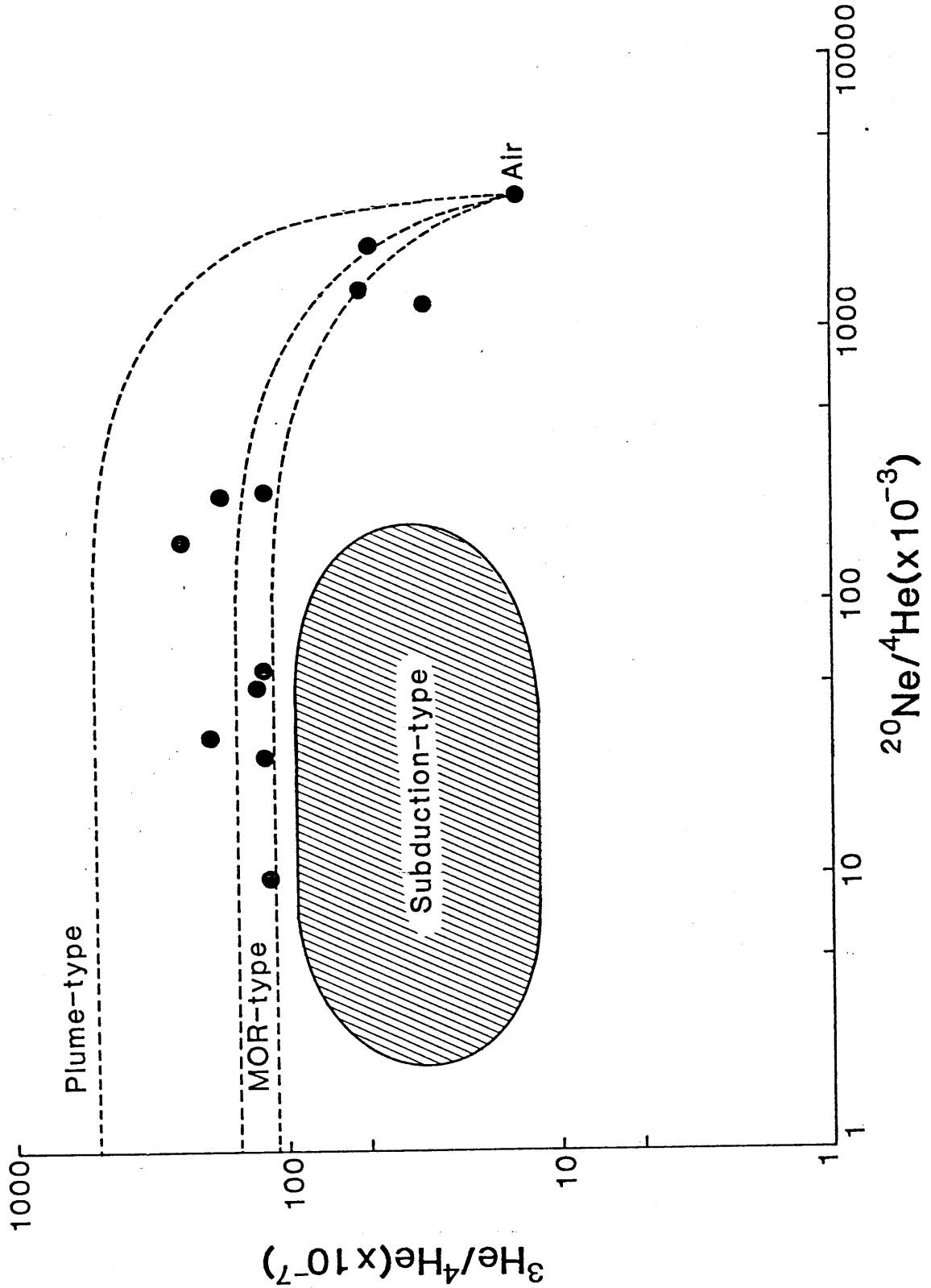

Figure 4-3. Correlation between the $^{3}He/^{4}He$ and $^{20}Ne/^{4}He$ ratio in Icelandic samples. Distribution of samples in the figure suggests that there exist three end members: atmospheric He, plume-type He and MOR-type He. The $^{3}He/^{4}He$ ratio of plume-type He is 5.0×10^{-5}. The $^{3}He/^{4}He$ ratio of MOR-type He is 1.25×10^{-5}.

fractionation of He and the other is the decay of ^{3}H.

Mass fractionation of He in gaseous samples may be attributed to the two processes. One is the solubility difference between ^{3}He and ^{4}He in the water. As gaseous samples may be affected by several stages of equilibrium between water and gas phases, mass fractionation may be significant. However, the $^{3}He/^{4}He$ ratio of fresh water observed in this study ($1.27\pm0.13 \times 10^{-6}$), which is in equilibrium condition with the atmosphere, agrees well with that of the atmosphere (1.40×10^{-6}) within the margin of experimental error. Therefore, fractionation due to solubility difference is not so important. The other process is partitioning of ^{3}He and ^{4}He between glass and crystal or among several minerals. Isotopic fractionation may occur during the mineral growth in the melt. The bulk of rock-forming minerals do not retain He, so that over 80 % of the He in rock is lost into underground fluids (Gerling, 1957). Therefore the different isotopic composition of He among minerals is averaged out and the fractionation may be neglected.

The other mechanism for changing the $^{3}He/^{4}He$ ratio is the decay of ^{3}H produced by nuclear explosions. ^{3}H is incorporated into rain and joins in the hydrological cycle. ^{3}He is produced by the beta decay of ^{3}H with a mean life of 18 years. Torgersen and Jenkins (1982) calculated the change of $^{3}He/^{4}He$ ratio based on this process. If 1000 T.U. of ^{3}H in rain during 1963 were allowed to decay in a closed system

for 25 years, a $^{3}He/^{4}He$ ratio similar to the mantle He would be result. A mixing of this 1000 T.U. ^{3}H in 1963 rain with crustal He produces almost the same value of the $^{3}He/^{4}He$ ratio as that observed in this study. Though such water should still contain over 250 T.U. ^{3}H, hot spring water, mineral spring water and deep well water in Japan generally contain less than 1 T.U. ^{3}H (Tanaka, 1974). Therefore, ^{3}He from ^{3}H decay is insignificant in this study.

Figure 4-4 shows a schematic diagram of the He isotopic signature for the earth. The primary components of He sources are primordial He such as MOR-type and plume-type, and radiogenic He such as oceanic crust and sediment and continental crust. Atmospheric He and subduction-type He are thought to be secondary components. Atmospheric He is a mixture of all the primary components degassed from the solid earth. Subduction-type He is a mixture of MOR-type and oceanic crust and sediment He. The $^{3}He/^{4}He$ and $^{20}Ne/^{4}He$ ratios of each source are estimated as follows:

a) Atmospheric He

The earth's atmosphere contains He in a concentration of 5.24×10^{-6} by volume, with an isotopic ratio for $^{3}He/^{4}He$ of 1.40×10^{-6}; this value is an average of three isotopic determinations by Mamyrin et al. (1970), Clark et al. (1976) and this work. The atmosphere also contains Ne in a concentration of 1.81×10^{-5} by volume, with isotopic ratios of $^{20}Ne/^{22}Ne$ (9.80) and $^{21}Ne/^{22}Ne$ (0.0290). Then the $^{20}Ne/^{4}He$ ratio of the atmosphere is easily calculated to be

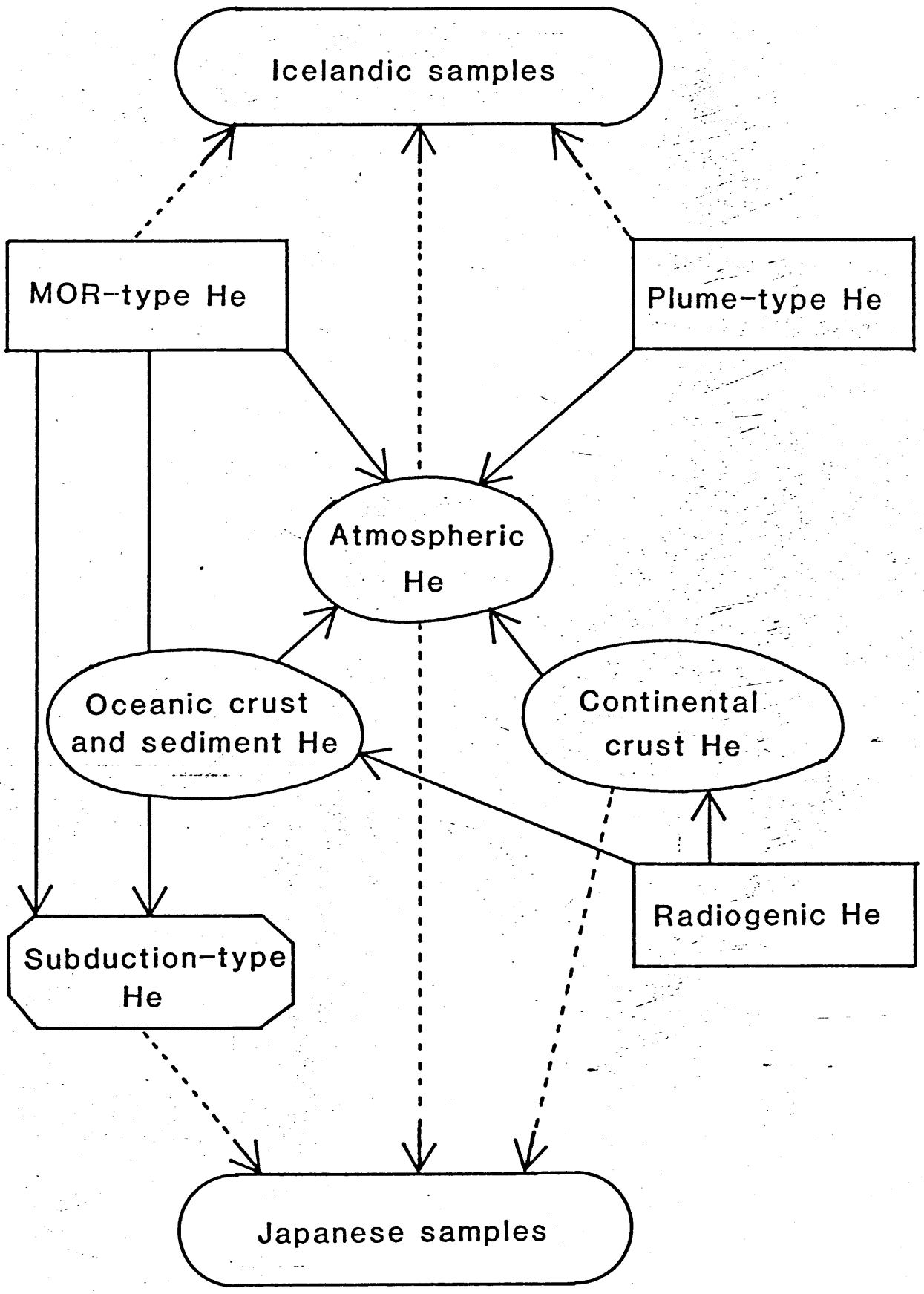

Figure 4-4. Schematic diagram of the He isotopic signature for the earth.

3.15.

b) MOR-type He

The $^{3}He/^{4}He$ ratios in young oceanic ridge basalts are very uniform for samples collected at different plate boundaries. The average $^{3}He/^{4}He$ ratio ($1.25\pm0.15 \times 10^{-5}$) for basalts is accepted as the He signature for the upper mantle (MOR-type).

On the other hand, the $^{20}Ne/^{4}He$ ratios and He concentrations in oceanic basalts are rather fluctuating irrespective of quite uniform $^{3}He/^{4}He$ ratios. Large variations in $^{20}Ne/^{4}He$ ratios, by more than three orders of magnitude, may be attributed to the following mechanisms: 1) dilution by in-situ radiogenic ^{4}He production; 2) diffusive loss of ^{4}He from basalt glass; 3) contamination by the atmospheric rare gases dissolved in sea water; and 4) mantle heterogenity for $^{20}Ne/^{4}He$ ratio.

If the dilution by in-situ radiogenic ^{4}He production is valid, $^{3}He/^{4}He$ ratio should decrease when the $^{20}Ne/^{4}He$ ratio increases. However, the $^{3}He/^{4}He$ ratio is almost constant so the first hypothesis is not likely. Kurz and Jenkins (1981) concluded that no significant diffusion will take place in less than 100 Ma for the typical basalt rim. Since analyzed oceanic basalts are younger ones, the second hypothesis is also not suitable. Dissolved atmosphere in sea water has higher Ne and lower He concentration than oceanic basalts, and most basalts glasses are products of active interaction between melting lava and sea water. Therefore, contamination

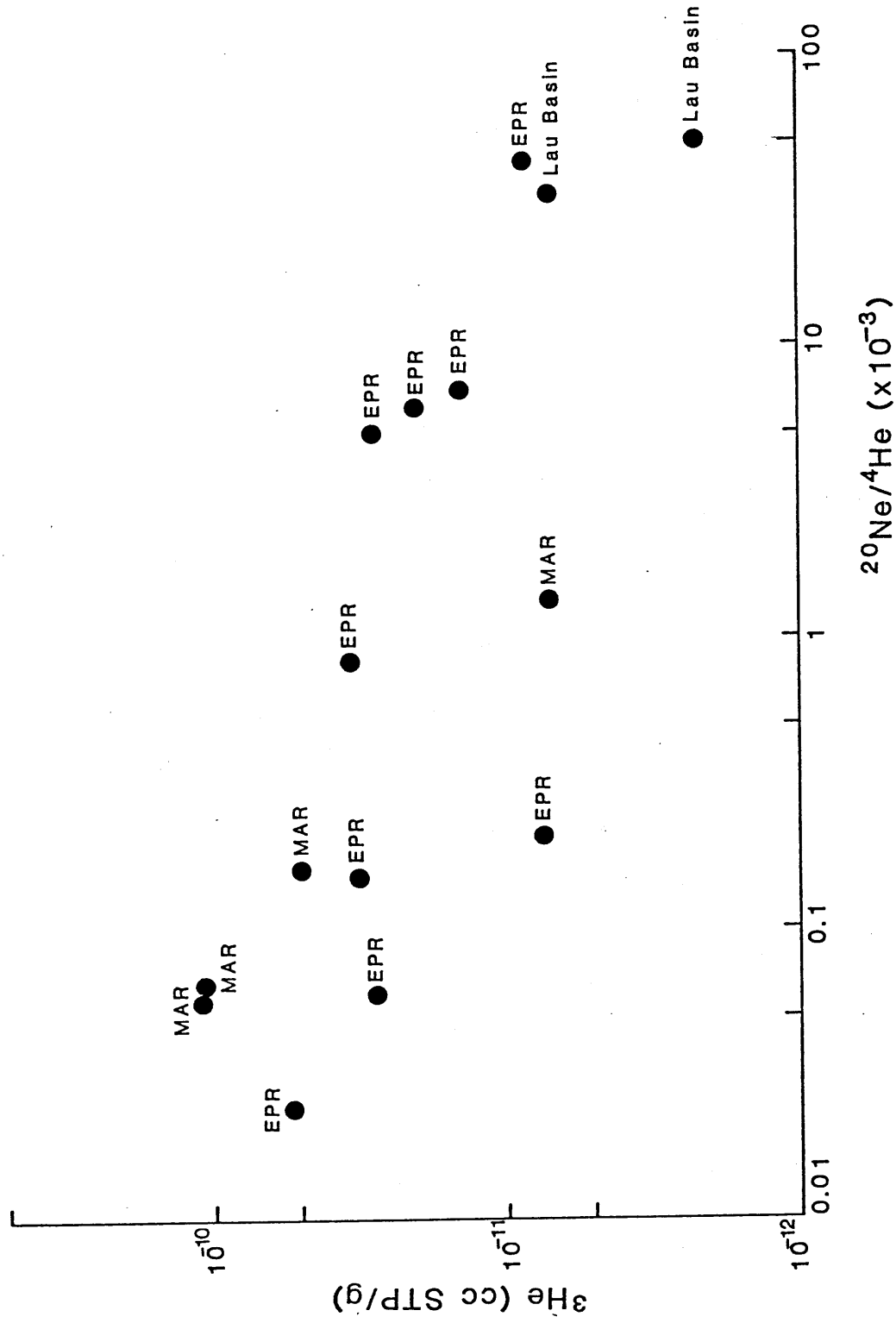

Figure 4-5. Correlation between ^{3}He contents and $^{20}Ne/^{4}He$ ratios in Mid-Oceanic Ridge Basalts (MORBs). Data are from Lupton and Craig (1975); Craig and Lupton (1976); Rison (1980)

by the atmospheric rare gases is plausible.

Figure 4-5 shows the relation between ^{3}He contents in MORB and $^{20}Ne/^{4}He$ ratios (Lupton and Craig, 1975, Lupton and Craig, 1976 and Rison, 1981). The higher is the ^{3}He content, the lower the $^{20}Ne/^{4}He$ ratio becomes. This tendency suggests that the variations in $^{20}Ne/^{4}He$ ratios in oceanic basalt samples are attributable to the extent of atmospheric contamination and not to mantle heterogenity. In this study, the $^{20}Ne/^{4}He$ ratio of the upper mantle material is assumed to be 2×10^{-5}, based on the values of uncontaminated oceanic basalt samples. If the $^{20}Ne/^{4}He$ ratio is assumed to be the highest among oceanic basalts, there is no change in calculated mantle contribution.

c) Subduction-type He

The $^{3}He/^{4}He$ ratios of volcanic gases from the Circum-Pacific zone, such as Kamchatka, Mt. Lassen and New Zealand, are up to 1.1×10^{-5}, and the maximum value is surprisingly uniform. Table 4-1 shows the highest $^{3}He/^{4}He$ ratios along a major sections of the convergent boundaries of the Circum-Pacific zone. The $^{3}He/^{4}He$ ratios of volcanic gases and geothermal fluids from Mt. Lassen in Calfornia (Craig et al., 1978), Uzon caldera in Kamchatka (Baskov et al., 1973), and Wairakei in New Zealand (Torgersen et al., 1982) are quite uniform; however, those of Agrihan Island in the Marianas (Craig et al., 1978), Kunashir Island in the Kurils (Baskov et al., 1973), and Honshu Island in Japan are sligtly lower than 1.1×10^{-5}. The maximum value ($1.1 \times$

Table 4-1. Subduction-type He

Name	Place	$^{3}He/^{4}He$ ($\times10^{-7}$)	$^{20}Ne/^{4}He$ ($\times10^{-3}$)
Mt. Lassen	California	113	<1.2
Agriham Island	Mariana	92	370
Uzon Caldera	Kamchatka	113	61
Kunashir Island	Kuril	88	-
Wairakei	New Zealand	115	3.5
Honshu Island#	Japan	96.5	62

#: this work.

Table 4-2. Plume-type He

Name	Place	$^{3}He/^{4}He$ ($\times10^{-7}$)	$^{20}Ne/^{4}He$ ($\times10^{-3}$)
Haleakala	Hawaii	515	6.3
Loihi	Hawaii	441	-
Kilauea	Hawaii	209	0.55
Yellowstone	Wyoming	216	-
Geysir2#	Iceland	235	170

#: this work.

10^{-5}) is accepted as the He signature for subduction-type magma.

The $^{3}He/^{4}He$ ratio of the subduction-type He is slightly lower than that of the MOR-type He. This implies that the $^{3}He/^{4}He$ ratio of the mantle material involved in the generation of andesitic and more acidic lavas at convergent plate margins are affected by some radiogenic contamination with lower $^{3}He/^{4}He$ ratios. This radiogenic material may be attributed to the remelted subducted oceanic crust or to sedimentary materials.

The $^{20}Ne/^{4}He$ ratios vary significantly from less than 1.2×10^{-3} to 3.7×10^{-1} irrespective of the uniform $^{3}He/^{4}He$ ratio. The high $^{20}Ne/^{4}He$ ratio may be attributed to contamination by the atmospheric rare gases. Hence, the lowest ratio of 1.0×10^{-3} is assumed as the subduction type $^{20}Ne/^{4}He$ ratio.

d) Plume-type He

Volcanic gases, ultramafic nodules and alkali basalts from the Hawaiian Islands show extremely high $^{3}He/^{4}He$ ratios (Craig and Lupton, 1976; Kaneoka and Takaoka, 1980; Kurz et al., 1982). The value of $(2 - 5) \times 10^{-5}$ is significantly higher than that for MOR-type He. In several other regions such as Iceland (Polak et al., 1975), Yellowstone (Craig et al., 1978) and the Ethiopian Rift Valley (Craig and Lupton, 1978), the $^{3}He/^{4}He$ ratios vary considerably; however, the highest ratio for each area is apparently higher than MOR-type He. These regions with the extremely high $^{3}He/^{4}He$

ratios seem to be closely related to so-called hot spots. Actually the precise nature of hot spots is not understood, but the geological evidence from both ocean basins and continents indicates that locally the mantle must be sufficiently hot to produce relatively large volumes of magma without the benefit of plate boundary processes. On the basis of the He isotope signature, whether what is occuring is physical upwelling of deep mantle material with a high $^3He/^4He$ ratio or upwelling of heterogeneous upper mantle material with a high $^3He/^4He$ ratio is not clear.

As is shown in Table 4-2, the highest $^3He/^4He$ ratio of about 5×10^{-5} is obtained for ultramafic nodules from Haleakala volcano (Kaneoka and Takaoka, 1980). This value is assumed as the He signature for the Plume-type He. Effort has been made to measure the $^{20}Ne/^4He$ ratios of hot spots. The $^{20}Ne/^4He$ ratios of Kilauea volcanic gas (Craig and Lupton, 1976) is assumed as the Plume-type $^{20}Ne/^4He$ ratio.

e) Continental crustal He

Detailed calculations by Morrison and Pine (1955) showed that the crustal production of ^3He in the continental crust is accounted for by nuclear reactions: $^6Li(n,\alpha)^3H(\beta^-)^3He$, and that the normal "crustal $^3He/^4He$ ratio" is calculated to be 10^{-7} based on the concentration of Li, U and Th in the crustal rock.

Later Gorshkov et al. (1966) improved the method for calculating the $^3He/^4He$ ratio in rocks and made some of the attendant parameters more exact. Comparison between the

measured and calculated $^{3}He/^{4}He$ ratios was carried out by Gerling et al. (1971). According to Zartman et al. (1961), crustal He in natural gases is not the He accumulated by the decay of highly concentrated U and Th in the deposit but is the He by the massive averaged granitic rocks. The $^{3}He/^{4}He$ ratio of crustal He should be calculated based on the averaged granitic rock. I made a calculation following the method of Gorshkov et al., (1966). The calculated result is 1.5×10^{-8} for averaged granitic rock.

Wetherill (1954) indicated that ^{20}Ne was also produced by the nuclear reaction: $^{17}O(\alpha,n)^{20}Ne$. Rison (1980) calculated that the production rate of ^{20}Ne in the crust is 3.7×10^{-21} cc STP/g yr. I made a similar calculation for the $^{20}Ne/^{4}He$ ratio based on the averaged granitic rock and the calculated ratio is 9.4×10^{-9} .

f)Oceanic crust and sediment He

Calculation for the $^{3}He/^{4}He$ and $^{20}Ne/^{4}He$ ratios of oceanic crust and sediment are made based on the concentration of Li, U and Th in the averaged subducting materials. The calculated $^{3}He/^{4}He$ and $^{20}Ne/^{4}He$ ratios are 1.2×10^{-7}, 5.0×10^{-8}, respectively.

4.1.3 Contribution of each component in natural gases in Japan

When He and Ne in natural gas samples are composed of atmosphere (A), continental crust (C) and subduction-type mantle (M)

components, the following equations are derived:

$$(^3He/^4He)_s = (^3He/^4He)_m \times M + (^3He/^4He)_c \times C + (^3He/^4He)_a \times A$$

$$(^{20}Ne/^4He)_s = (^{20}Ne/^4He)_m \times M + (^{20}Ne/^4He)_c \times C + (^{20}Ne/^4He)_a \times A$$

$$M + C + A = 1$$

where subscript s, m, c and a represent sample, subduction type, continental crust and atmosphere, respectively.

Since the $^{20}Ne/^4He$ ratio of the atmosphere is significantly higher than those of the mantle and crust, it is possible to use the ratio as an indicator of air contamination. The corrected He isotopic ratio of gaseous samples due to air incorporation during sampling and natural incorporation as a part of the hydrological cycle is obtained from the following calculation:

$$(^3He/^4He)_{corr.} = ((^{20}Ne/^4He)_a \times (^3He/^4He)_s - (^3He/^4He)_a \times (^{20}Ne/^4He)_s)/((^{20}Ne/^4He)_a - (^{20}Ne/^4He)_s)$$

The mixing ratios of the three components, subduction type mantle, continental crust and atmosphere, were calculated for typical samples and are shown in Table 4-3. A similar approach for estimating the mixing ratios of these three components in natural gases was made by Kamenskiy et al. (1976).

The calculated contribution of subduction-type mantle in samples with high $^3He/^4He$ ratios from Shirahone (#52) and Arima (#85) hot springs and Satsumaio-iodake (#98) volcanic fumarole are 87.5 %, 83.7 % and 86.5 %, respectively.

Table 4-3. Mixing ratio of each component

No.	Name	$^{3}He/^{4}He$ ($\times10^{-7}$)	$^{20}Ne/^{4}He$ ($\times10^{-3}$)	Mantle (%)	Crust (%)	Air (%)
28	Awanoyu	90.1	5.9	81.9	17.9	0.2
42	Heiwajima	1.37	10	1.1	98.6	0.3
52	Shirahone	96.5	62	87.5	10.6	1.9
53	Meiji	92.4	83	83.7	13.7	2.6
65	Omaezaki	1.02	150	0.2	95.1	4.7
81	Byakko	11.0	17	9.8	89.7	0.5
82	Aichyuya	17.3	10	15.6	84.1	0.3
85	Arima	92.2	27	83.7	15.5	0.8
90	Shikano	16.6	9.4	14.9	84.8	0.3
98	Satsuma-iodake	95.4	59	86.5	11.7	1.8
100	Itoman	0.747	2.9	0.5	99.4	0.1

Therefore, the Island Arc type magma in Japan is characterized as having 90 % of subduction-type He and 10 % crustal He. Itoman (#100) natural gas and Heiwajima (#42) and Omaezaki (#65) water well gases show almost pure crustal origin at more than 95 %; mantle contribution is very small. Hence, emission of primordial He in the Island Arc is not observed everywhere but only in limited regions such as volcanic and geothermal areas. Hot springs and mineral springs at Shikano (#90), Byakko (#81) and Yuya (#82) show $^{3}He/^{4}He$ ratios similar to that of the atmosphere. However, He is greatly enriched in these samples when their $^{20}Ne/^{4}He$ ratios are compared to that of the atmosphere. Calculated atmospheric contribution is negligibly small and observed $^{3}He/^{4}He$ ratios are explained by mixing of subduction-type He (15 %) and crustal He (85 %).

Consequently, $^{3}He/^{4}He$ ratios of gaseous samples in the Japanese Islands are not uniform but show large variation, which is attibuted to the mixing of three components, atmospheric He, subduction-type mantle He and crustal He.

4.1.4 He signature in Iceland

There are some common features between the Japanese Islands and Iceland. Both islands have many hot springs, active volcanoes and earthquakes. However, from the view point of geotectonic structure, Iceland is clearly different from the Japanese Islands. One of the differences is that

stress field of the Japanese Islands is compressional, while that of Iceland is tensional. In Iceland, there are no deep earthquake. The volcanoes are fissure type and are distributed symmetrically with respect to the central belt (median zone). The belt has many faults, linear fractures and volcanoes and is considered to be located on the Mid-Atlantic Ridge. The comparison of rare gas isotopic ratios between Iceland and the Japanese Islands is tectonically important, since Iceland lies on a divergent plate boundary, whereas the Japanese Islands are on a convergent plate boundary.

The distribution of the $^{3}He/^{4}He$ ratios observed for the present study in Iceland agrees well with that of Kononov et al. (1974). Figure 2-22 shows sampling points and observed $^{3}He/^{4}He$ ratios of thermal fluids and gaseous samples in this study. Gaseous samples collected at the northeastern part of the central belt have typical MOR-type ratios ranging from 1.12×10^{-5} to 1.26×10^{-5}. Therefore, the northeastern part of the island is considered to be a normal MOR-region. On the other hand, samples collected at the southern part of the island, excluding strongly air-contaminated samples such as Laugarvatu (#108), Reykjanes Geysir (#109) and Reykjanes 1 (#111), indicate that the southern part has some contribution of more primitive He from the mantle distict of the MOR-type.

The extremely low contribution of the crustal He in Icelandic samples compared to those from the Japanese Islands

is explained by the absence of crustal materials in a divergent type of plate boundary.

4.2 He isotopic distribution in various geotectonic provinces of the Japanese Islands

He isotopic studies of terrestrial samples during the past decade have shown that the $^3He/^4He$ ratio of mantle-derived He is not uniform and that variation of the ratio is found in association with different tectonic environments such as the Mid-Oceanic Ridge, Island Arc and Hot Spot. Craig et al. (1978) found elevated and uniform $^3He/^4He$ ratios in volcanic gases from the Circum-Pacific volcanoes. However, in this study a large variation in $^3He/^4He$ ratios was observed in the Japanese Islands. For example, some natural reservoirs show radiogenic He ratios. In order to explain the variation in the ratio, the relation between the $^3He/^4He$ ratio and the geotectonic structure of the sampling region was investigated.

4.2.1 $^3He/^4He$ ratios in sedimentary plains

The Kanto Plain extends on the coastal side of the volcanic front in the North-East Japan Arc. The plain is a large later Cenozoic sedimentary basin. The Tertiary mountains surrounding the plain become low toward the plain, and their basement is continuous with Neogene granitic rock beneath the sediment. The thickness of the sedimentary layer is more than 2000 m at the northwest side of the plain (near Takasaki) and to the north of Tokyo Bay. In the

central-south part of the plain, the thickness becomes more than 4000 m. At the Iwatsuki deep well drilled for seismological research, the bottom of Neogene is 2900 m deep. The upper, about 2000 m layer above the basement is composed of Miocene sandstone, mudstone, conglomerate and tuff. This layer is covered with Quaternary oceanic sediment called the Kazusa formation, about 800 m deep (Kakimi et al., 1973; Fukuda et al., 1974). There are large amounts of CH_4-rich natural gases incorporated with saline water in the Kazusa formation.

Figure 4-6 shows the sampling locations of CH_4-rich natural gases in the plain and the $^3He/^4He$ ratios together with the thickness of the sedimentary layer. The samples from Narashino (#38), Yokoshiba (#39), Shirako (#40) and Chonan (#41) are fuel gases from gas fields in the southern Kanto Plain, where large-scale artificial pumping of underground water has been carried out to obtain fuel gas in the area. The discharging rates of gases are greater than 5000 m^3/d. These samples are characterized by high concentrations of CH_4, up to more than 90 %, and He content less than one-tenth that of the atmosphere. Heiwajima (#42) water well gas was collected on the coast of Tokyo Bay. The chemical characteristics of the well are similar to those of the fuel gas in the southern Kanto Plain.

The $^3He/^4He$ ratios of these samples are apparently lower than that of the atmosphere; they vary from 1.37×10^{-7} to 3.49×10^{-7}. These low ratios reflect well the non-magmatic

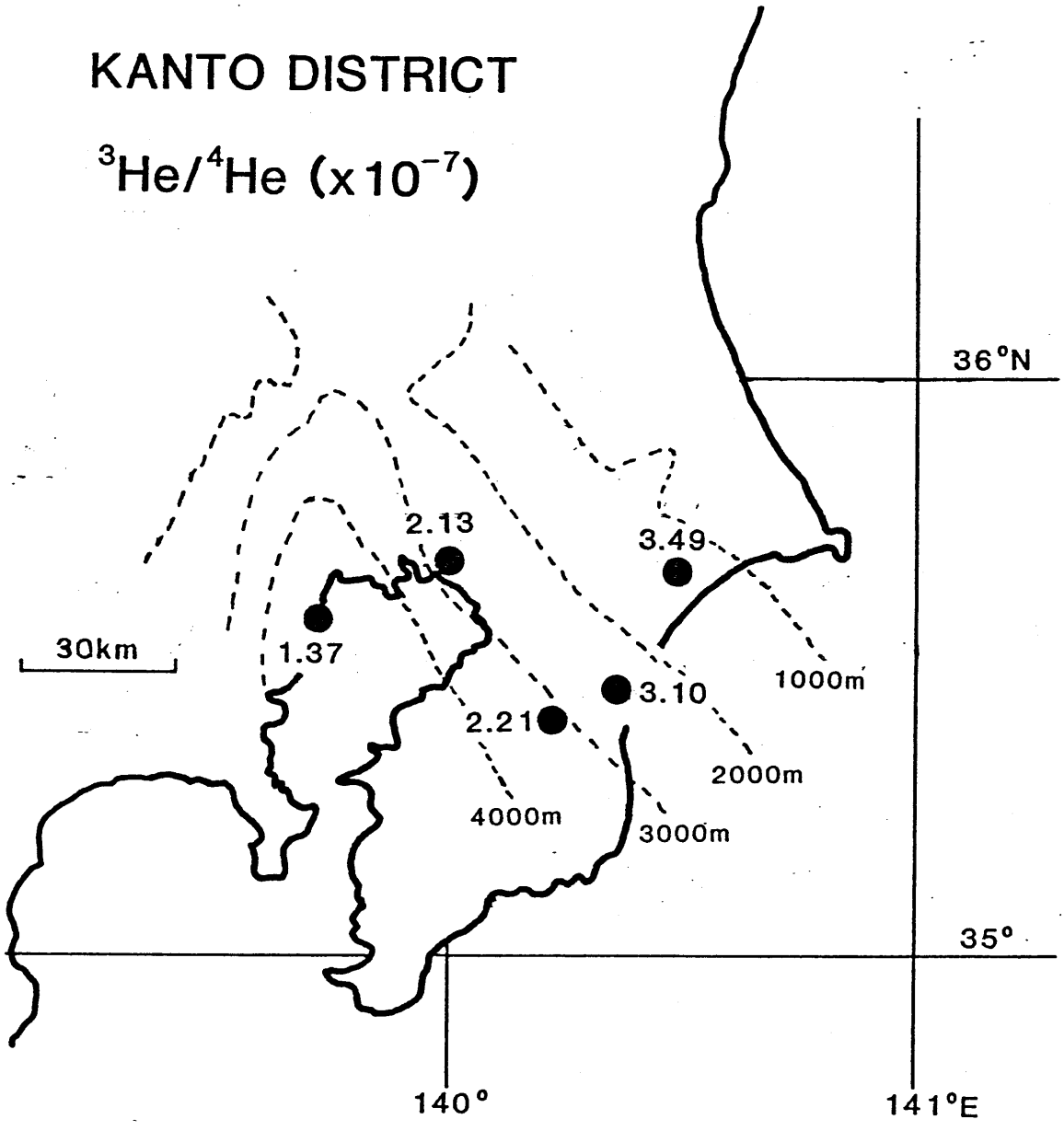

Figure 4-6. Sampling locations and the $^3He/^4He$ ratios of CH_4-rich natural gases in the Kanto Plain. The unit of the $^3He/^4He$ ratio is expressed as 10^{-7}. The thickness of the sedimentary layer is also shown.

features of the region. As is shown in Figure 4-6, there is a close relation between the thickness of sedimentary layer and the $^3He/^4He$ ratio of CH_4-rich natural gas. Table 4-4 indicates the thickness of the layer, the observed $^3He/^4He$ ratios and the corrected $^3He/^4He$ ratios for atmospheric contamination. At the Heiwajima (#42) well, the thickness of the layer is larger than 4000 m and the $^3He/^4He$ ratio is 1.33×10^{-7}. Yokoshiba (#39) natural gas has the highest $^3He/^4He$ ratio among them and its thickness is smallest at about 1500 m. The thicker the sedimentary layer is, the lower is the $^3He/^4He$ ratio observed. This tendency suggests that He with a low $^3He/^4He$ ratio in these samples is mainly radiogenic He produced by the radioactive decay of U and Th in the sedimentary materials. The contribution of the radiogenic He becomes larger in thicker sedimentary layers.

The corrected $^3He/^4He$ ratios are plotted against the thickness of the sedimentary layer in Figure 4-7. The relation between the $^3He/^4He$ ratio and the thickness is described as:

$$(^3He/^4He)_d = -7.06 \times 10^{-11} \times d + 3.94 \times 10^{-7}$$

where d and $(^3He/^4He)_d$ denote the thickness of the sedimentary layer and the $^3He/^4He$ ratio corresponding. On the surface where the thickness equals 0 m, the $^3He/^4He$ ratio according to the equation is to be 3.94×10^{-7}, which is apparently higher than the calculated $^3He/^4He$ ratio (1.5×10^{-8}) assuming average granitic rock due to nuclear reactions. There should be a slight contribution of the

Table 4-4. Thickness of sedimentary layer in the southern Kanto district and corrected $^{3}He/^{4}He$ ratio

No.	Name	$^{3}He/^{4}He$ ($\times10^{-7}$)	$^{20}Ne/^{4}He$ ($\times10^{-3}$)	$(^{3}He/^{4}He)_{corr.}$ ($\times10^{-7}$)	thickness (m)
38	Narashino	2.13	20	2.05	2100
39	Yokoshiba	3.49	71	3.25	1300
40	Shirako	3.10	210	2.32	2600
41	Chonan	2.21	240	1.24	3500
42	Heiwajima	1.37	10	1.33	4000

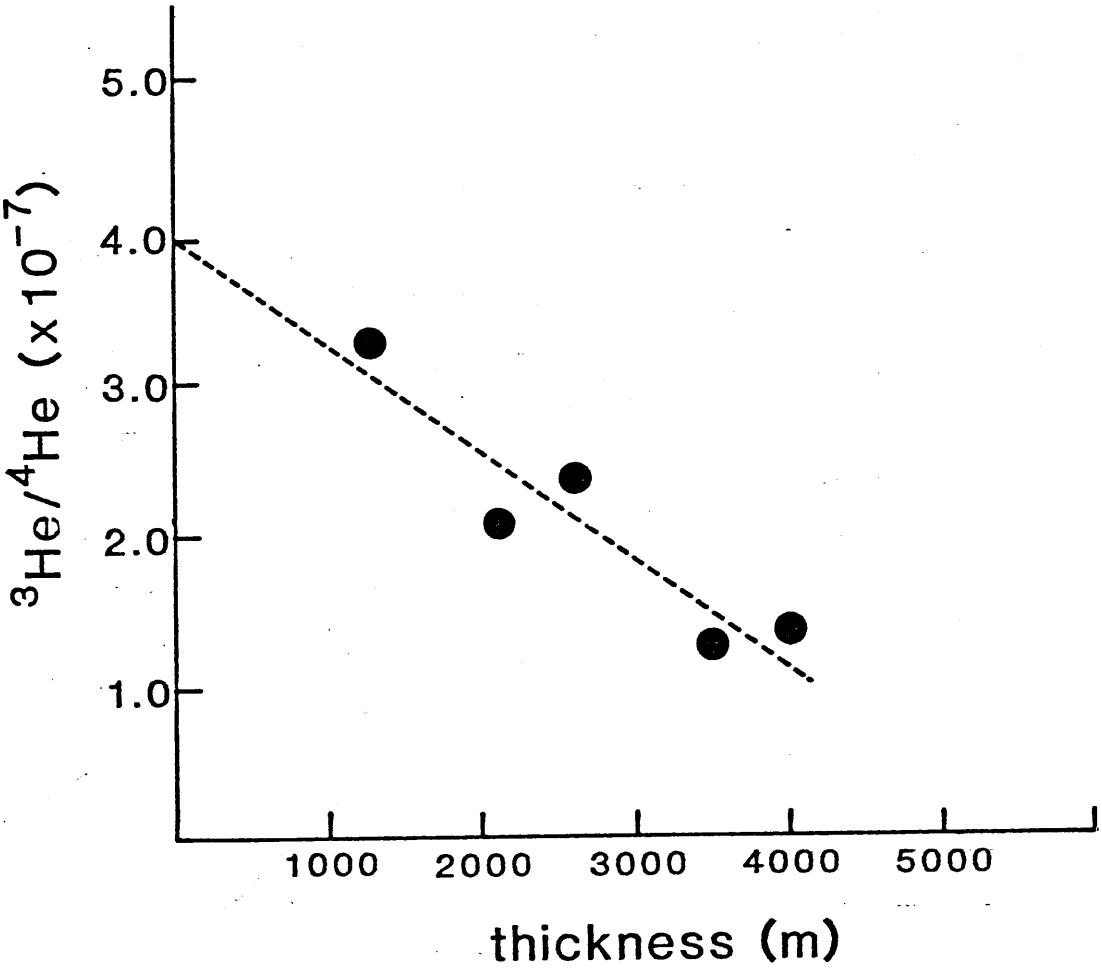

Figure 4-7. Correlation between the thicknesses of the sedimentary layer and the corrected $^3He/^4He$ ratios for CH_4-rich natural gases. Correction was made to eliminate atmospheric contamination.

mantle-derived He in the basement rock (granitic He). On the other hand, the calculated $^3He/^4He$ ratio for the sedimentary material in the region becomes 1.2×10^{-7}, which shows good agreement with the corrected $^3He/^4He$ ratio in deeper regions such as Heiwajima (#42) and Chonan (#41). Therefore, the $^3He/^4He$ ratios in both areas are attributed to purely sedimentary type He.

Consequently, even in the Island Arc, the emission of primordial He is quite low above the thick sedimentary layer. The $^3He/^4He$ ratio was observed in the thicker sedimentary layer in the Kanto Plain. This tendency suggests that He with a low $^3He/^4He$ ratio in the plain is mainly attributed to a mixture of radiogenic components of granitic He and sedimentary He.

4.2.2 $^3He/^4He$ ratios in volcanic areas

According to a previous study, areas with high $^3He/^4He$ ratios are closely correlated with the regional volcanic activity. The transportation of primordial He from the mantle to the ground surface in volcanic regions may be attributed to the pressure of upward migrating flow. The ordinary diffusion velocity of He in crystalline and sedimentary rock is extremely small, and additional radiogenic He from the U and Th in rock may be dominant. Therefore, if we observe He emission with a high $^3He/^4He$ ratio on the surface of the earth, there must be a carrier of

He from the mantle. In the Japanese Islands, high $^3He/^4He$ ratios are usually observed in areas where molten magma may exist beneath the ground surface. In order to verify the presence of carrier of the primordial He in the subduction zone, I have investigated ^3He emission in an area with a single strato-volcano.

Mt. Ontake volcano, with an elevation of 3,063 m, is located in Central Honshu (35°54'N, 137°29'E). The first eruption of this volcano in historical time took place on October 28, 1979; several new craters were formed and large amounts of volcanic ash and steam ejected. The previous magmatic activity is estimated to have occurred about 23,000 year B.P. The volcano had been believed to be dormant, but weak geothermal activities with fumaroles were observed at the southwestern flank of the central cone. The mountain is a strato-volcano with a possible small caldera, and the main rock type is pyroxene andesite (Sawada, 1981). There is no active volcano within a radius of about 40 km from Mt. Ontake.

Sampling sites were ten hot springs located within a radius of 25 km of the volcano; their $^3He/^4He$ ratios are shown in Figure 2-19. Sampling sites, elevations and distances from the central cone of the volcano and chemical compositions are shown in Table 4-5 together with $^3He/^4He$ and $^{20}Ne/^4He$ ratios. The major chemical constituent of most samples is CO_2 except for Nigorigo (#77) hot spring gas which is a N_2-CO_2 mixture. Concentrations of He vary from less

Table 4-5. Distances from the central cone of Mt. Ontake and $^3He/^4He$ ratios.

Name	No.	Distance (km)	Elevation (m)	$^3He/^4He$ ($\times10^{-7}$)	$^{20}Ne/^4He$ ($\times10^{-3}$)	N_2* (%)	CH_4* (%)	CO_2* (%)	He* (ppm)
Nigorigo	77	4.2	1850	86.1	31	38.5	0.32	56.5	93
Nigorikawa	56	7.6	1700	76.3	230	6.6	<0.01	91.3	5.1
Kanose	55	8.0	1350	81.3	12	1.1	<0.01	96.5	4.5
Kiso	57	9.6	1500	68.0	6.7	6.3	0.11	89.8	53
Akigami	80	14.0	1150	48.1	400	5.1	3.6	85.0	1.5
Shitajima	78	14.2	750	26.0	1300	2.3	<0.01	90.0	<0.5
Yuya	79	15.0	800	30.1	27	11.6	0.01	80.0	1.7
Kakehashi	58	21.0	800	41.7	44	2.2	1.03	93.1	14
Shojima	59	22.2	750	28.3	59	0.3	0.08	94.6	8.1
Shikanoyu	60	25.4	800	23.9	14	2.4	0.87	97.0	3.3

*: Urabe (1982)

than 0.5 ppm to 93 ppm. The highest $^{3}He/^{4}He$ ratio, 8.61 x 10^{-6}, was observed for gas at Nigorigo (#77) hot spring. This hot spring was the sampling site closest to the central cone, at a distance of 4.2 km. The larger the distance is, the lower the $^{3}He/^{4}He$ ratio of gas sample becomes. At Shikanoyu (#60) hot spring, 25.4 km away from the cone, the ratio was the lowest among those sampled with the value of 2.39 x 10^{-6}. This ratio is still significantly higher than the atmospheric ratio, however, and a small contribution of ^{3}He derived from the mantle is evident.

In Figure 4-8, a positive correlation between the observed $^{3}He/^{4}He$ ratios and distances of the sampling site from the cone is clearly seen. The $^{3}He/^{4}He$ ratios decrease almost linearly with the distance from the cone; however, no correlation between $^{20}Ne/^{4}He$ ratios and distances was observed. If the cause of decrease in the $^{3}He/^{4}He$ ratio observed for sites in circumference is attributed to the mixing of atmospheric He and the primordial He, the observed $^{20}Ne/^{4}He$ ratio should increase with a decrease in the $^{3}He/^{4}He$ ratio. In the present case, however, there is no correlation between $^{3}He/^{4}He$ ratios and $^{20}Ne/^{4}He$ ratios. The $^{3}He/^{4}He$ ratios corrected for atmospheric contamination are almost the same as the observed $^{3}He/^{4}He$ ratios. Therefore, the tendency of $^{3}He/^{4}He$ variation is due to the dilution of primitive He with radiogenic He in basement rock. The relation between the $^{3}He/^{4}He$ ratios and the distances from the cone is expressed as the following linear equation:

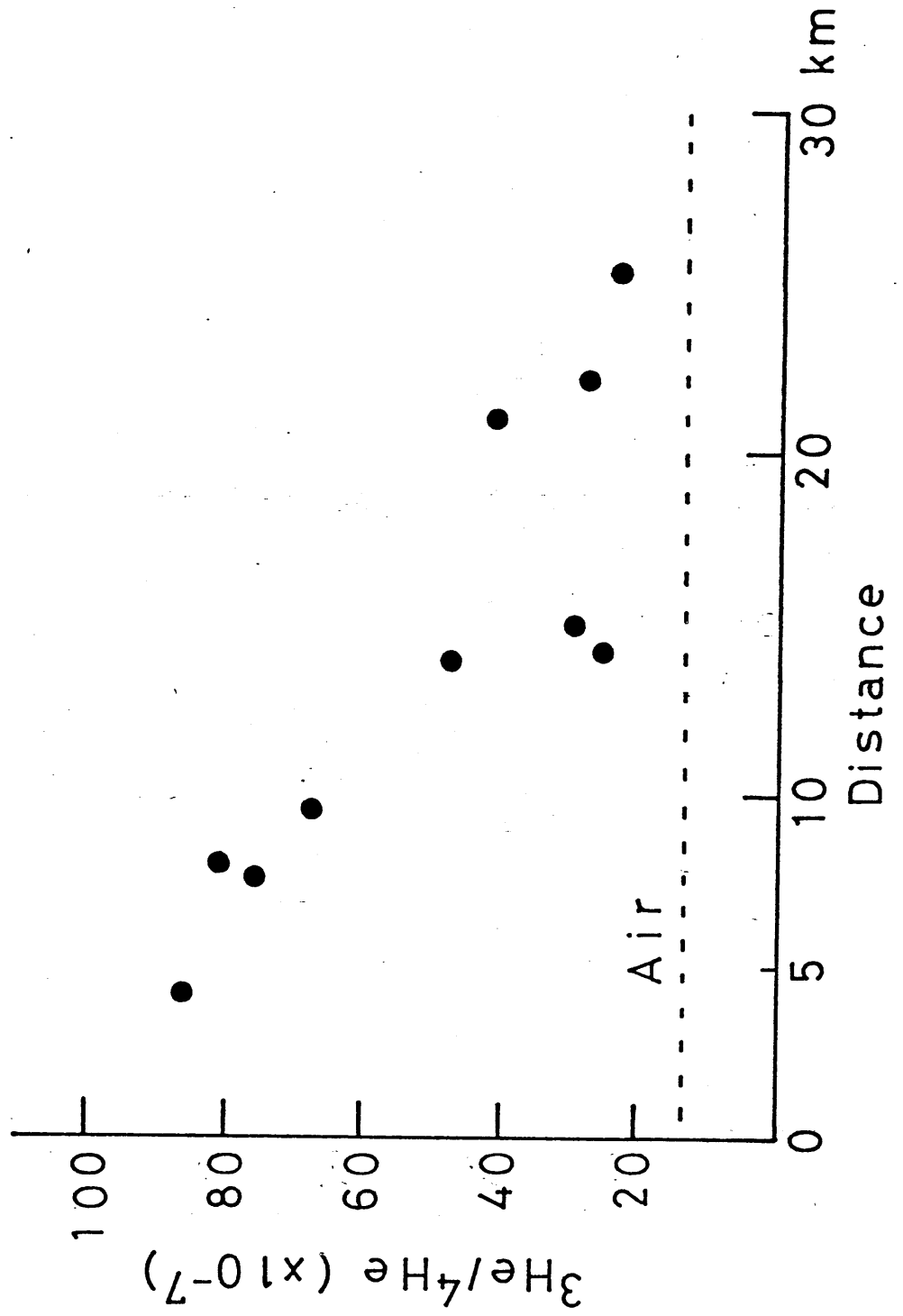

Figure 4-8. Correlation between the distance of the sampling site from the vent of Mt. Ontake and the $^3He/^4He$ ratio.

$$(^3He/^4He)_d = 9.43 \times 10^{-6} - 0.307 \times 10^{-6} \times d$$

where d and $(^3He/^4He)_d$ denote the distance of the sampling site from the central cone and the $^3He/^4He$ ratio at the site, respectively. The extrapolated value of the $^3He/^4He$ ratio at the central cone (a distance of 0 km) is 9.43×10^{-6}. This value is slightly lower than the MOR-type He but is in good agreement with the subduction-type He (admixture of 80% MOR-type He and 20% crustal He). The calculated ratio at the distance of 26.2 km equals the atmospheric value. This radius of 26.2 km is significantly larger than the 5 km topographical feature of the volcanic edifice. The effective range of an independent volcano similar to Mt. Ontake may be about 25 km, based on the $^3He/^4He$ ratio measurement.

The diffusion coefficient of He in sedimentary rock is estimated to be 3.93×10^{-5} cm^2/s (Ohsumi and Horibe, 1981). It takes more than 2×10^6 year to migrate the distance of 1 km of sedimentary layer by the simple diffusion process. Since the diffusion coefficient of He in ordinary crystalline rock is considered to be much smaller than that in sedimentary rock, transport velocity in the basement rock must be extremely small. In addition, radiogenic He from radioactive decay of U and Th in rock may be dominant over primitive He. The slightly elevated $^3He/^4He$ ratios observed in the area surrounding the volcano are not attained by the diffusion of primordial He from a conduit of the uprising magma of the volcano, but it may be necessary to have transportation by media such as thermal fluids. The tendency

of the $^{3}He/^{4}He$ ratio to decrease with distance from the cone may be attributed to changes in mixing ratio between the primitive He (with thermal fluids as carrier) and the radiogenic He produced in basement rock. Since the major chemical components of hot spring gases are CO_2 and N_2, those chemical species may be predominant candidates for the role of carrier of He.

In conclusion, the emission of primitive He in a volcanic area is larger at a site close to the cone than at the circumference. This tendency suggests that the carrier of primitive ^{3}He is the material flow of an uprising magma containing volatiles. Farther from the cone, the primitive He was transported through the fissures to the ground surface by thermal fluids. During the process, radiogenic He from the crustal rocks is added to the primitive He.

4.2.3 $^{3}He/^{4}He$ ratios across the Island Arc

The Tohoku district, in the northeastern part of Japan, is considered to be a typical island arc system. Generally, an island arc is characterized by four major features: (1) trench, (2) forearc (arc-trench gap), (3) volcanic arc and (4) back-arc (marginal sea). These are arrayed parallel to one another. The well-defined boundary of the forearc and the volcanic arc is called a volcanic front. The corresponding four major geographical features for the Tohoku district are (1) the Japan trench, (2) the Kitakami mountain

range - Sendai plain - Abukuma mountain, (3) a chain of active volcanoes such as Kurikoma, Zao, Adatara and Nasudake, and (4) the Japan Sea.

Geophysical data, including seismic velocities, terrestrial heat flow, gravity anomalies and crustal movement, taken from the east-west cross-section at 39°N of the northeastern part of Japan well represent features of the island arc system (Yoshii, 1979a). The presence of the binary planes of the focal depth distribution of microearthquakes reflects the characterictics of the tectonic sturcture of the trench-arc system. Shallow earthqukes, including many great earthquakes, occur in the wedge points under the trench-arc gap (Hasegawa et al., 1978). The occurrences of these earthquakes, together with crustal deformation, terrestrial heat flow anomalies and gravity anomalies observed in the Tohoku district, are attributed to the relative motion of the overlying plate and subducting oceanic lithosphere.

The locations of sampling sites of hot springs and mineral springs in the Tohoku district and the observed $^{3}He/^{4}He$ ratios are shown in Figure 4-9 together with the volcanic front. The $^{20}Ne/^{4}He$ ratios, water temperatures, major chemical compositions, He concentrations and distances from the trench to sampling sites are listed in Table 4-6. There is no relation between $^{3}He/^{4}He$ and $^{20}Ne/^{4}He$ ratios. The $^{20}Ne/^{4}He$ ratios are generally low except for Fukura (#29) well. Therefore, the main cause of variation in $^{3}He/^{4}He$

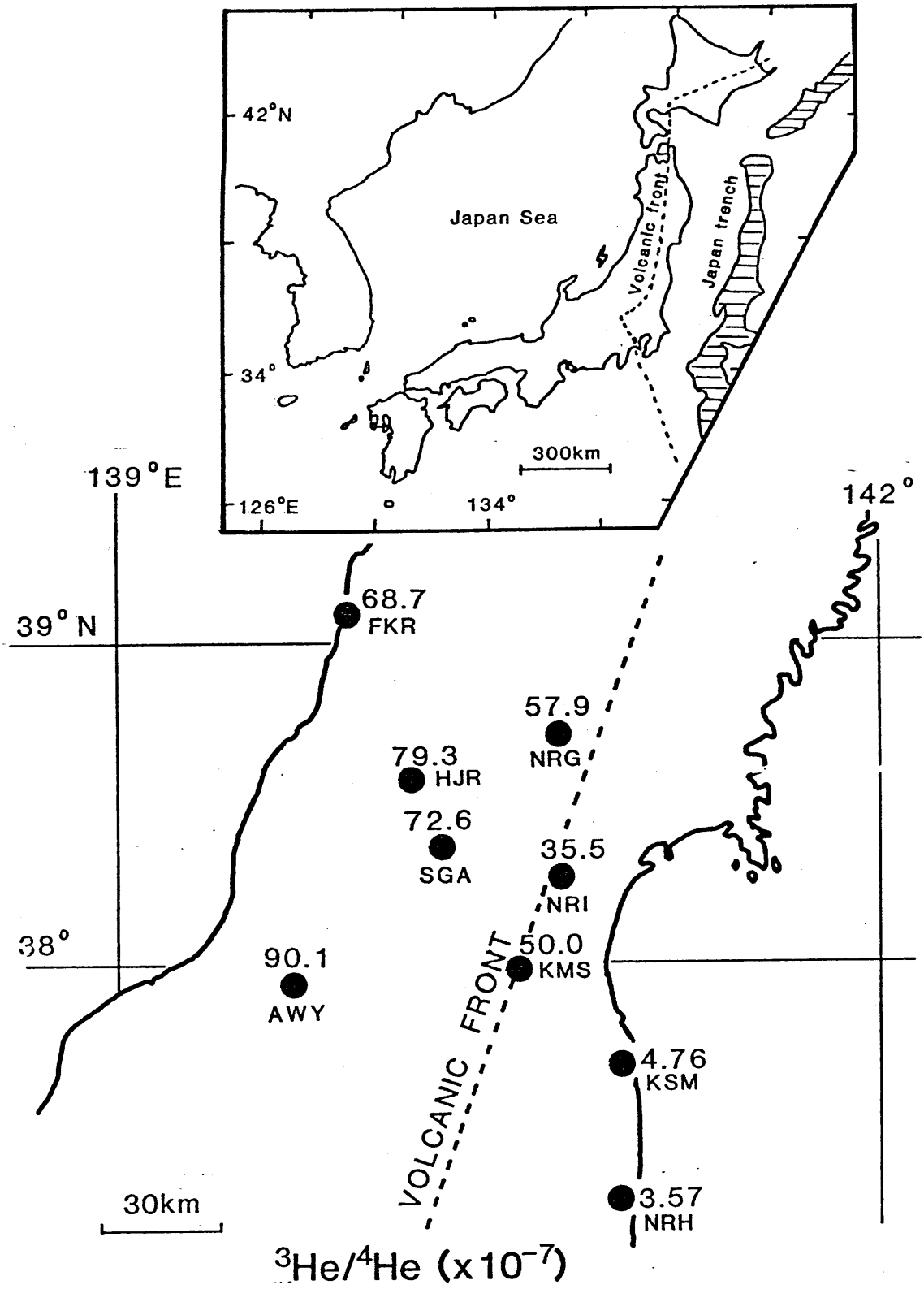

Figure 4-9. Sampling locations of hot springs and mineral springs in the Tohoku district. The $^3He/^4He$ ratios and code names are shown together with the position of the volcanic front. The unit of the $^3He/^4He$ ratio is expressed as 10^{-7}.

Table 4-6. Distances from the trench and $^{3}He/^{4}He$ ratios

Name	No.	Distance (km)	$^{3}He/^{4}He$ (10^{-7})	$^{20}Ne/^{4}He$ ($\times10^{-3}$)	CH_4* (%)	CO_2* (%)	N_2* (%)	He* (ppm)
Naraha	33	239	3.57	37	61	0.14	34	140
Kashima	32	255	4.76	2.9	<0.1	<0.1	98	6900
Nariai	25	295	35.5	56	<0.1	42	56	70
Kamasaki	24	298	50.0	41	<0.1	9.3	90	260
Narugo	23	314	57.9	78	<0.1	81	3.9	1.9
Sagae	27	338	72.6	50	24	2.0	63	100
Hijiori	26	354	79.3	260	<0.1	33	54	2.4
Awanoyu	28	371	90.1	5.9	<0.1	99	<0.1	1.4
Fukura	29	394	68.7	520	30	68	0.67	30

*: Urabe (1982)

ratio is not the mixing of the atmosphere but an addition of radiogenic He to the primordial He.

The relation between the observed $^3He/^4He$ ratios of gas samples in the Tohoku district and distances from the trench to sampling sites is shown in Figure 4-10. This is a profile of the $^3He/^4He$ ratios in the land area overlying a subduction zone, perpendicular to the trench axis. At the east coast side of the island (Naraha (#33) and Kashima (#32) wells), at a distance of about 250 km from the trench axis, the $^3He/^4He$ ratios are extremely low with values of (3 - 5) x 10^{-7}. The lowest ratio is observed at the easternmost site (Naraha (#33) well): the value of 3.57×10^{-7} is less than one-third of the atmospheric ratio, and a significant contribution of radiogenic He is apparent. The extremely low $^3He/^4He$ ratios observed in the forearc region are consistent with the observation that no magma production is in progress in the region.

Closer to the volcanic front, the $^3He/^4He$ ratio becomes significantly higher. The Nariai (#25) mineral spring, about 5 km east of the front, has a higher $^3He/^4He$ ratio than that of the atmosphere. The value of 3.55×10^{-6} is about 10 times higher than that of sites facing the Pacific Ocean. This higher $^3He/^4He$ ratio may be attributed to the leakage of primordial He brought with an uprising magma on the west side of the volcanic front. Just on the volcanic front, the $^3He/^4He$ ratio at Kamasaki (#24) hot spring is 5.00×10^{-6}, about 4 times higher than that of the atmosphere but as low

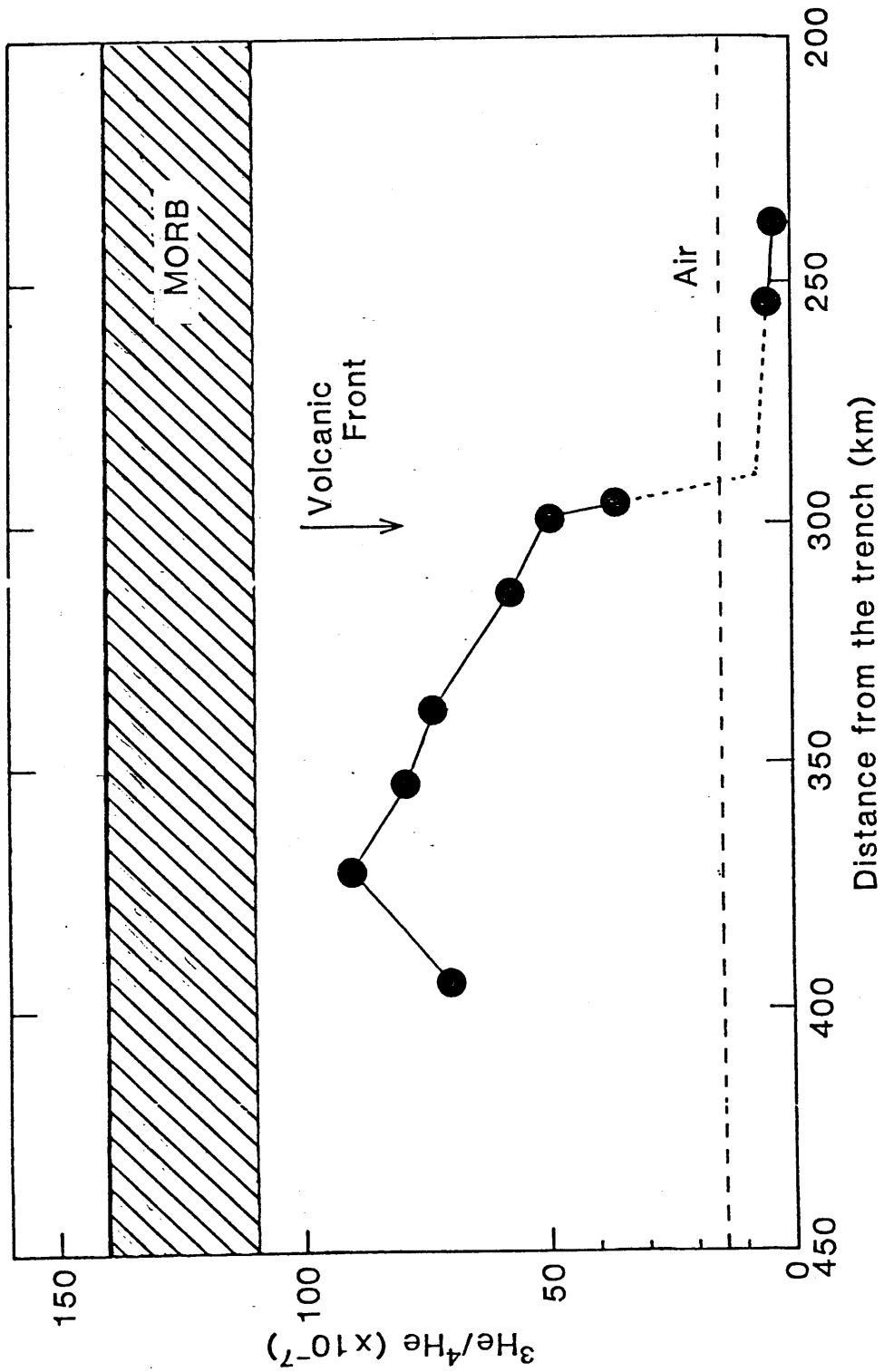

Figure 4-10. Correlation between the distance of the sampling site from the trench axis and the $^3He/^4He$ ratio.

as one-third of the MOR-type He. This implies that crustal contamination is more significant in the island arc region than along the Mid-Oceanic Ridge.

Further to the west within the volcanic arc, $^{3}He/^{4}He$ ratios become gradually higher. At Awanoyu (#28) hot spring, 370 km away from the trench, the ratio reaches a maximum value of 9.01×10^{-6}. The value is over 6 times the atmospheric ratio and is almost equivalent to that of volcanic gas in the Circum-Pacific region (subduction-type He).

Hedge and Knight (1969) showed a similar tendency for lead and strontium isotopes of volcanic rocks in the Tohoku district. The $^{238}U/^{204}Pb$ ratios range from 2.4 in tholeiitic basalt on the east side to 11.0 in alkali basalt at the west end of the volcanic arc. The isotopic composition is slightly less radiogenic on the west side of the volcanic arc. Recently, Notsu (1982) reported that the $^{87}Sr/^{86}Sr$ ratios of volcanic rocks in the Tohoku district decrease from the east side (0.7038 - 0.7045) to the west side (0.7028 - 0.7038). The variation was interpreted to be caused by sediments accompanied by a slab. The contribution of the slab becomes smaller away from the volcanic front, because the upper surface of the slab is deeper toward the back side of the arc.

The $^{3}He/^{4}He$ distribution is well correlated with terrestrial heat flow data for the area across the trench-arc system. General features of heat flow distribution in and

around the northeastern Japan Arc are described as follows: Low heat flow values (less than 42 mW/m^2) are predominant in the forearc region being affected by the subducting oceanic lithosphere, and high heat flow values (greater than 84 mW/m^2) are observed in the volcanic arc region and beneath the Japan Sea (Uyeda and Horai, 1964; Yoshii, 1979b).

Sediment subduction along the convergent plate margin has been discussed. It was long thought that sediments are too soft and too light to subduct and always become accreted to the landward plate after being scraped off the subducting plate. Deep-sea drilling results, however, show that quite often the contrary is the case (von Huene and Uyeda, 1981). Sediments do subduct. He isotopic variations observed in the volcanic arc region may indicate that sediments brought with a downgoing slab do not reach the western edge of the volcanic arc. That is, the $^3He/^4He$ ratio variations may be attributed to the difference in the amount of subducting sediment which is enriched in ^4He, in the source region of magma. In order to confirm the hypothesis, more extensive work on He isotopic analyses, including volcanic gases, will be needed in the region.

In conclusion, $^3He/^4He$ ratios in gas samples show a good correlation with the geotectonic structure of the island arc system in the Tohoku district. There is a close relation between the $^3He/^4He$ ratios and the distances from sampling sites to the trench. Samples collected in the forearc region show radiogenic values. Closer to the volcanic front, the

ratio becomes significantly higher. From the site just on the front to the west side of the volcanic arc, the $^{3}He/^{4}He$ ratios increase gradually. At the point 370 km from the trench, the $^{3}He/^{4}He$ ratio reaches a maximum value.

4.2.4 General trend of $^{3}He/^{4}He$ ratios in the Japanese Islands

According to the study of Isomi (1968), four orogenies occurred in the Japanese Islands. They are called the Variscan, Pacific, Himayalan and Alpine orogenies. Considering the age and the spatial distribution of the orogenic zone, the Alpine orogenic belt is apparently different from the other three orogenic belts. Hence, the tectonic situation of a certain area in Japan is identified from the view-points of both Alpine and pre-Alpine orogenies. Eight tectonic provinces proposed by Sumi (1979) are used in this study. They are shown in Figure 4-11, and their characters are described, together with their $^{3}He/^{4}He$ signatures, as follows:

VPH-1 zone: Zone of Variscan, Pacific and Himalayan orogenies in Northeast Japan. There is no Quaternary volcanic activity at all. Tertiary volcanic rocks are found occasionally at the boundary of the AV-1 zone. In the south part of the zone, granitic rocks of later Himalayan orogenies are observed.

Samples collected in the VPH-1 zone are Kojo (#14)

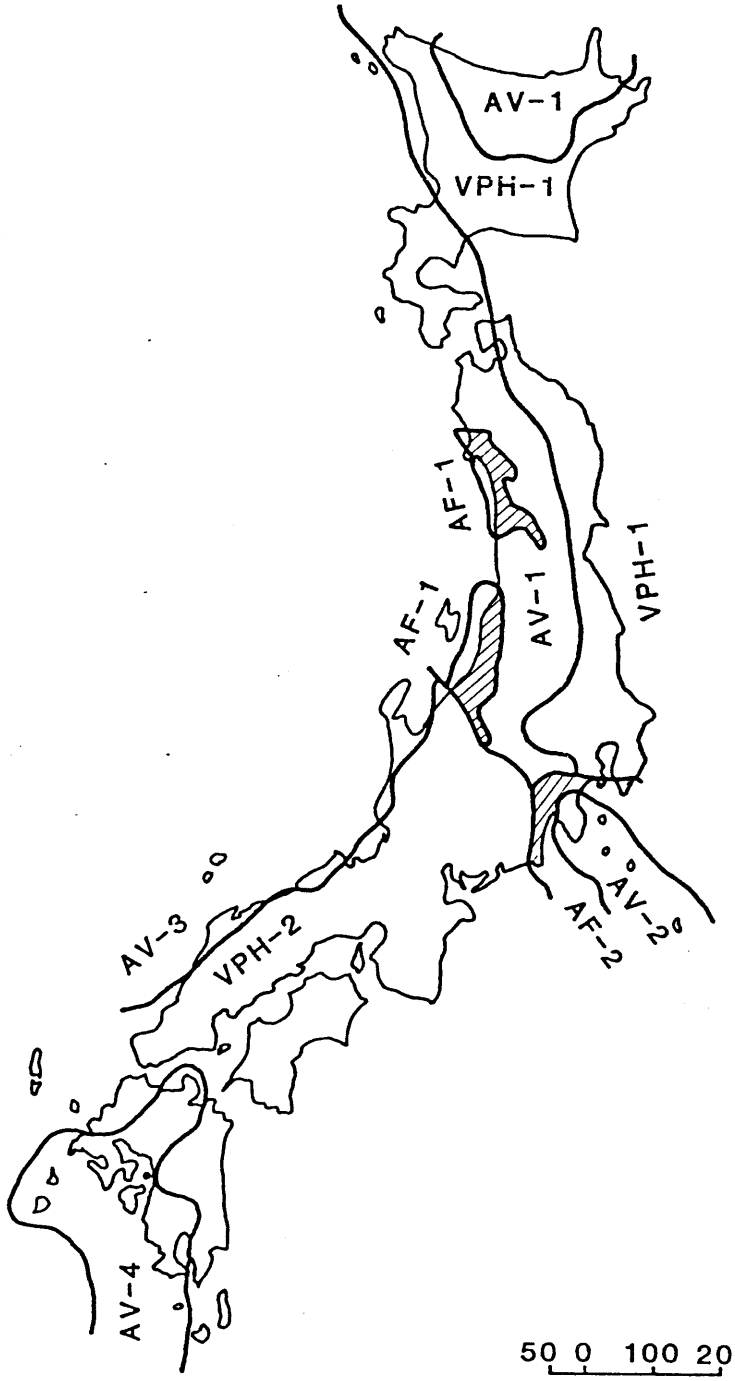

Figure 4-11. Eight tectonic provinces in the Japanese Islands (after Sumi, 1979). VPH: zone of Variscan, Pacific and Himalayan orogenies, AV: zone of Neogene to recent volcanism, AF: zone of Neogene folding. The AV and AF zones show high $^{3}He/^{4}He$ ratios whereas the VPH zones indicate radiogenic values.

spring water at the boundary of AV-1 in the Hokkaido district, Naraha (#33) and Kashima (#32) water well gases in the Tohoku district, Isobe (#36) and Arafune (#37) mineral spring gases at the boundary of AV-1 in the Kanto district and CH_4-rich natural gases from the Kanto Plain. The mean value of the $^3He/^4He$ ratio in the zone (ten samples) is $(6.0 \pm 5.3) \times 10^{-7}$, generally lower than that of the atmosphere. This suggests that there is no passage of He from the upper mantle to the surface. Several samples facing the AV-1 zone, such as those from Kojo mineral spring, have a higher $^3He/^4He$ ratio than that of samples collected in the central part of the zone, such as those from Heiwajima (#42) well. This tendency is explained by the leakage of primordial He from the AV-1 zone.

VPH-2 zone: Zone of Variscan, Pacific and Himalayan orogenies in Southwest Japan. In the easternmost part of the zone, facing the boundary of the AV-4 zone, are the large Quaternary volcanic calderas of Aso and Ata. Along the coast of the Seto Inland Sea, Tertiary volcanic rocks are found. At the coast of the Pacific Ocean, granite and rhyolite of the later Himalayan orogenies are observed.

Excluding the samples around Rokko mountain, such as those from Arima (#85), Minatoyama (#86) and Takarazuka (#87) hot springs, gaseous samples from the VPH-2 zone in the Chubu and Kinki districts usually have medium $^3He/^4He$ ratios, almost equal to the atmospheric value. The mean He isotopic ratio of the group (seven samples) is $(15.2 \pm 5.4) \times 10^{-7}$,

slightly higher than that of the VPH-1 zone. About 10 % of the mantle-derived He in the zone may be attributed to pre-Alpine orogenic activity. If the samples around Rokko mountain are included, the mean value of the $^{3}He/^{4}He$ ratio becomes $(3.2 \pm 3.0) \times 10^{-6}$, and the standard deviation would be rather large. Hence, the high $^{3}He/^{4}He$ ratios of these samples together with the high temperature of spring water are not well explained by the characteristics of the proposed geotectonic provinces.

AV-1 zone: Zone of Neogene to recent volcanism in the Northeast Japan. Thick layers of Miocene submarine volcanic rocks are distributed in this region. They are weathered and changed to greenish color, producing chlorite and sericite, zeolite, prehnite and pumpelynite. Basement rocks are products of Variscan, Pacific or Himalayan orogenies.

Most of the hot spring gases and thermal fluids in Hokkaido, Tohoku and Chubu district are located in the AV-1 zone. Generally, they have higher $^{3}He/^{4}He$ ratios than that of the atmosphere. The mean value of the ratio, $(5.3 \pm 2.3) \times 10^{-6}$, is about 50 % of subduction-type He. This He is attributed to the Quaternary volcanic activity in the zone.

AV-2 zone: Zone of Neogene to recent volcanism in the Izu district. Rock type is the same as AV-1. However, the basement rock is not well understood. This zone crosses the main direction of the Japan Arc and belongs to the Philippine plate.

Samples collected in the AV-2 zone are four hot spring

waters and two volcanic fumaroles. The $^{20}Ne/^{4}He$ ratios of these springs suggest strong contamination by atmospheric He. However, the $^{3}He/^{4}He$ ratios are slightly higher than that of the atmosphere except for that from the Mine (#63) hot spring sample. The He/ He ratios of Hakone volcanic fumaroles (Owakudani (#45) and Yunohanazawa (#46)) are the typical subduction type.

AV-3 and AV-4 zone: Zone of Neogene to recent volcanism in the Hokuriku - Sanin district and in the Kyushu district. Rock type is the same as that of AV-1; the basement was formed during the Variscan orogeny in AV-3 and the Pacific or Himalayan orogenies in AV-4.

Hot spring gases and thermal fluids are collected in the Sanin district of the AV-3 zone. Volcanic fumaroles of Satsuma-iodake (#98) and gas and water samples from surrounding hot springs in the island belong to the AV-4 zone. These eight samples show high $^{3}He/^{4}He$ ratios with a mean value of $(6.2 \pm 1.9) \times 10^{-6}$, approximately equal to that of the AV-1 zone.

AF-1 zone: Zone of Neogene folding on the Japan Sea side of Honshu. A thick and folded layer of Neogene is found. There are some Quaternary volcanoes such as Chokai and Myoko.

Most of the petroleum gases in the oil fields of Akita and Niigata prefecture are located along the AF-1 zone. Suprisingly, samples from this zone have high $^{3}He/^{4}He$ ratios, as high as those of the AV-1 zone. The mean value of the $^{3}He/^{4}He$ ratio (nineteen samples) is $(5.1 \pm 2.5) \times 10^{-6}$. This

mantle-derived He is not attributed to Quaternary volcanism but to the older volcanism.

AF-2 zone: Zone of Neogene folding on the Pacific side of Honshu. The same layer as that in AF-1 is observed. There is a typical Quaternary volcano, Mt. Fuji.

Three samples were collected in the AF-2 zone, from Shimobe (#43) hot spring, Kusashio (#44) natural gas and Omaezaki (#65) water well. The Shimobe (#43) and Kusashio (#44) samples have higher $^{3}He/^{4}He$ ratios than that of the atmosphere: 5.68×10^{-6} and 2.82×10^{-6}, respectively. On the other hand, the ratio of Omaezaki (#65) well is extremely low, 1.02×10^{-7}. This suggests that the Omaezaki region does not belong to AF-2 but to VPH-2.

AV-1, 2, 3 and 4 zones show high $^{3}He/^{4}He$ ratios, and the mantle-derived He is attributed to Quaternary volcanism. AF-1 and AF-2 zones indicate similar high $^{3}He/^{4}He$ ratios but these are not due to Quaternary volcanism. VPH-1 and 2 zones show low $^{3}He/^{4}He$, ratios and the value is explained by low emission of ^{3}He and large production of radiogenic He in the sedimentary or old basement layer in the zone.

4.3 Rare gas and some geochemical problems

4.3.1 Chemistry of gaseous samples

According to previous investigations (Moureu, 1923; Zobel, 1952; Zartman et al., 1961 and others), gaseous samples are classified into several types based on the major components such as CO_2, N_2 and CH_4. Chemical compositions were compiled for gaseous samples in Japan.

Chemical analyses of 222 gaseous samples in total are compiled. The compilation shows that representative types of major constituents are (1) CH_4-rich gas (concentration of CH_4 and other hydrocarbons is more than 75 %), 113 samples; (2) N_2-rich gas, 41; (3) CO_2-rich gas, 32; (4) N_2-CH_4 mixed gas (total concentration of CH_4 and N_2 is more than 75 %), 28; (5) Others (CH_4-CO_2 mixture, N_2-CO_2 mixture and N_2-O_2 mixture), 8. He concentrations differ significantly among these types. The means of He concentration in N_2-CH_4 mixed gas and N_2-rich gas are the highest among them, and the values are 590 ppm and 560 ppm, respectively. The lowest value of averaged He concentration was found in the CO_2-rich gas. The value is 2.7 ppm, 200 times lower than that of N_2-CH_4 mixed gas and N_2-rich gas. CH_4-rich gas has a medium value of 49 ppm. These variations in He content may be due to differences in the production mechanisms of these gases.

Table 4-7 indicates correlation coefficients between He content and N_2, CH_4 and CO_2 for each type. There is no apparent correlation between He content and major chemistry

Table 4-7. Correlation between He and N_2, CH_4, and CO_2 contents

	He-N_2	He-CH_4	He-CO_2
CH_4-rich	0.305	-0.197	-0.150
N_2-rich	0.250	-0.135	-0.080
CO_2-rich	0.633	0.241	-0.526
CH_4-N_2 mixed	0.093	-0.067	-0.205
others	-0.439	0.095	0.491
total	0.318	-0.140	-0.158

Table 4-8. Reservoir and amount of carbon in the earth

	Conversion into CO_2
Air	2.3×10^{12} t
Water (Ocean)	1.4×10^{14} t
(Fresh)	1.3×10^{16} t
Coal and Oil	1×10^{13} t
Living matter	7×10^{12} t
Sediment as organic	2.2×10^{16} t
as carbonate	4.0×10^{16} t
Igneous rock	3.3×10^{16} t

after Wedephol (1963)

except for CO_2-rich gas. The coefficient between He and N_2 in CO_2-rich gas shows good correlation, and that between He and CO_2 is negatively correlated. This tendency suggests that He is accompanied by N_2 or admixed to N_2 at first and then diluted by CO_2. If the origin of He is clarified, the origin of N_2 and CO_2 may be suggested.

The chemical compositions of gaseous samples, which were collected in this study were measured by Urabe (1982) using the gas chromatography method. A similar tendency to previous investigation was observed; the results can be summarized as follows. A total of 85 gaseous samples are classified into six groups according to major chemical constituents: (1) CH_4-rich gas, 27; (2) N_2-rich gas, 12; (3) CO_2-rich gas, 26; (4) N_2-CH_4 mixed gas, 5; (5) N_2-CO_2 mixed gas, 10; (6) Others (N_2-CH_4-CO_2 and CO_2-CH_4 mixed gas), 5. He concentration is the highest in N_2-rich and N_2-CH_4 mixed gas. N_2-CO_2 mixed gas has medium He content. The lowest value is observed in CO_2-rich gas and CH_4-rich gas. There is a close relation between N_2 content and He content in gaseous samples: the samples with high He content always have high N_2 content. This tendency was attributed to the mixing between N_2-rich gas with high He content and CO_2-rich gas, as described before.

4.3.2 Rare gas and origin of N_2-rich and CO_2-rich gas

Figure 4-12 shows the relation between He content in

gaseous samples and $^{3}He/^{4}He$ ratios. He concentration in gaseous samples show wide variation, from less than 0.5 ppm to 6,900 ppm. There is no significant correlation between He content and $^{3}He/^{4}He$ ratios. This implies that He content is controlled by the extent of dilution by major chemical constituents, whereas $^{3}He/^{4}He$ ratios may be attributed to another mechanism such as magmatic activity.

Relations between CO_2-rich gas, N_2-rich gas and $^{3}He/^{4}He$ ratios in natural gases are described as follows.

a) CO_2-rich gas

The origin of CO_2 in natural gases has been discussed in terms of several processes (Irwin and Barnes, 1980): (1) mantle-derived CO_2, (2) releasing of CO_2 by weathering of igneous rocks, (3) thermal decomposition of carbonates by magmatic heat, (4) decomposition of carbonates by inorganic chemicals like magmatic acids, (5) bacterial decomposition of organic materials and (6) biological respiration. Reservoirs and amount of carbon in the earth have been estimated by Wedepohl (1963) and are listed in Table 4-8. Considering the amount of each reservoir, the origin of CO_2 in natural gases is mainly due to (1) mantle-derived CO_2 and (2) sedimentary or recycling CO_2. If the origin of He in CO_2-rich gas is clarified, it may be possible to estimate the origin of CO_2.

Figure 4-13 shows the relation between the $^{3}He/^{4}He$ ratio in CO_2-rich gas and CO_2 content. There is an apparent difference between hot spring gases (•) and mineral spring

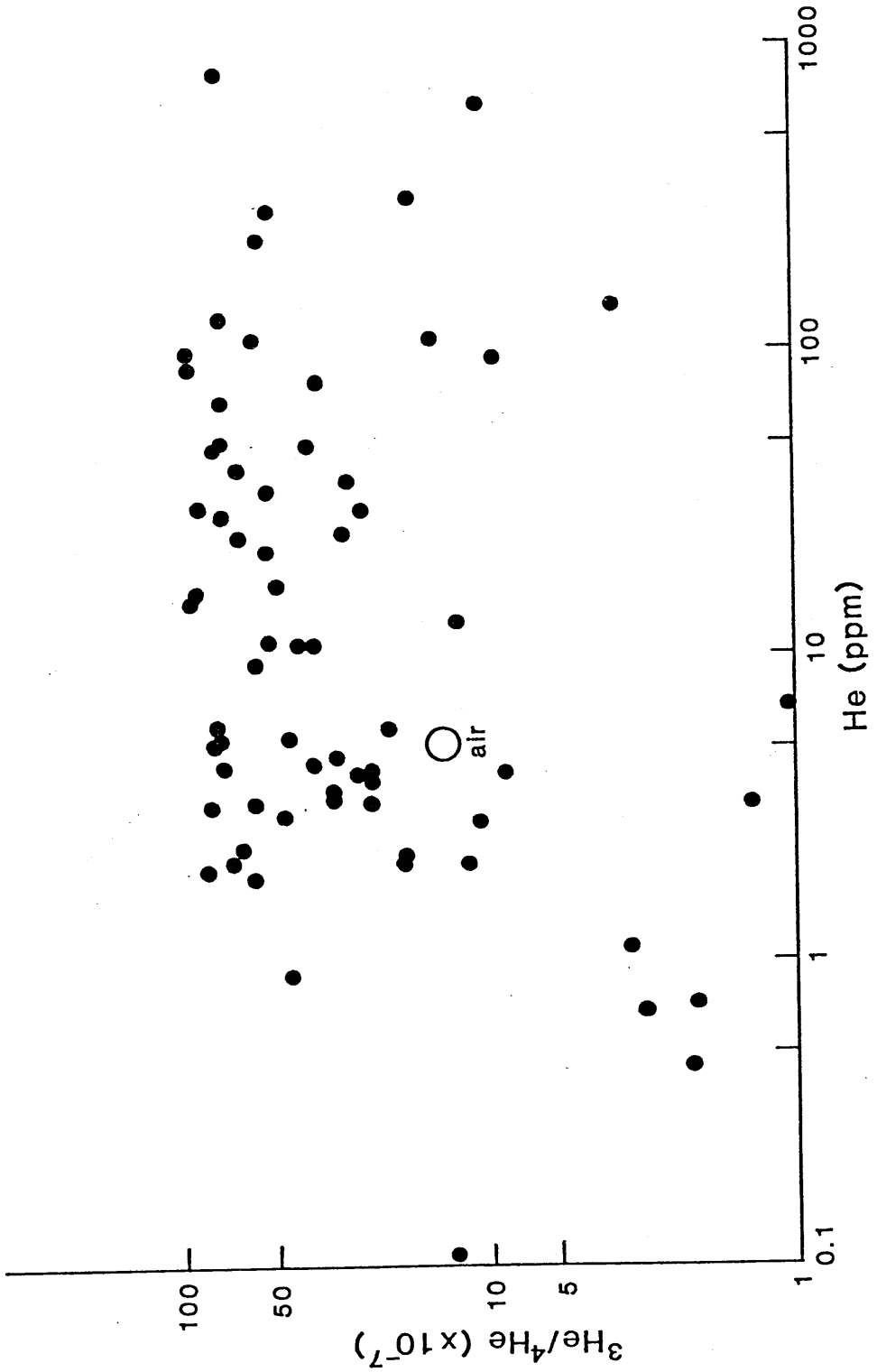

Figure 4-12. Correlation between He content and $^3He/^4He$ ratio in Japanese samples.

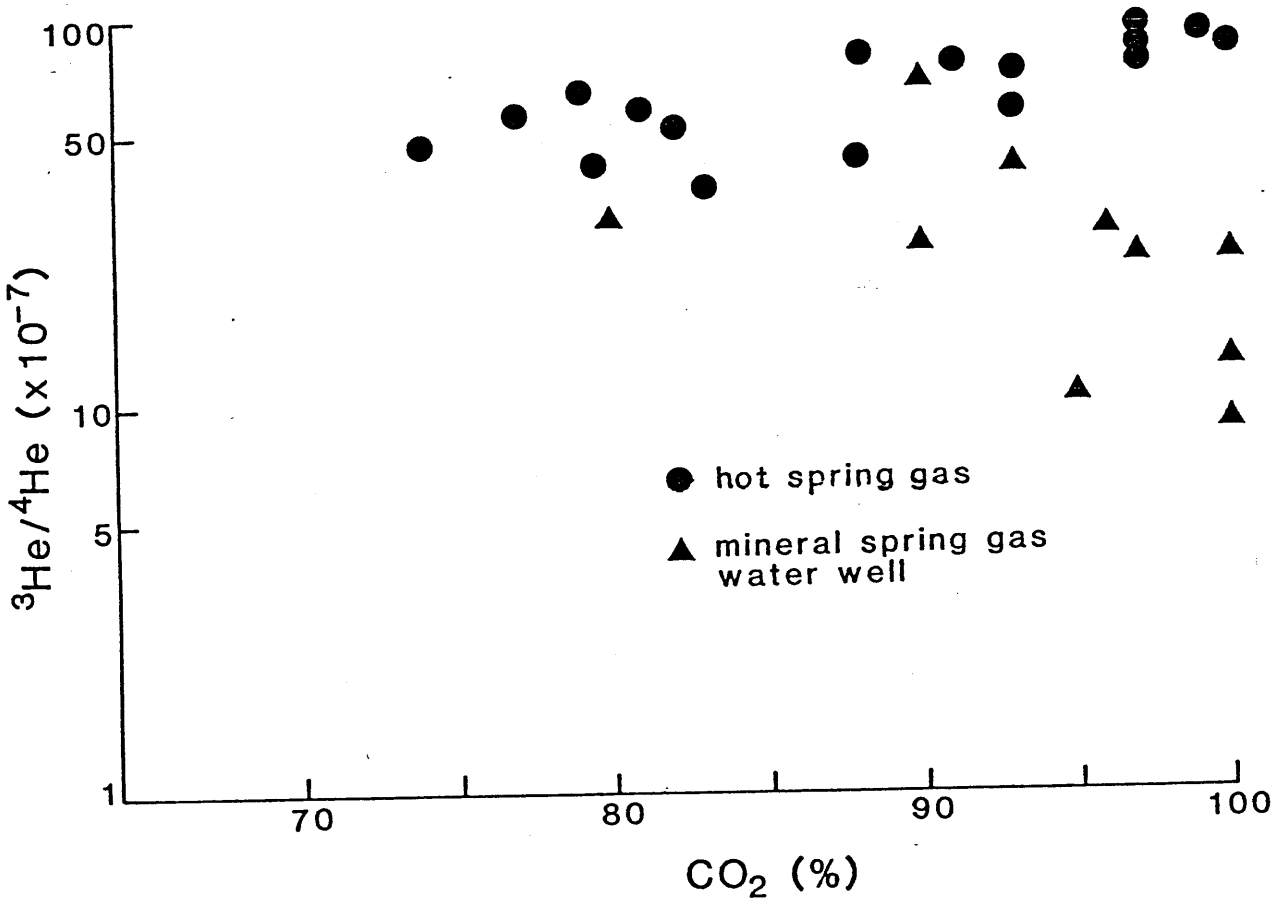

Figure 4-13. Correlation between CO_2 content and $^3He/^4He$ ratio in CO_2-rich gas samples.

gases (▲). The $^3He/^4He$ ratios of hot spring gases increase when CO_2 contents increase, whereas in mineral spring gases and water well gases, the $^3He/^4He$ ratios show a negative correlation with CO_2 content.

The $^3He/CO_2$ ratios of CO_2-rich gases were calculated. The ratio of hot spring gases vary from 11 x 10^{-12} to 320 x 10^{-12} with the mean value of 77 x 10^{-12}. Mid-Ocanic Ridge Basalt has a $^3He/CO_2$ ratio of 2.2 x 10^{-10} (HRX 6B from EPR 21 °N: Marty et al., 1982) and 5.2 x 10^{-10} (Popping rock from MAR 36 N: Marty, 1982). The $\delta^{13}C$ of these two samples indicate possible mantle origin with values of - 5.0 ‰ and - 7.8 ‰, respectively (Moore et al., 1977; Pineau et al., 1976). Therefore, the $^3He/CO_2$ ratios of mantle-derived materials are estimated to be 2 - 5 x 10^{-10}. Although the elemental fractionation of $^3He/CO_2$ ratios should account for changes of a factor of 2 or 3, observed $^3He/CO_2$ ratios in several hot spring gases (Yunokawa (#8), Otoshibe (#9), Matsushiro (#47) and Arima (#85)) are quite similar to MORB. This fact and the correlation between $^3He/^4He$ ratios and CO_2 content in hot spring gases suggest that CO_2 in these samples may be partly attributed to mantle-derived materials.

On the other hand, $^3He/CO_2$ ratios of mineral spring and water well gases indicate significantly lower values than hot spring gases, except for Kiso and Kakehashi mineral springs. The ratios vary from 0.63 to 19 x 10^{-12}, and the mean value is 5.6 x 10^{-12}. Considering the negative correlation between $^3He/^4He$ ratios and CO_2 contents in mineral spring and

water well gases, CO_2 in these gaseous samples may be sedimentary or recycled CO_2.

b) N_2-rich gas

The origin of N_2 in natural gas has been discussed by Zartman et al. (1961): (1) an introduction of atmospheric N_2, (2) release of N_2 by bacterial decomposition of N_2-bearing compounds, (3) release of N_2 by inorganic chemical breakdown or organic compounds, (4) the liberation of inorganic N_2 from igneous rocks and (5) mantle-derived N_2. One of the processes explaining the presence of N_2 in a natural gas sample is incorporation of air in the pore space of various reservoir rocks. If the air is included in the sediments, they will contain not only N_2 but other atmospheric gases as well. When gases have a N_2/Ar ratio approximately equal to that in air, the nitrogen is due to atmospheric contamination.

Figure 4-14 shows the relation between the $^3He/^4He$ ratio and N_2 contents in gaseous samples. There is no relation between $^3He/^4He$ ratios and N_2 contents. However, the $^3He/^4He$ ratios of hot spring gases (●) are generally higher than those of mineral springs and water wells (▲).

As is shown in Table 3-7, several N_2-rich gas samples have $^{40}Ar/^{36}Ar$ ratios greater than 295.6, the value of atmospheric Ar. These gases appear to be a mixture of radiogenic Ar (Ar_{rad}) and atmospheric Ar (Ar_{air}). The fraction, e, of the total Ar that is atmosphere is given by the expression

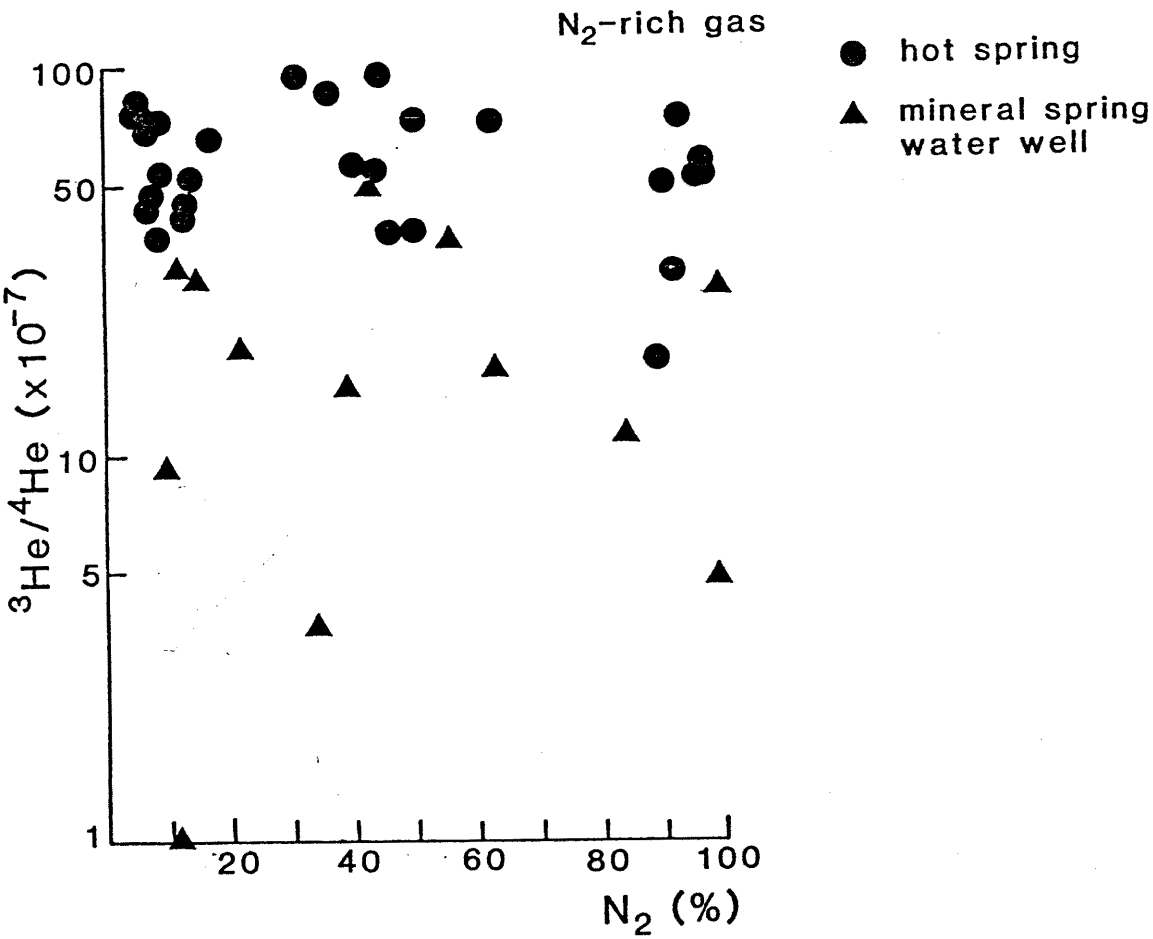

Figure 4-14. Correlation between N_2 content and $^3He/^4He$ ratio in gaseous samples.

$$e = Ar_{air}/Ar_{total} = 296.8/(({}^{40}Ar/{}^{36}Ar)_s + 1.2)$$

where $({}^{40}Ar/{}^{36}Ar)_s$ is the ratio in the sample. N_2 to Ar_{air} ratio (N_2/Ar_{air}) is given by the expression

$$(N_2/Ar_{air}) = N_{2s}/Ar_s \times 1/e$$

where N_{2s} and Ar_s are concentrations of N_2 and Ar in these samples, respectively. The calculated (N_2/Ar_{air}) ratios for samples vary from 47 to 245. The atmospheric ratio of N_2 to Ar is 84, and the ratio for the dissolved gases in water in equilibrium with the atmosphere at 20 C°is 38. It may be reasonable to postulate a simple mechanism of gas solution and effervescence, which could account for a factor of 2 or 3 change in the atmospheric (N_2/Ar) ratio. Therefore, a large fraction of N_2 in these gases can reasonably be attributed to the incorporated air.

Considering both the N_2/Ar_{air} ratios and the lack of relation between ${}^3He/{}^4He$ ratio and N_2 content, variations in N_2 content in gaseous samples are attributed to the following mechanism. At first original gas highly enriched in He, with various ${}^3He/{}^4He$ ratios and chemical compositions, are incorporated with N_2 and Ar from atmosphere with low He content. Then the mixture is diluted by the CO_2-rich gas or CH_4-rich gas.

4.3.3 Petroleum gases on the coastal area of the Japan Sea

Much of the hydrocarbon content of the earth has been or

is being explored. There is strong evidence of biogenic origin based on the carbon isotopic composition (Nakai, 1960; Colombo et al., 1966, 1970; Stahl 1968, 1974).

Two different processes are responsible for the formation of methane-rich natural gas in nature: (A) biogenic methane, originating mostly from the microbial decomposition of organic matter; (B) thermogenic methane, originating from thermal processes on organic matter at high temperature. Natural gas has been attributed to biogenic sources in each process.

The origin of petroleum is not well understood. Petroleum deposits and gases associated with such deposits are accompanied by fossils of marine microbes. Most authors consider that petroleum is derived from marine organic materials. Although an appreciable amount of data on the carbon isotopic composition of crude oil are available (Fuex, 1977; Stahl, 1977, 1979), its source material is not easily identified. Maturity, migration and decomposition by bacteria may have an influence on the $\delta^{13}C$-values of oil.

Recently, hydrothermal vents at 21°N on the East Pacific Rise were discovered to be discharging turbid water at up to 400°C; mixtures of hydrothermal plumes with ambient sea water contain significant amounts of dissolved H_2 and CH_4 as well as He with high $^3He/^4He$ ratio (Welhan and Craig, 1979). Subsequent studies show the occurrence of methane discharge in the ridge crest (Lupton and Craig, 1981; Horibe et al., 1982). Emission of nonbiological methane was suggested on

the Mid-Oceanic Ridge.

What is the origin of CH_4-rich natural gas and petroleum gas in the subduction zone? The formation of CH_4-rich gas in Japan is discussed based on the $^3He/^4He$ ratios of He in these gases. Generally, petroleum gas has a higher $^3He/^4He$ ratio than natural gas. The ratios of petroleum gases on the coast of the Japan Sea vary from 1.18 to 8.65×10^{-6}, and most samples indicate a higher $^3He/^4He$ ratio than that of the atmosphere. This suggests that a part of CH_4 in these petroleum gases has a non-biological origin is derived from the mantle accompanied by primitive He. The ^3He to total hydrocarbon ratios ($^3He/HC$) of hydrothermal plumes are from 3.0×10^{-7} to 4.7×10^{-8} (Welhan and Craig, 1979). Popping rocks from MAR 36°N have ratios of 3.3×10^{-8} (Pinau et al., 1976; Marty, 1982). CH_4 can be in equilibrium in the basalt-water system by the reaction:

$$CO_2 + 4H_2 = CH_4 + 2H_2O$$

Therefore, CH_4 in popping rocks may be derived from the mantle. Petroleum gas on the Japan Sea coast has a $^3He/HC$ ratio of 2.5×10^{-12} to 3.7×10^{-10}. This implies that about 1 % of hydrocarbon may be derived from the mantle at maximum. Considering the occurrence of appreciable amount of petroleum gas in the area, a significant amount of non-biological hydrocarbon may be found on the coast of Japan Sea.

On the other hand, the $^3He/^4He$ ratio of natural gas on the coast of the Pacific Ocean varies from 1.37×10^{-7} to

3.49×10^{-7}. This suggests that the He in natural gas in the area is of radiogenic origin. The $^{3}He/HC$ ratios of natural gas vary from 4.5×10^{-13} to 1.1×10^{-13} and are quite low compared to that of Popping rock. Therefore, the contribution of mantle-derived hydrocarbon seems to be negligiblly small, and the origin of natural gas on the coast of the Pacific Ocean is in sedimentary material.

In conclusion, several CH_4-rich petroleum gases on the coast of the Japan Sea have significantly high $^{3}He/^{4}He$ ratios, approximately equal to that of volcanic fumarole. A mantle-derived CH_4 is thought to be included in these petroleum gases.

4.3.4 Hot spring classification based on the D/H and $^{18}O/^{16}O$ ratios and relation to $^{3}He/^{4}He$ ratios

According to the compilation of hot springs and mineral springs (Sumi, 1975), the total number of springs in Japan is 2237. They include 110 springs whose water temperature is higher than 90 °C and about 300 springs higher than 60° C. Most of the thermal spring systems are closely associated with Quaternary volcanoes; however, some of them have no relation with active volcanoes. Matsubaya et al. (1973) proposed a classification of hot springs on the basis of chloride ion content and isotopic compositions of hydrogen and oxygen. There are four groups: (1) Arima brine type, (2) Green tuff type, (3) Costal type and (4) Volcanic type. The

$^{3}He/^{4}He$ ratio of each type are discussed together with signatures of hydrogen and oxygen isotopic ratios and chemistry of each type.

(1) Arima brine type Arima (#85) is located on the northern slope of the Rokko Mountains, north of Kobe. The Rokko Mountains are composed of upper Cretaceous granitic rock, which intruded into Arima rhyolite of a similar age (Kasama, 1968). Takarazuka (#87) is located on the eastern extension of the Rokko granite. Matsubaya et al. (1973) found wide dispersions of $\delta^{18}O$ and δD values from meteoric values of $\delta^{18}O$ = - 8.2 ‰ and δD = - 50 ‰ to highly shifted values of + 6.5 ‰ and -27.8 ‰, respectively, in these springs. The isotopic values of these brines vary proportionally with chloride concentrations irrespective of changes in temperature, carbonate concentration, and locality. Matsubaya et al. (1973) explained that these sample waters are mixtures of local meteoric waters and a saline brine of Cl^{-} = 43,700 ppm, $\delta^{18}O$ = + 8‰ and δD = - 30 to -25 ‰. The latter is attributed to the "residual magmatic, metamorphic or geothermal" fluid associated with upper Cretaceous rhyolite-granitic rocks.

The observed $^{3}He/^{4}He$ ratios of Arima (#85) and Takarazuka (#87) hot spring gases are 9.22×10^{-6} and 8.15×10^{-6}, respectively. These values are approximately equal to the $^{3}He/^{4}He$ ratios of active volcanic gases. Since intrusion of Rokko granite occurred in the upper Cretaceous, the accumulated radiogenic He is not small.

In order to clarify whether the residual magmatic fluid is the principal source of such a high $^3He/^4He$ ratio, I calculated the change in $^3He/^4He$ ratio due to the addition of radiogenic He. Several assumptions are necessary: (1) U and Th contents in Rokko granite are 5 ppm and 20 ppm, respectively. (2) Initial contents of ^3He and ^4He in a magma are 5×10^{-11} cc STP/g and 5×10^{-6} cc STP/g, respectively. (3) The age of Rokko granite is 60 Ma. The calculation indicates that the $^3He/^4He$ ratio of Rokko granite would be 6.3×10^{-7} at present, which is extremely low compared to the observed ratios. If the contents of U and Th in the granite are one-fifth of the assumed values and the initial contents of ^3He and ^4He in the magma are two times higher than the assumed values, the calculated ratio becomes 3.9×10^{-6}, still lower than the observed ratio. This may imply that there is another magma source which intruded later than upper Cretaceous or that initial $^3He/^4He$ ratios of Rokko granite were significantly higher than that of the subduction type He.

(2) Green tuff type Most of the thermal springs in this group are in the "green tuff" region that contain Miocene geosynclinal sediments with abundant submarine pyroclastic rocks and lava flows. The "green tuff" is also the host rock for many "Kuroko" ore deposits. The "green tuff" region along the coast of the Japan Sea (Niigata, Yamagata and Akita Prefectures) is one of the oil and natural gas fields of Japan. According to Matsubaya et al. (1973),

^{18}O and D values of waters in the "green tuff" region vary along the lines of "Craig's meteoric water plot" (Craig, 1963). Therefore, the waters are thought to be recycled meteoric waters. The waters are neutral sodium chloride sulfate type with high salinity and high SO_4/Cl ratios.

Some of the hot spring gases and petroleum gases in the "green tuff" regions were measured. Samples obtained from the "green tuff" region which have no relation to the Quaternary volcano are Misasa and Sekigane hot springs and some petroleum gases (Kita-Yurihara (#22), Hirai (#74), Nakadori (#75) and Kita-Katagai (#72)). These have high $^3He/^4He$ ratios ranging from 6.20×10^{-6} to 8.65×10^{-6}. A calculation similar to that used for Arima type is made for estimating aging effect. Assumptions are as follows: (1) U and Th contents in green tuff materials are 1.0 and 3.0 ppm. (2) Initial contents of ^3He and ^4He in magma are 5×10^{-11} cc STP/g and 5×10^{-6} cc STP/g. (3) The age of green tuff is 15 Ma. Results of calculation indicate that the $^3He/^4He$ ratio of "green tuff" would be 3.8×10^{-6} at present, about two times lower than the observed $^3He/^4He$ ratios. Since there is no evidence for recent intrusion in the "green tuff" regions, the observed high $^3He/^4He$ ratio may be attributed to an extremely high $^3He/^4He$ ratio in the initial condition such as plume-type He.

(3) Coastal type This type has a strong relation to Quaternary volcanoes in Japan. Matsubaya et al. (1973) showed that most of thermal waters along the oceanic coast

are isotopically intermediate between oceanic and local meteoric waters and are considered to be mixtures of the two types of waters. This coastal thermal water reveals that the water is not simply diluted by sea water but is generally depleted in terms of chloride normalized concentration, Na^+, Mg^{2+}, and SO_4^{2-} and enriched in Ca^{2+} and K^+ relative to sea water. Matsubaya et al. (1973) concluded that this tendency is due to chemical interaction between sea water and reservoir rocks in the thermal system.

Only three thermal water samples of this type were collected in this study. They are Atagawa (#62), Mine (#63) and Osawa (#64) hot springs in the Izu Peninsula, Shizuoka Prefecture. The $^3He/^4He$ ratios of these samples show medium values ranging from 9.2×10^{-7} to 4.53×10^{-6}. Since the $^{20}Ne/^4He$ ratios of the samples are about half that of the atmosphere, there is significant contamination by the air. Such contribution of air may be attributed to the interaction between magmatic fluid and sea water.

(4) Volcanic type A thermal water system of strong volcanic affilation is widely distributed in the Japanese Islands. Most of the collected samples in this study are classified as this type. Observed $^3He/^4He$ ratios vary from slightly higher values than the air value to the typical Island Arc value. The relation between the $^3He/^4He$ ratio and volcanic activity will be discussed later.

4.3.5 Heat source of hot springs

Considering the geological setting of hot spring regions, Kobayashi (1941) classified the heat source of hot springs into four groups as follows: (a) Quaternary volcanic rock (Quaternary type), (b) Tertiary volcanic rock and plutonic rocks (Tertiary type), (c) Mesozoic intrusive rock and plutonic rock (Mesozoic type), (d) Sedimentary and metamorphic rock (Sedimentary type).

A Quaternary type heat source seems to originate in molten magma derived from partial melting of the mantle by diapir uprising, accompanied by primordial He. Heat sources of Tertiary type and Mesozoic type are also magma, but the age of the derived magma is older than that of the Quaternary type. The heat source of sedimentary type is not well understood. Renner et al. (1975) considered the principal heat source for geothermal systems to be (1) heat directly related to the earth (volcanic heat) and (2) heat related to the geothermal gradient or general increase in temperature with depth as a consequence of conductive heat flow (gradient heat). The sedimentary type heat source may be this gradient heat. Recently, Torgersen and Jenkins (1982) indicated that the $^{3}He/^{4}He$ ratio of a geothermal system is useful to determine whether the system is active volcanic or passive volcanic.

In this study it can be concluded that He with high $^{3}He/^{4}He$ ratio is mainly brought from the upper mantle by uprising magma. If the heat source of hot springs and

geothermal regions is magma at a high temperature, there will be a relation between the heat discharged by a hot spring and the $^{3}He/^{4}He$ ratio of the hot spring gas. Figure 4-15 shows the histogram of $^{3}He/^{4}He$ ratios for three groups of springs classified by water temperature. There is an apparent tendency for hot springs with high temperatures (more than 42°C) to have high $^{3}He/^{4}He$ ratios with small variations in the values. Mineral springs with their low temperatures (less than 25° C) have lower $^{3}He/^{4}He$ ratios than hot springs, with wide variations in the values.

Based on the $^{3}He/^{4}He$ ratios and the temperatures of water, hot springs and mineral springs in Japan are divided into four groups: (1) high $^{3}He/^{4}He$ ratios and high temperature, (2) high $^{3}He/^{4}He$ ratios and low temperature, (3) low $^{3}He/^{4}He$ ratio and high temperature, (4) low $^{3}He/^{4}He$ ratio and low temperature. Most hot springs in Quaternary volcanism belong to the high $^{3}He/^{4}He$ ratio and high temperature (1) group. Since mass transfer of magmatic He to a fluid is geologically improbable without the accompaning transfer of heat, the presence of magmatic He in a hot spring of Quaternary volcanism implies a direct transport of heat and mass from magma by fluid movement.

In Kiso (#57) and Kakehashi (#58) mineral springs, high $^{3}He/^{4}He$ ratio and low temperature was observed. These springs are a mixture of a small amount of magmatic fluid and a large amount of meteoric water at low temperature. Heiwajima (#42) water well is a typical sample of low $^{3}He/^{4}He$

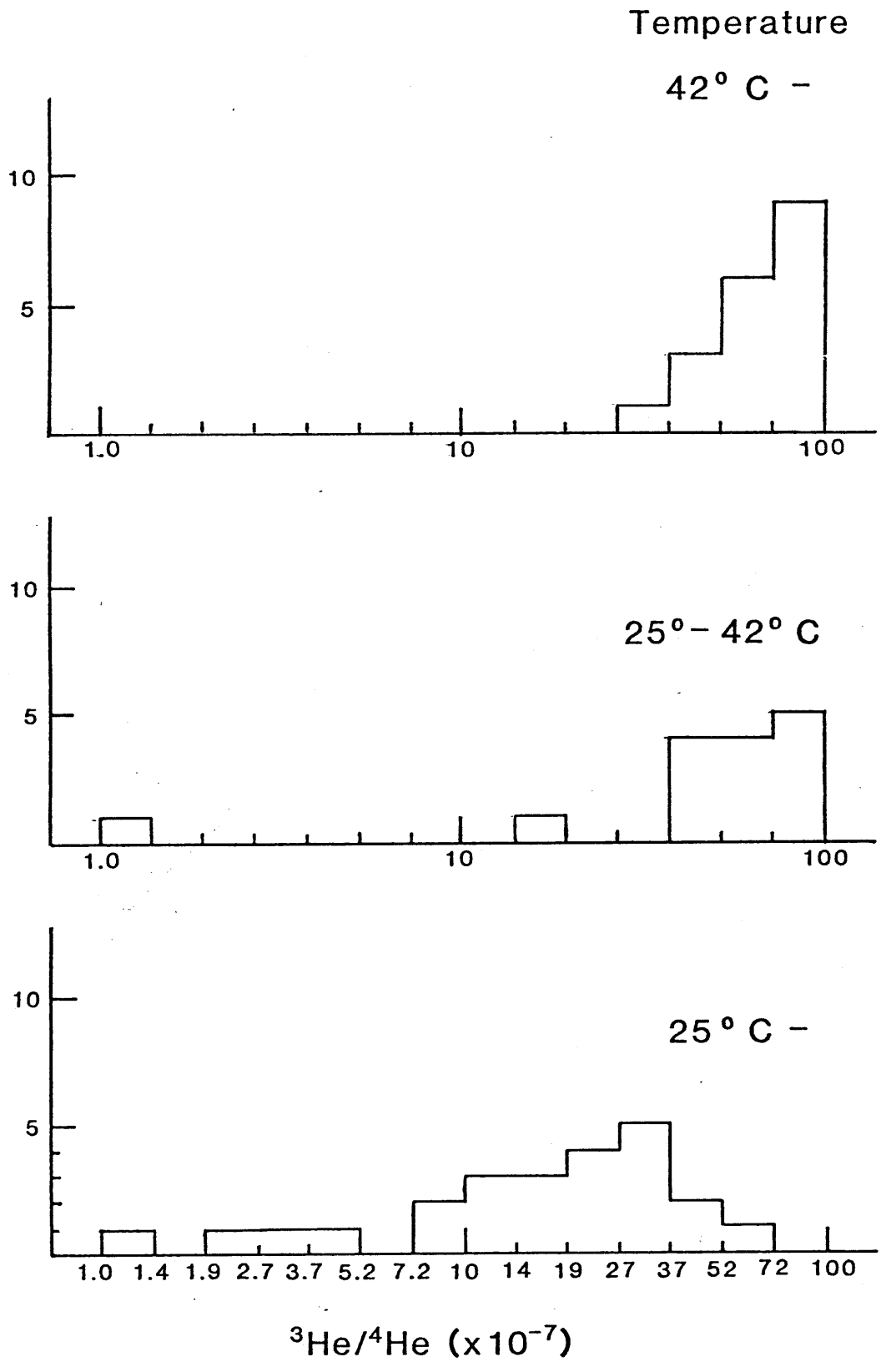

Figure 4-15. Histogram of the $^3He/^4He$ ratios for three spring groups classified by water temperature. Hot springs with high temperatures (>42°C) have higher $^3He/^4He$ ratios, whereas mineral springs with low temperatures (<25°C) have low $^3He/^4He$ ratios.

ratio and high temperature. The temperature of the water is almost 37°C and the $^{3}He/^{4}He$ ratio of bubble gas shows radiogenic value (1.37×10^{-6}). Since the depth of the bore hole is about 900 m, this temperature is attributed to the normal "gradient heat". Most mineral springs and water wells in sedimentary layer and old basement rock show low $^{3}He/^{4}He$ ratio and low temperature.

Figure 4-16 shows the relation between the $^{3}He/^{4}He$ ratio and the heat discharging rate of hot springs. The heat discharging rate is calculated as the product of the water temperature and the discharging rate of water. In the low heat discharging zone in the figure ($Q < 1 \times 10^{4}$ kcal/min), the $^{3}He/^{4}He$ ratios show large variation, whereas in the high zone ($Q > 5 \times 10^{4}$ kcal/min), the $^{3}He/^{4}He$ ratios are generally constant with higher values. This suggests that the heat sources of hot spring regions with a high heat discharging rate are usually a direct transport of heat and mass from magma by fluid movement.

In conclusion, there is a close relation between the $^{3}He/^{4}He$ ratios and heat discharging rates of hot springs. The $^{3}He/^{4}He$ ratio of the high heat discharging spring is generally high, which implies direct transport of both heat and mass from magma by fluid movement. The source of springs with medium high heat discharging and radiogenic $^{3}He/^{4}He$ ratio is thought to be the normal conductive heat flow of the earth.

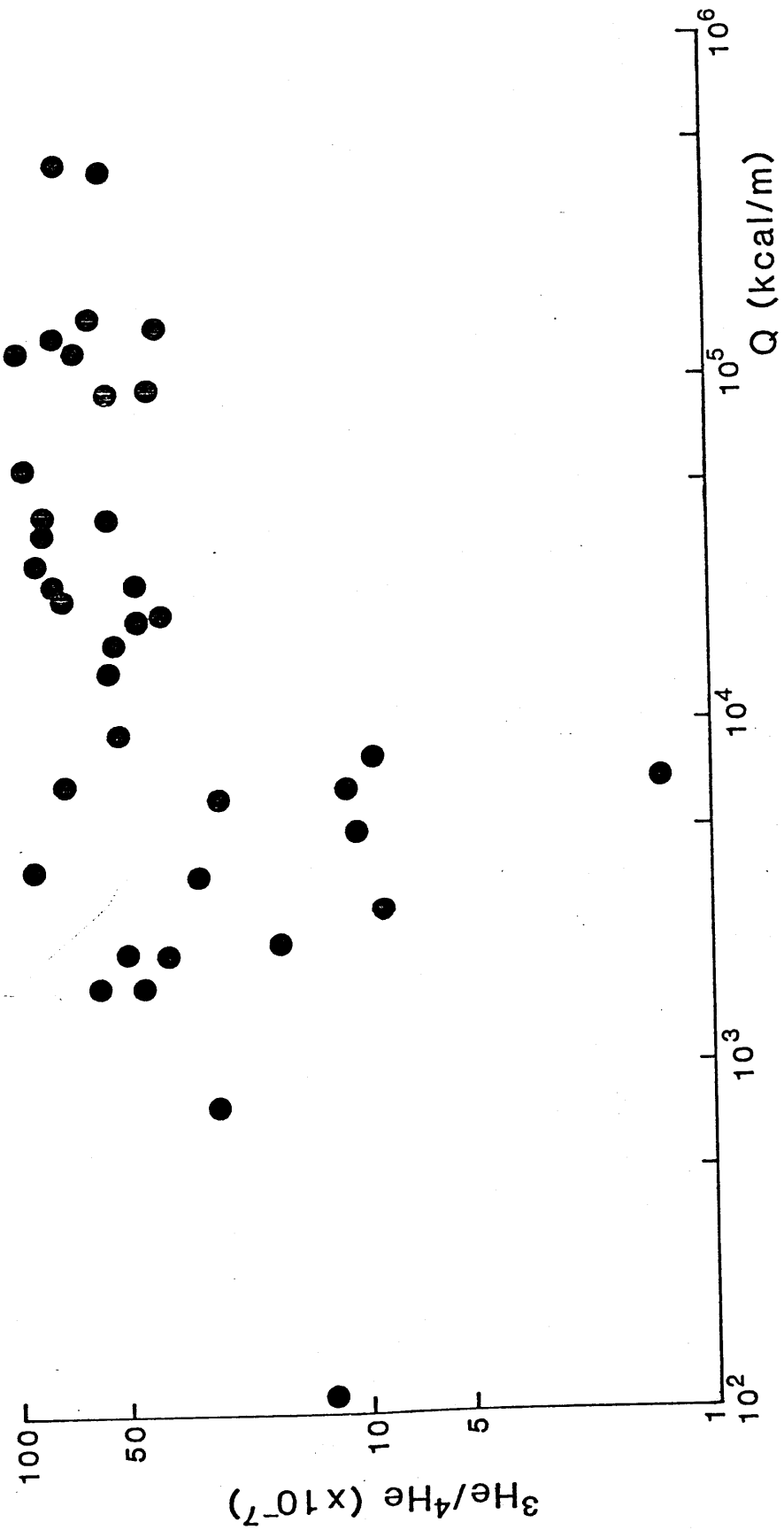

Figure 4-16. Correlation between the heat discharging rates of hot springs and their $^3He/^4He$ ratios. The low discharging springs have large variations in $^3He/^4He$ ratios, whereas the high discharging springs have high and uniform $^3He/^4He$ ratios.

V. Conclusion

Observed $^{3}He/^{4}He$ ratios of natural gas and thermal fluids in the Japanes Islands vary significantly, by about two order of magnitude, from 7.47×10^{-8} to 9.65×10^{-6}. Pevious investigators proposed the constancy of the $^{3}He/^{4}He$ ratios (from 7.0×10^{-6} to 1.1×10^{-5}). The $^{20}Ne/^{4}He$ ratios of these samples vary from 8.8×10^{-4} to 4.49, and there is no correlation between $^{3}He/^{4}He$ and $^{20}Ne/^{4}He$ ratios. Since the $^{20}Ne/^{4}He$ ratio of the atmosphere is significantly higher than that of the mantle and crust, it is possible to use the ratio as an indicator of air contamination.

The $^{3}He/^{4}He$ ratios generally correlate with the subduction-related tectonic structure of the Japanese Islands. The $^{3}He/^{4}He$ ratios are as low as on the order of 10^{-7} for samples in the area facing the Pacific Ocean and in most of the alluvial plains. In the zone along the volcanic front and the areas immediately west of the front, the ratios are as high as $(5 - 9) \times 10^{-6}$.

The data on samples from the Japanese Islands distribute in a triangle-like region in the $^{3}He/^{4}He$ - $^{20}Ne/^{4}He$ diagram, which suggests that there exist three end members for He: atmsopheric He, mantle-derived He (subduction-type He) and continental crustal He. The mixing ratios of the respective three components can be calculated based on the observed $^{3}He/^{4}He$ and $^{20}Ne/^{4}He$ ratios. The calculated subduction-type He contribution for samples from volcanic geothermal area is

about 90 % at maximum. Island Arc type magma in Japan may be characterized as having 80 % MOR-type He and 20 % crustal He. This crustal He may be attributed to the remelted subducted oceanic crust or to sedimentary materials.

(1) In the Kanto Plain, a large sedimentary basin of later Cenozoic origin, observed $^{3}He/^{4}He$ ratios are significantly lower than that of the atmosphere. These low ratios are attributed to the non-magmatic activity of the region. In the basin, the $^{3}He/^{4}He$ ratios are found to be negatively correlated with the thickness of the sedimentary layer. This implies that the observed variation is attributed to the mixing of two radiogenic components, sedimentary He ($^{3}He/^{4}He$ = 1 x 10) and granitic He (4 x 10^{-7}). The deeper the sedimentary layer is, the larger the contribution of the sedimentary He becomes.

(2) The emission of primordial He in the area around Mt. Ontake is larger at sites closer to the central cone than at circumference. This tendency suggests that the carrier of primitive He is the material flow containing volatiles by the uprising magma. At the sites farther from the cone, the primitive He was transferred through fissure to the ground surface by thermal fluids. During such a process, the radiogenic He from the crustal rock added to the primitive He.

(3) In the Tohoku district, there is a close relation between the $^{3}He/^{4}He$ ratios and the distances from sampling sites to the Japan Trench. Samples collected in the forearc region show radiogenic $^{3}He/^{4}He$ ratios (granitic He). Closer to the volcanic front, the ratio becomes significantly higher. From the site just on the front to the west side of the volcanic arc, the $^{3}He/^{4}He$ ratios increase gradually. This profile suggests that there is a passage of primitive He from the mantle on the west side of the volcanic front region but not on the east side in the Tohoku district.

(4) The high $^{3}He/^{4}He$ ratios of natural gases and fluids are considered to be a useful indicater of magmatic fluid and applicable to estimating the heat sources of hot springs. The $^{3}He/^{4}He$ ratios of hot spring gases generally correlate with the heat discharging rates of the springs except in a few cases. For a high heat discharging spring, the $^{3}He/^{4}He$ ratio is usually high. This implies a direct transport of both heat and mass from magma by fluid movement. On the other hand, the source of a medium heat discharging spring with radiogenic $^{3}He/^{4}He$ ratio is thought to be the general increase of conductive heat flow of the earth.

(5) Several CH_4-rich petroleum gases on the coast of the Japan Sea have significantly high $^{3}He/^{4}He$ ratios, approximately equal to the ratio of volcanic fumaroles in Japan. CH_4-rich natural gases on the coast of the Pacific

Ocean show radiogenic ratios. This suggests that formation mechanisms of hydrocarbon on the two coasts are different. CH_4 in natural gases is attributed to normal biological origins in the sedimentary layer, whereas a part of CH_4 in petroleum gas may have inorganic origins in the mantle.

(6) Icelandic gases and thermal fluids were measured in order to compare the He isotopic signature of the subduction zone and with that of the Mid-Oceanic Ridge. The results show that He isotopic compositions of Icelandic samples are attributed to the mixing of three components: MOR-type He, plume-type He and atmospheric He. Gaseous samples collected at the northeastern part of the central belt (median zone) have typical MOR-type ratios, whereas the south part of the island indicates apparently higher $^3He/^4He$ ratios than that of the MOR-type. The extremely low contribution of crustal He in Icelandic samples compared to that in Japanese samples is explained by the absence of crustal materials in a divergent type of plate boundary.

References

Aldrich, L. T. and Nier, A. O. (1948) The occurrence of ^3He in Helium. Phys. Rev., 74, 1590-1594.

Alvarez, L. W. and Cornog, K. (1939) ^3He in Helium. Phys. Rev. 56, 379.

Bartlett, N. (1962) Xenon hexafluoroplatinate (5), $Xe^+[PtF_6]^-$. Proc. Chem. Soc. (london), 1962, 218.

Basford, J. R., Dragon, J. C., Pepin, R. O., Coscio, M. R. and Murthy, V. R. (1973) Krypton and Xenon in lunar fines. Proc. Fourth Lunar Sci. Conf. Geochem. Cosmchim. Acta Suppl., 4, 1915-1918.

Baskov, Y. A., Vetshteyu, V. Y., Surikov, S. N., Tolstikhin, I. N., Malyuk, G. A. and Mishna, T. A. (1973) Isotope composition of H, O, C, Ar and He in hot springs and gases in the Kurile-Kamchatka volcanic region as indicators of formation conditions. Geokhimiya, 1973, 180-189.

Boulos, M. S. and Manuel, O. K. (1971) The xenon record of extinct radio activities in the earth. Science, 174, 1334-1336.

Brown, H. (1952) Rare gas and the formation of the earth's atmosphere. in The Atmosphere of the Earth and Planets Revised edition, edited by G. P. Kuiper, pp. 258-266, Univ. of Chicago Press.

Butler, W. A., Jeffery, P. M., Reynolds, J. H. and Wasserburg G. J. (1963) Isotopic variations in terrestrial xenon.

J. Geophys. Res., 68, 3283-3291.

Claassen, H. H., Selig, H. and Malm, J. G. (1962) Xenon-tetrafluoride. J. Chem. Soc., 84, 3593.

Clarke, W. B., Beg, M. A. and Craig, H. (1969) Excess ^{3}He in the sea: evidence for terrestrial primordial helium. Earth Planet. Sci. Lett., 6, 213-220.

Clarke, W. B., Jenkins, W. J. and Top, Z. (1976) Determination of tritium by mass spectrometric measurement of ^{3}He. Int. Jour. App. Rad. Isotopes, 27, 515-522.

Colombo, U., Gazzarrini, F., Gonfiantini, R., Sironi, G. and Tongiorgi, E. (1966) Measurement of $^{13}C/^{12}C$ isotope ratios on Italian natural gases and their geochemical interpretation. Advances in organic geochemistry, 1964. pegamon Press., Oxford, pp. 279.

Colombo, U., Gazzarrini, F., Gonfiantini, R., Knenper, G., Teichmuler, M. and Teichmuler, R. (1970). Das C^{12}/C^{13} Verhaltnis von Kohlen und kohlenburtigem Methan. CR 6e Congr. Int. Strat. Geol. Carbonifi., Sheffield 1967, 2, 557.

Craig, H. (1963) The isotopic geochemistry of water and carbon in geothermal areas. Nucl. Geol. Geotherm. Areas. edited by E. Tongiorgi, pp. 17-53.

Craig, H. and Lupton, J. E. (1976) Primordial neon, helium and hydrogen in oceanic baslts. Earth Planet. Sci. Lett. 31, 369-385.

Craig, H. and Lupton, J. E. (1978) Helium isotope variations: evidence for mantle plumes at Yellowstone,

Kilauea and the Ethiopian Rift valley. EOS Trans. AGU 59, 1194.

Craig, H., Lupton, J. E., Welhan, J. A. and Poreda, R. (1978) Helium isotope ratios in Yellowstone and Lassen Park volcanic gases. Geophys. Res. Lett. 5, 897-900.

Craig, H., Lupton, J. E. and Horibe, Y. (1978) A mantle helium component in Circum-Pacific volcanic gases: Hakone, the Marianas and Mt. Lassen. In Terrestrial Rare Gases, edited by E. C. Alexander and M. Ozima, Japan Sci. Soc. Press. Adv. Earth Planet. Sci. 3, 3-16.

Craig, H., Lupton, J. E. and Horowitz, R. M. (1979) Isotopic geochemistry and hydrology of geothermal waters in the Ethiopian Rift Valler. SIO Reference No. 77-14, U. C. San Diego.

Crookes, W. (1895) The spectrum of the gas from Cleveite. Chem. News, 71.

Dalrymple, G. B. and Moore, J. G. (1968) Argon-40: Excess in submarine pillow basalts from Kilauea volcano, Hawaii Science, 161, 1132-1135.

Eberhardt, P., Eugster, O. and Marti, K. (1965) A redetermination of the composition of atmospheric neon. Z. Naturforsch, 20A, 623-624.

Eugester, O., Eberhardt, P. and Geiss, J. (1967) The isotopic composition of krypton in unequilibrated and gas rich chondrites. Earth Planet. Sci. Lett., 2, 385-390.

Fuex, A. N. (1977) The use of stable carbon isotopes in

hydrocarbon exploration. J. Geochem. Explor., 7, 155.

Fukuda, O., Takahashi, H., Oyagi, N. and Suzuki, H. (1974) Basement of Kanto plain, Chisitsu news, 234, 8-17.

Funkhouser, J. G. and Naughton, J. J. (1968) Radiogenic helium and argon in ultramafic inclusions from Hawaii. J. Geophys. Res., 73, 4604-4607.

Funkhouser, J. G., Fisher, D. E. and Bonatti, E. (1968) Excess argon in deep-sea rocks. Earth Planet. Sci. lett., 5, 95-100.

Gerling, E. K. (1957) Helium migration from minerals and rocks. Tr. Rad. Inst. im. V. G. Khlopova, AN SSSR, 6, 1957.

Gerling, E. K., Mamyrin, B. A., Tolstikhin, I. N. and Yakorleva, S. S. (1971) Helium isotope composition in some rocks. Geochem. Int., 8, 755-761.

Gorshkov, G. V., Zyabkin, V. A., Letkovskaya, N. M. and Tsvetkov. O. S. (1966) The natural neutron background of the atmosphere and the earth's crust. Atomizdat, Moscow., 1966.

Hasagawa, A., Umino, N. and Takagi, A. (1978) Double-planed deep seismic zone and upper-mantle structure in the North eastern Japan Arc. Geophys. J. R. Astron. Soc., 54, 281-296.

Hedge, C. E. and Knight, R. J. (1964) Lead and strontium isotopes in volcanic rocks from northern Honshu, Japan. Geochem. J., 2, 15-24.

Hennecke, E. W. and Mannuel, O. K. (1975) Noble gases in

an Hawaiian xenolith, Nature, 257, 778-780.

Hooker, P. J., Condomines, M., O'Nions, R. K. and Oxburgh, E. R. (1982) Helium and other isotopic variations in the Krafka rifting zone, Iceland. EOS Trans., AGU 63 457.

Hoppe, R., Dahne, W., Mattauch, H. and Rodder, K. M. (1962) Fluorierung von Xenon. Angew. Chem. 74, 903.

Horibe, Y., Kim, K. R. and Craig, H. (1982) Deep ocean hydrothermal vents in Mariana trough. Abstracts of Fifth Intern. Conf. on Geochron. Cosmochron. and Isotope Geol., Nikko Park, Japan, 154.

Irwin, W. P. and Barnes, I. (1980) Tectonic relations of carbon dioxide discharges and earthquakes. J. Geophys. Res., 85, 3115-3121.

Isomi, H. (1968) Tectonic map of Japan, 2. geologic provinces, (1:2000000). Geological survey of Japan.

Janssen, P. J. C. (1868) Lettre ecrite de Madras le 22 juillet 1868. Compt. Rend., 67, 494.

Kakimi, T., Kinugasa, Y. and Kimura, M. (1973) Quaternary tectonic map, Tokyo, (1:500000). Geological Survey of Japan.

Kamenskiy, I. L., Lobkov, V. A., Prasdvov, E. M., Beskrov, N. S., Kudryavtseva, E. I., Anufriyev, G. S. and Pvlov, V. P. (1976) Components of the upper mantle in the volcanic gases of Kamchatka (according to He, Ne, Ar and C isotopy). Geokhimiya, 1976, 682-694.

Kaneoka, I. and Takaoka, N. (1978) Excess ^{129}Xe and high

$^{3}He/^{4}He$ ratios in olivine phenocrysts of Kapuho lava and xenolithic dunites from Hawaii. Earth Planet. Sci. Lett., 39, 382-386.

Kaneoka, I., Takaoka, N. and Aoki, K. (1978) Rare gases in mantle-derived rocks and minerals. In Terrestrial Rare Gases, edited by E. C. Alexander and M. Ozima, Adv. Earth Planet. Sci., 3, 71-84.

Kaneoka, I. and Takaoka, N. (1980) Rare gas isotopes in Hawaiian ultramafic nodules and volcanic rocks: constraints on genetic relationships. Science, 208, 1366-1368.

Kasama, T. (1968) Granitic rocks of the Rokko mountains, Kinki district, Japan. J. Geol. Soc. Japan, 74, 147-158.

Kirsten, T., Richter, H. and Storzer, D. (1982) Rare gas isotope systematics of submarine basalts and glasses. Abstracts of Fifth Intern. Conf. on Geochron. Cosmochron and Isotope Geol. Nikko Park, Japan, 183-184.

Kobayashi, G. (1941) Geological classification of hot springs in Japan and the relation between spring discharges and geotectonic line. J. Geol. Soc. Japan., 608, 460-464.

Kockarts, G. (1973) Helium in the terrestrial atmosphere. Space Sci. Reviews, 14, 723-757.

Kononov, V. I., Mamyrin, V. A., Polak, B. G. and Khabarin, L. V. (1974) Helium isotopes in gases of Icelandic hydrothermare. Dokl. Akad. Nauk. USSR., 217, 172-175.

Kurz, M. D. and Jenkins, W. J. (1981) The distribution of helium in oceanic basalt glasses. Earth Planet. Sci. Lett., 53, 41-54.

Kurz, M. D., Jenkins, W. J. and Hart, S. R. (1982) Helium isotopic systematics of oceanic islands and mantle heterogenety. Nature, 297, 43-47.

Kyser, T. K. and Rison, W. (1982) Systematics of rare gas isotopes in basic lavas and ultramafic xenoliths. J. Geophys. Res., 87, 5611-5630.

Lupton, J. E. and Craig, H. (1975) Excess ^{3}He in oceanic basalts: evidence for terrestrial primordial helium. Earth Planet. Sci. Lett., 26, 133-139.

Lupton, J. E. and Craig, H. (1981) A major ^{3}He source on the East Pacific Rise. Science, 214, 13-18.

Mamyrin, B. A., Tolstikhin, I. N., Anufriyev, G. S. and Kamenskiy, I. L. (1969) Isotopic analysis of terrestrial helium on a magnetic resonance mass spectrometer. Geokhimiya, 1969, 595-602.

Mamyrin, B. A., Anufriyev, G. S., Kamenskiy, I. L. and Tolstikhin, I. N. (1970) Determination of the isotopic composition of atmospheric helium. Geokhimiya, 1970, 721-730.

Marty, B. (1982) Private communication.

Marty, B., Zashu, S. and Ozima, M. (1982) Two noble gas components in a Mid-Atlantic Ridge basalt. Submitted to Nature.

Matsubaya, O., Sakai, H. Kusachi, I. and Sakake, H. (1973) Hydrogen and oxygen isotopic ratios and major element chemistry of Japanese thermal water systems. Geochem. J., 7, 123-151.

Matsubayashi, O., Matsuo, S., Kaneoka, I. and Ozima, M. (1978) Rare gas abundance pattern of fumarolic gases in Japan Volcanic Areas. In Terrestrial Rare Gases. Edited by E. C. Alexander and M. Ozima. Japan Sci. Soc. Press, Tokyo, 155-170.

Moore, J. G., Batchelder, J. N. and Cunniugham, C. G. (1977) CO_2-filled vesicles in Mid-Oceanic Basalts. J. volcanol. geotherm. Res., 2, 309-327.

Morrison, P. and Pine, J. (1955) Radiogenic origin of the helium isotopes in rock. Ann. N. Y. Acad. Sci., 62, 71-92.

Moureu, C. (1923) Les gaz rares des gaz naturels. J. Chem. Soc., 123, 1905-1947.

Nagao, K., Takaoka, N., Matsuo, S., Mizutani, Y. and Matsubayashi, O. (1980) Change in rare gas composition of the fumarolic gases from the Showa-shinzan volcano. Geochem. J., 14, 139-143.

Nagao, K., Takaoka, N. and Matsubayashi, O. (1981) Rare gas isotopic compositions in natural gases of Japan. Earth Planet. Sci. Lett., 53, 175-188.

Nakai, N. (1960) Carbon isotope fractionation of natural gas in Japan. J. Earth Sci. Nagoya Univ., 8, 174-180.

Nier, A. O. (1950) A redetermination of the relative

abundances of the isotopes of carbon, nitrogen, oxygen, argon and potassium. Phys. Rev., 77, 789-793.

Noble, C. S. and Naughton, J. J. (1968) Deep ocean basalts: Inert gas content and uncertainties in age dating. Science, 162, 265-267.

Notsu, K. (1982) Strontium isotope composition in volcanic rocks from Japan. J. Volcanol. Geotherm. Res. in print

Ohsumi, T. and Horibe, Y. (1981) Diffusion coefficinents of rare gases in oceanic sediments. Proc. Ann. Meeting of Geochem. Soc. Japan, 1981, 267.

Ozima, M. (1975) Ar isotopes and earth-atmosphere evolution models. Geochim. Cosmochim. Acta, 39, 1127-1134.

Ozima, M. and Alexander, E. C. (1976) Rare gas fractionation patterns in terrestrial samples and the earth-atmosphere evolution model. Rev. Geophys. Space Phys., 14, 385-390.

Ozima, M. and Zashu, S. (1982) Noble gases in submarine pillow volcanic glasses. Submitted to Earth Planet. Sci. Lett.

Paul, W. and Steinwedel, H. (1953) Ein neues Massenspektrometer ohne Magnetfield. Z. Naturforsch, 82, 448-450.

Phinney, D., Tennyson, J. and Frick, U. (1978) Xenon in CO_2 well gas revisited. J. Geophys. Res., 83, 2313-2319.

Pineau, F., Javoy, M. and Bottinga, Y. (1970) $^{13}C/^{12}C$ ratios of rocks and inclusions in popping rocks of the

Mid-Atlantic Ridge and their bearing on the problem of isotopic composition of deep-seated carbon. Earth Planet. Sci. Lett., 29, 413-421.

Polak, B. G., Kononov, V. I., Tolstikhin, I. N., Mamyrin, B. A. and Khabarin, L. (1974) The helium isotopes in thermal fluids. In Thermal and Chemical Problems of Thermal waters., edited A. T. Johnson, Int. Assoc. Hydrol. Sci. Publ., 119, 15-29.

Poreda, R., Craig, H. and Schilling, J. G. (1980) $^{3}He/^{4}He$ variations along the Reykjanes Ridge. Eos Trans. AGU61 1158.

Ramsay, W. (1895) Terrestrial Helium. Nature, 51, 512.

Renner, J. L., White, D. E. and Williams, D. L. (1975) Hydrothermal convection systems. In Assessment of Geothermal Resources of the United States, 1975. Edited D. E. White and P. L. Williams, U.S.G.S. circular 726.

Rison, W. (1980) Isotpic studies of the rare gases in igneous rocks: implications for the mantle and atmosphere. Ph. D. Thesis, Univ. Calif., Berkeley.

Rubey, W. W. (1951) Geologic histry of sea water. Bull. Geol. Soc. Am., 62, 1111-1147.

Sawada, Y. (1981) Annual reports of the world volcanic eruptions in 1979., Bul. volcanic eruptions, 19, 49-51.

Smith, S. P. and Reynolds, J. H. (1981) Excess ^{129}Xe in a terrestrial samples as measured in a pristine system. Earth Planet. Sci. Lett., 54, 236-238.

Stahl, W. (1968) On the origin of natural gases in northwest Germany. Erdol Kohle, 21, 514.

Stahl, W. (1974) Carbon isotope fractionations in natural gases. Nature (London) 251, 134-135.

Stahl, W. (1977) Carbon and nitrogen isotopes in hydrocarbon research and exploration. Chem. Geol., 20, 121-149.

Stahl, W. (1979) Carbon isotopes in petrolium geochemistry. In Lectures in isotope geology. Eedited E. Jager and J. C. Hunziker. Springer, Berlin, Heidelberg, New York.

Staudacher, T. and Allegre, C. J. (1982) Terrestrial xenology. Earth. Planet. Sci. Lett., 60, 389-406.

Stroud, L., Meyer, T. O. and Emerson, D. E. (1967) Isotopic abundance of neon, argon and nitrogen in natural gases. U. S. Bur. Mines. Rept. Invest. 1967, 6936.

Sumi., K. (1975) Catalogue of hot springs and mineral springs in Japan. Geological Survey of Japan.

Sumi., K. (1979) The relationship of the rates of convective heat discharge to the tectonic provinces in Japan. Bull. Geol. Survey Japan, 28, 277-325.

Tanaka, K. (1974) Estimation of the rate of precipitation recharge to the groundwater by tritium measurements. Chikukagaku, 7/8, 9-16.

Torgersen, T. and Jenkins, W. J. (1982) Helium isotopes in geothermal systems: Iceland, The Geysers, Raft River and Steam bout Springs. Geochim. Cosmochim. Acta, 46, 739-748.

Torgersen, T., Lupton, J. E., Sheppard, D. and Giggenback, W.

(1982) He isotope variations in the thermal areas of New Zealand. J. Volcanol. Geotherm. Res., 12, 283-298.

Urabe, A. (1982) Geochemical study on natural gases in Japan. Master Dissertation, Univ. Tokyo, 82-87.

Uyeda, S. and Horai, K. (1964) Terrestrial heat flow in Japan. J. Geophys. Res., 69, 2121-2141.

von Huene, R. and Uyeda, S. (1981) A summary of results from the IPOD transects across the Japan, Mariana and Middle-America convergent margins. Oceanol. Acta, 1981, Proc. 26th, Intn. Geol. Congress. Geol. Conti. Margins. Symp., Paris, July 7-17.

Weiss, R. F. (1971) The solubility of nitrogen, oxygen and argon in water and sea water. Deep Sea Res., 17, 721-735.

Wedepohl, K. H. (1963) Einige Uberlegungen zur Geschicht des Meermassers. Fortscher. Geol. Rheinl. Westf. 10, 129.

Welhan, J. A. and Craig, H. (1979) Methane and hydrogen in East Pacific Rise hydrothermal fluids. Geophys. Res. Lett., 6, 829-831.

Wetherill, G. W. (1954) Variations in the isotopic abundances of neon and argon extracted from radioactive minerals. Phys. Rev., 96, 679-683.

Yoshii, T. (1979a) A detailed cross-section of the deep seismic zone beneath northeastern Honshu, Japan. Tectonophysics, 55, 349-360.

Yoshii, T. (1979b) Compilation of geophysical data around

the Japanese island (1). Bull. Earthq. Res. Inst., 54, 75-117.

Zartman, R. E., Wasserburg, G. J. and Reynolds, J. H. (1961) Helium, argon and carbon in some natural gases. J. Geophys. Res., 66, 277-306.

Zobell, C. E. (1952) Part played by bacteria in petroleum. J. Sed. Petr., 22, 42-49.